Characterization of Structure and Function of Microbial Communities in

Synechocystis sp. PCC6803 Photobioreactors

by

Alexander Simon Zevin

A Dissertation Presented in Partial Fulfillment
of the Requirements for the Degree
Doctor of Philosophy

Approved April 2015 by the
Graduate Supervisory Committee:

Bruce E. Rittmann, Co-Chair
Rosa Krajmalnik-Brown, Co-Chair
Willem F. J. Vermaas

ARIZONA STATE UNIVERSITY

May 2015

ABSTRACT

Creating sustainable alternatives to fossil fuel resources is one of the greatest

challenges facing mankind. Solar energy provides an excellent option to alleviate

modern dependence on fossil fuels. However, efficient methods to harness solar energy

are still largely lacking. Biomass from photosynthetic organisms can be used as

feedstock to produce traditional fuels, but must be produced in great quantities in order to

meet the demands of growing populations. *Cyanobacteria* are prokaryotic photosynthetic

microorganisms that can produce biomass on large scales using only sunlight, carbon

dioxide, water, and small amounts of nutrients. Thus, *Cyanobacteria* are a viable option

for sustainable production of biofuel feedstock material. Photobioreactors (PBRs) offer a

high degree of control over the temperature, aeration, and mixing of cyanobacterial

cultures, but cannot be kept sterile due to the scales necessary to meet domestic and

global energy demands, meaning that heterotrophic bacteria can grow in PBRs by

oxidizing the organic material produced and excreted by the *Cyanobacteria*. These

heterotrophic bacteria can positively or negatively impact the performance of the PBR

through their interactions with the *Cyanobacteria*. This work explores the microbial

ecology in PBR cultures of the model cyanobacterium *Synechocystis* sp. PCC6803

(*Synechocystis*) using microbiological, molecular, chemical, and engineering techniques.

I first show that diverse phylotypes of heterotrophic bacteria can associate with

Synechocystis-based PBRs and that excluding them may be impossible under typical PBR

operating conditions. Then, I demonstrate that high-throughput sequencing can reliably

elucidate the structure of PBR microbial communities without the need for pretreatment

to remove *Synechocystis*

16S rRNA genes, despite the high degree of polyploidy found in *Synechocystis*. Next, I

establish that the structure of PBR microbial communities is strongly influenced by the

microbial community of the inoculum culture. Finally, I show that maintaining available

phosphorus in the culture medium promotes the production and enrichment of

Synechocystis biomass in PBRs by reducing the amount of soluble substrates available to

heterotrophic bacteria. This work presents the first analysis of the structure and function

of microbial communities associated with *Synechocystis*-based PBRs.

ACKNOWLEDGEMENTS

TABLE OF CONTENTS

Page

iv

LIST OF TABLES

LIST OF FIGURES

viii

Chapter 1

Introduction

1.1 Renewable energies and sustainability

Concerns over global climate change, dependence on foreign oil, and resource limitations have spurred the search for reliable renewable energy sources. Burning fossil fuels generates carbon dioxide (CO_2) gas, a major greenhouse gas that contributes substantially to global climate change (Solomon et al., 2009). Furthermore, fossil fuel resources are finite, and unchecked consumption may leave future generations of human society without the energy resources necessary to fuel and support continually growing populations (Rittmann, 2008). To extend the longevity of fossil resources, mankind has developed many clever methods of harvesting fossil fuel resources, such as deep-sea drilling, hydraulic fracturing, and recovery of oil from bituminous sands. However, these methods cause damage to the environment, do nothing to reduce CO_2 emissions, and do not change the fact that consumption of fossil resources is unsustainable (Kelly et al., 2010; Miller and Robert, 2011; Peterson et al., 2012).

Renewable, environmentally sound energy sources are required to ensure the long-term sustainability of human society. Unfortunately, no current renewable energy sources provide the same energy density, convenience, and versatility as fossil fuels. Furthermore, current renewable energy sources do not produce the amount of energy that is needed to support a growing and developing society (Rittmann, 2008). Because of this, society must develop a diverse repertoire of sustainable energy sources to replace fossil fuels. This new energy landscape will likely include wind, geothermal, nuclear, and solar sources (Gross et al., 2003). Solar energy is by far the most bountiful source of energy on the planet,

1

annually providing the Earth with far more energy than is needed to power human society

(Morton, 2006). However, efficient methods to capture and convert solar energy into

useful forms on large scales are still lacking.

1.2 Renewable energy from photosynthetic biomass

Photosynthesis is the biological process in which light, CO_2, and water are used to

produce organic matter and molecular oxygen. Photosynthetic organisms fix CO_2 and

produce oxygen by using energy from freely available sunlight. The organic matter

generated through photosynthesis can become a source of renewable energy for human

society.

Energy from biomass currently makes up only 10-14% of the world's energy

consumption, and is used disproportionately in developing nations (Kaltschmitt et al.,

2003). The most common way that biomass is used, particularly in developing countries, is

through direct combustion, such as of wood. However, biomass can be processed to

produce combustible oils, ethanol, or biogases such as methane (Kaltschmitt et al., 2003;

Saxena et al., 2009). Currently, most of photosynthetic biomass that the developed world

used for energy comes from plant-based sources such as corn or sugar cane. However,

these sources are not sustainable on a large scale, as they compete with human food

sources, require arable land for cultivation, and cannot be cultivated in sufficient quantities

(Chisti, 2008). Biodiesel is another important biofuel that can be made from the lipids

extracted from photosynthetic biomass. This process involves transesterification of lipids

to form fatty acid methyl esters. Currently, most biodiesel in the United States is produced

2

from soybeans, which also competes with human food supply and cannot meet the domestic demand for liquid transportation fuels (Chisti, 2007).

Photosynthetic microorganisms, including *Cyanobacteria* and eukaryotic algae, are another potential source of renewable biomass. These microalgae have higher photosynthetic efficiencies and areal yields than terrestrial plants, and they do not require arable land for cultivation. Most importantly, biomass from these sources does not compete with human food supplies and can be cultivated domestically (Chisti, 2007). Although microalgal biofuels have great promise, several challenges are preventing large-scale deployment of the technology.

The first, and arguably largest, challenge is to produce sufficient quantities of biomass to meet the energy demands of a first-world economy. Replacing 1% of U.S. annual consumption of petroleum requires around 31 million tons of microalgal biomass, and current culturing methods are not productive enough to meet these demands (Chisti, 2013). This challenge is directly addressed in this work and will be more thoroughly explored in the following sections.

The second challenge is harvesting and dewatering the biomass, which is seen as a major roadblock to the economic viability of micoalgal biofuels due to the high-energy inputs associated with harvesting technologies. A number of methods are available for harvesting biomass including centrifugation, flocculation, filtration, or flotation. While each technology has advantages and disadvantages, none has emerged as superior (Uduman et al., 2010). The final challenge is the conversion of microalgal biomass into different feedstock and fuels. One method is the direct conversion of biomass into biocrude oil through a process termed hydrothermal liquefaction (HTL), which employs high

3

temperatures and pressures to convert microalgal biomass directly into a biocrude oil that has similar energy content to petroleum and can potentially be co-refined in existing petroleum refineries, meaning that modern infrastructure may be suitable for production of renewable fuels. HTL has the added benefit of using wet biomass slurries, bypassing the need to completely dry the biomass (Barreiro et al., 2013). Alternately, lipids can be extracted from microalgal biomass and converted into biodiesel through a transesterification process (Sheng et al., 2011b). Lipid recovery from microalgal biomass can be enhanced through the use of pretreatments such as pulsed electric fields (Lai et al., 2014; Sheng et al., 2011c). Energy also can be recovered from microalgal biomass (lipid extracted or not) as methane through anaerobic digestion or as ethanol through fermentation (Brennan and Owende, 2010).

1.3 *Cyanobacteria*: a unique tool for large-scale production of biomass

Compared to eukaryotic algae, prokaryotic cyanobacteria have several key advantages. First, lipid accumulation in *Cyanobacteria* is directly related to photosynthetic activity and biomass production, whereas nutrient limitation or some other stress factor is required for lipid accumulation in eukaryotic microalgae (Sheng et al., 2011b). Second, *Cyanobacteria* are more amenable to genetic engineering than eukaryotic algae, allowing for rapid strain improvement and providing an avenue for production of specific high-value compounds, such as fatty acids (Liu et al., 2011b; Vermaas, 1998). *Cyanobacteria* also are known to produce a wide range of bioactive compounds that have uses outside of the renewable energy sector (Abed et al., 2009). Finally, *Cyanobacteria* can have higher areal biomass yields than eukaryotic microalgae (Mata et al., 2010).

4

Cyanobacteria are oxygenic photoautotrophs, meaning they produce molecular oxygen and organic matter from light energy and carbon dioxide (Ducat et al., 2011). Thus, biofuels derived from *Cyanobacteria* are carbon neutral: i.e., every carbon dioxide molecule released as a result of oxidizing biofuels derived from *Cyanobacteria* was recently fixed from the atmosphere and incorporated into the cyanobacterial biomass.

Synechocystis sp. PCC6803 (*Synechocystis*) is an especially well characterized cyanobacterium that exhibits robust photoautotrophic growth. *Synechocystis* was the first photoautotrophic organism to have a fully sequenced genome and has served as a model organism in numerous studies in both the molecular and engineering fields (Knoop et al., 2010; Sheng et al., 2011b; Vermaas, 1998). *Synechocystis* has already been used as a platform for production a number of biofuel and feedstock compounds including ethanol and fatty acids (Liu et al., 2011a; Liu et al., 2011b; Ortiz-Marquez et al., 2013). Furthermore, *Synechocystis* contains genetic pathways capable of directly producing alkanes, suggesting the potential for direct production of common transportation fuels (Schirmer et al., 2010).

1.4 Photobioreactors for mass cultivation of cyanobacterial biomass

Cyanobacteria can be cultivated on large scales in either open-pond or closed-photobioreactor (PBR) systems. Compared to open ponds, PBRs offer important advantages, including improved control over culture temperature, reduced water loss to evaporation, and reduced risk of culture contamination. Moreover, PBRs can achieve much higher biomass densities in less space than open ponds (Chisti, 2007; Pulz, 2001). PBRs come in a variety of sizes and configurations including tubular, flat plate, column,

and stirred tank, although tubular and flat plate photobioreactors appear to provide the most optimal conditions for mass cultivation of cyanobacterial biomass, especially in terms of light delivery (Lakaniemi et al., 2012b; Pulz, 2001).

In order for biofuels derived from cyanobacterial biomass to be competitive with petroleum-based fuels, they must be inexpensive to produce (Chisti, 2013). Since PBRs are intrinsically more expensive to build and maintain than open ponds, it is critical to reduce operational costs as much as possible, while increasing biomass production (Chisti, 2007). The culture medium and PBR vessel cannot be sterilized, as this would be costly and is practically impossible at large scale. Although PBRs reduce the risk of culture contamination by heterotrophic bacteria, the requirement to not sterilize the medium and growth vessel means that heterotrophic bacteria are likely to colonize PBR cultures, a phenomenon that is already documented (Lakaniemi et al., 2012a; Lakaniemi et al., 2012b).

Previously, our group characterized important operational aspects of PBR cultures of *Synechocystis* in order to understand how limitations in light, inorganic carbon, and nutrient supply may limit biomass productivity in PBRs. One key finding of these studies was that inorganic carbon (C_i) supply could become limiting when *Synechocystis* efficiently takes up the available C_i, and applying more CO_2 could alleviate this (Kim et al., 2010a). These studies also demonstrated that macronutrients, particularly phosphate, could also be limiting in PBRs for which the goal is high biomass productivity (Kim et al., 2010b). Thus, methods to improve C_i and nutrient delivery are required to prevent these limitations from halting production in industrial PBR settings.

1.5 Implications of microbial ecology in PBR operations

Microbial ecology is the study of communities of microorganisms and their interactions with each other and their environment. Those that study microbial communities seek to determine which microorganisms are present in the system, what their metabolic capabilities are, which metabolic pathways are actually being used, and how the different members of the community affect one another. Microbial ecology has implications in many biotechnological processes including wastewater treatment, bioremediation technologies, microbial fuel cell technologies, and PBRs (Rittmann et al., 2006; Rittmann et al., 2008).

In natural settings, heterotrophic bacteria almost always are found in association with *Cyanobacteria*. Heterotrophic bacteria grow by oxidizing the organic compounds produced by the cyanobacteria and produce CO_2 as a result, which can be used as a carbon source by the *Cyanobacteria* (Abed et al., 2007; Berg et al., 2009; Eiler and Bertilsson, 2004; Li et al., 2011; Prasad et al., 2013). Heterotrophic bacteria can benefit *Cyanobacteria* by reducing oxygen saturation in the culture, increasing the availability of micronutrients, and recycling macronutrients from decaying biomass (Keshtacher-Liebson et al., 1995; Mouget et al., 1995; Purvina et al., 2010). However, predatory heterotrophic bacteria can be detrimental to *Cyanobacteria*, by causing cell lysis that ends in termination of the cyanobacterial culture (Radhidan and Bird, 2001). Furthermore, heterotrophic bacteria may compete with the cyanobacteria for nutrients, or consume a valuable bioproduct excreted by the *Cyanobacteria* (Bratbak and Thingstad, 1985; Liu et al., 2011b). The impact of heterotrophic bacteria on PBR operations must considered since they cannot be excluded from industrial-scale cultures and may provide important benefits

7

to the system. Thus, the structure and function of PBR microbial communities must be addressed in order to successfully bring PBR technologies to the industrial scale.

1.6 Types of heterotrophic bacteria associated with *Cyanobacteria*

Most of the available data regarding the particular types of heterotrophic bacteria associated with *Cyanobacteria* come from natural settings, such as cyanobacterial blooms in lakes. One such study showed that *Alphaproteobacteria*, mostly from the genera *Sphingopixys* and *Rhodobacter*, dominated the community of heterotrophic bacteria associated with a bloom of the toxic cyanobacterium *Microcystis* (Li et al., 2011). Another study showed that cyanobacterial blooms in four lakes, each with different types of *Cyanobacteria*, had different types of associated heterotrophic bacteria (Eiler and Bertilsson, 2004). Thus, the communities of heterotrophic bacteria that associate with naturally occurring cyanobacterial populations may differ depending on the species of *Cyanobacteria* and the environment.

1.7 Soluble microbial products in PBRs

All bacteria produce soluble microbial products (SMP) as a part of their normal metabolism. SMP are very heterogeneous organic materials and can be further categorized as utilization-associated products (UAP) or biomass-associated products (BAP). UAP result directly from oxidation of an electron donor, while BAP result from hydrolysis of biomass or extracellular polymeric substances (EPS) (Laspidou and Rittmann, 2002). UAP tend to be smaller and more easily biodegraded than BAP (Ni et al., 2011a). Importantly, SMP produced by autotrophic bacteria can support the growth of heterotrophic bacteria (Ni

8

et al., 2011b). Thus, SMP produced by *Cyanobacteria* are likely the major carbon source and electron donor for the heterotrophic bacteria that grow in PBRs.

While SMP produced by cyanobacteria have not been well characterized, a variety of studies have been conducted on EPS produced by *Cyanobacteria*. EPS produced by *Synechocystis* are composed mostly of polysaccharides and proteins (Panoff et al., 1988). The polysaccharide fraction is highly enriched in glucose, but also contains a number of other monosaccharide subunits (Fisher et al., 2013). The high proportion of carbohydrates in *Synechocystis* EPS indicates that it is potentially a very important energy source for heterotrophic bacteria that associate with *Synechocystis*. Indeed, it has been demonstrated that heterotrophic bacteria can grow using EPS extracted from *Cyanobacteria* as a sole carbon source and electron donor (Giroldo et al., 2003; Li et al., 2009). Because SMP and EPS are closely related (Laspidou and Rittmann, 2002; Ni et al., 2011a), it is likely that SMP produced by *Synechocystis* are also highly enriched in saccharide moieties. Another carbon source and electron donor available to heterotrophic bacteria in PBRs is decaying biomass (Laspidou and Rittmann, 2002). Compared to EPS-derived substrates, the products resulting from cellular decay are probably richer in proteins and lipids.

Heterotrophic bacteria in a PBR have two major functions: depolymerizing and solubilizing EPS to SMP and subsequently biodegrading the SMP; and biodegrading the SMP that results from decay of cyanobacterial and heterotrophic cells. While it is perfectly possible for one type of heterotrophic bacteria to perform both of these functions, it is equally likely that distinct groups of heterotrophic bacteria biodegrade SMP either from EPS or from cellular biomass.

1.8 A multidisciplinary approach to manage microbial ecology in *Synechocystis*-based PBRs

The PBR presents a wonderful opportunity to integrate tactics from multiple disciplines to understand the complex interactions between *Synechocystis* and heterotrophic bacteria. Next generation sequencing (NGS) allows for rapid phylogenetic profiling of microbial communities (Liu et al., 2012), but can be costly, requires intensive bioinformatics analysis, and is not useful as a rapid diagnostic of microbial communities. The combination of NGS techniques with other potentially high throughput phylogenetic analyses, such as terminal-restriction fragment length polymorphism (T-RFLP) (Liu et al., 1997) and quantitative real-time polymerase chain reaction (qPCR) (Zhang et al., 2011), can provide a robust system for rapidly profiling the structure and dynamics of PBR microbial communities.

Classical microbiological techniques to isolate bacteria used in tandem with these molecular techniques can help to understand more fully the growth kinetics of the heterotrophic bacteria that live in the PBR. These empirically derived kinetic constants can then be used to inform mathematical models to predict the growth of heterotrophic bacteria in PBRs and to provide PBR operators with information on how to manage the heterotrophic bacteria.

Bulk chemical analyses of chemical oxygen demand (COD), dissolved organic carbon (DOC), carbohydrates, and proteins are useful to measure the available substrates in the PBR and provide a convenient way to assess the function of PBR microbial communities. Determining how the growth of heterotrophic bacteria affects the relative levels of these substrates may help to elucidate the preferred substrates of heterotrophic

bacteria. Knowing the preferred substrates of dominant heterotrophic bacteria, along with the effects of those bacteria on *Synechocystis*, will provide options for mitigating the impact of undesirable heterotrophic bacteria on PBR performance.

1.9 Objectives and summary of work

The major goals of this work are to examine the structure and function of PBR microbial communities and to develop methods to manage PBR microbial communities. Chapter 2 focuses on understanding the structure of the microbial communities using culture-dependent and culture-independent methods to assess the heterotrophic bacteria present in PBR cultures. Chapter 3 expands upon this by examining the growth kinetics of some of the cultured bacteria from Chapter 2 under PBR-like conditions, and it presents a simple mathematical model to predict heterotrophic growth in *Synechocystis*-based PBRs.

Chapter 4 presents a qPCR assay for specific detection of *Synechocystis* 16S rRNA genes and a magnetic capture hybridization technique for specific removal of *Synechocystis* 16S rRNA genes from pools of gDNA extracted from *Synechocystis*-based PBRs. Chapter 5 demonstrates that the inoculum used to start *Synechocystis*-based PBRs has a strong influence on the microbial community that develops in that PBR. Finally, Chapter 6 shows that phosphate limitation is associated with higher levels of SMP and heterotrophic bacteria in *Synechocystis*-based PBRs, demonstrating that nutrient availability is critical for driving production of *Synechocystis* biomass. Chapter 7 provides a summary and ideas of future research.

Taken together, the research presented here provides a fundamental analysis of microbial community structure and function in *Synechocystis*-based PBRs and provides

11

tools to manage, monitor, and thoroughly characterize PBR microbial communities. Detailed summaries of each technical chapter are provided below.

Chapter 2. Phylogenetic characterization of heterotrophic bacteria isolated and enriched from photobioreactor (PBR) cultures of *Synechocystis* sp. PCC6803

The first step toward understanding PBR microbial communities is to determine the types of heterotrophic bacteria most commonly associated with PBR cultures of *Synechocystis* sp PCC6803. Towards this goal, I isolated and enriched heterotrophic bacteria from different PBRs and compared the phylogenetic distribution of these heterotrophic bacteria to the distribution of heterotrophic bacteria detected directly in PBR cultures using 16S rRNA gene sequencing.

I isolated 65 heterotrophic bacteria distributed across five main classes: *Actinobacteria, Alpha/Beta/Gammaproteobacteria,* and *Bacilli*, with *Gammaproteobacteria* being the most common. I then used EcoPlates to show that representative isolates from each class could grow on a variety of carbon substrates, but that the substrates containing organic nitrogen were the most favorable. I enriched heterotrophic bacteria from two different PBRs using either acetate of glucose as a carbon source. All four enrichment cultures had different heterotrophic bacteria, but the enrichments from the same PBR were more similar to one another than they were to the enrichments from the other PBR. The types of heterotrophic bacteria detected in the enrichment cultures were similar to those that were isolated.

Chapter 3. Kinetic characterization of heterotrophic bacteria isolated and enriched from *Synechocystis* sp. PCC6803-based photobioreactors

In this chapter, I provided simple and complex carbon substrates for growth of the heterotrophic bacteria described in Chapter 2 and evaluated their growth kinetics. The goal of this work was to understand the growth rates of heterotrophic bacteria in PBR-like settings in order to develop effective strategies to manage heterotrophic bacteria in PBR settings. I selected one of the fastest growing isolates (*B2*, *Pseudomonas stutzeri*) to further characterize and compared it to a mixed community of heterotrophic bacteria enriched from a PBR (*ENR1*), which was dominated by bacteria from the classes *Alphaproteobacteria* and *Cytophagia*.

First, I conducted a series of batch experiments to measure important kinetic parameters for the different heterotrophic bacteria. One important parameter was the maximum specific growth rate, which represents how rapidly the bacterial population will grow in a chemostat culture. Another kinetic parameter determined for the heterotrophic bacteria was cellular yield, which measures the efficiency of the bacteria to convert the growth substrate into biomass. The final kinetic parameter measured through these experiments was the Monod constant (K_m), which can be thought of as the affinity of the bacteria for a particular substrate (Kovárová-Kovar and Egli, 1998). I demonstrated that, when provided with very labile substrates such as acetate, glucose, or laurate, *P. stutzeri* grew more rapidly than *ENR1*. However, *P. stutzeri* and *ENR1* had similarly low K_m values for these substrates, indicating that even low substrate concentrations could support the growth of heterotrophic bacteria in PBRs. I then examined the growth of *ENR1* on SMP harvested from a *Synechocystis* PBR. I showed that the SMP could support some

13

growth of ENR1, but the growth was much slower than it was for the more labile

substrates, demonstrating that PBR effluent probably contains relatively recalcitrant SMP.

I then used a mathematical model to predict the growth of the heterotrophic bacteria

in a PBR setting. This analysis showed that heterotrophic bacteria could grow very well

when labile substrates were provided, even at very short hydraulic retention times (HRTs).

Even recalcitrant SMP could support the growth of heterotrophic bacteria in the range of

HRTs at which *Synechocystis* PBRs are typically operated, indicating that it may be

difficult to exclude heterotrophic bacteria from PBR cultures by operating at HRTs

normally used in practice.

Chapter 4. Removal of *Synechocystis* sp. PCC6803 16S rRNA genes does not
significantly improve resolution of heterotrophic bacteria in 16S rRNA-based
microbial community analysis

In this chapter, I used and validated a qPCR assay developed by Jonathan

Badalamenti for specific detection of *Synechocystis* 16S rRNA genes. I then developed a

novel magnetic capture hybridization (MCH) technique to specifically remove

Synechocystis 16S rRNA genes from pools of genomic DNA (gDNA) extracted from

Synechocystis-based PBRs with the goal of improving detection of low-abundance

heterotrophic bacteria with high-throughput sequencing and T-RFLP assays.

First, I showed that the *Synechocystis* specific qPCR assay is quantitative and can

quantify the abundance of *Synechocystis* 16S rRNA gene copies with reasonable accuracy.

Furthermore, I showed that the *Synechocystis* specific qPCR assay can be used in

conjunction with previously described total bacterial qPCR assays to predict the abundance of heterotrophic bacteria in PBRs.

Next, I validated the MCH method for specific removal of *Synechocystis* 16S rRNA genes using gDNA extracted from two different *Synechocystis*-based PBRs. First, I showed with qPCR that the MCH method successfully reduced the concentration of total bacterial and *Synechocystis* 16S rRNA gene sequences. Next, I used high-throughput sequencing to assess the community structure in the PBR gDNA samples and MCH treated samples. I showed that, in general, the MCH treatment decreased the relative proportion of 16S rRNA gene sequences assigned to *Synechocystis* and increased the relative proportion of 16S rRNA gene sequences assigned to heterotrophic bacteria, showing that the MCH treated samples may more accurately represent the distribution of heterotrophic bacteria in *Synechocystis*-based PBRs. However, the MCH treatment did not lead to the discovery of heterotrophic phylotypes that were not detected in the untreated samples. I then showed that the MCH treatment could improve the number of non-*Synechocystis* terminal-restriction fragments (T-RFs) detected in T-RFLP assays. However, this was only the case for PBRs with a relatively high abundance of *Synechocystis* 16S rRNA genes.

Finally, I demonstrated that the MCH capture probe shared at least nine base pairs of sequence similarity with a variety of non-*Synechocystis* 16S rRNA genes, as well as with a variety of non-16S rRNA genes (protein coding genes) in the genomes of *Synechocystis* and other bacteria. From this, I concluded that the MCH capture probe was not sufficiently specific to *Synechocystis* 16S rRNA genes. Taken together, the results presented in this chapter showed that high-throughput sequencing was sufficient to uncover all of the microbial diversity in *Synechocystis*-based PBRs without the need to remove *Synechocystis*

15

16S rRNA genes prior to sequencing analysis. Thus, this MCH technique was not used for the high-throughput 16S rRNA gene sequencing analyses in the subsequent chapters.

Chapter 5. Effects of inoculum source on the structure of microbial communities in *Synechosyctis* sp. PCC6803-based photobioreactors

After identifying the types of heterotrophic bacteria found in PBRs and characterizing them in terms of growth kinetics, the next goal was to develop strategies to manage PBR microbial communities. Towards this goal, I conducted four PBR experiments that were operated under identical environmental conditions. Two PBRs (PBRA and PBRA2) were started with the same starter culture (inoculum), while the other two PBRs (PBRB and PBRC) were started using different inocula. PBRA and PBRA2 had nearly identical microbial communities and performed similarly in terms of overall biomass production. PBRB and PBRC each had unique microbial communities and performed differently than one another, although PBRB performed similarly to PBRA and PBRA2.

To further investigate the impact of the inoculum on PBR microbial community structure, I conducted a simple batch test. First, I obtained three flasks of *Synechocystis* culture from three different sources. I then used those flasks to inoculate three experimental flasks each, for a total of nine flasks. I then grew the nine flasks under identical conditions for 96 hours. Finally, I examined the microbial communities in each of the inoculum and experimental flasks using 16S rRNA gene sequencing and T-RFLP. Both techniques demonstrated that the microbial communities in each set of experimental flasks were more similar to one another and the respective inoculum flask than they were to the other sets of flasks.

16

From all the results, I concluded that the microbial community in the inoculum played a major role in shaping the microbial community that develops in PBRs. I demonstrated that light microscopy was not sufficient to detect heterotrophic bacteria in these inocula and that molecular methods were more sensitive and more appropriate for determining the purity of PBR inocula than was light microscopy. Finally, I showed strong agreement between the 16S rRNA gene sequencing and T-RFLP data, demonstrating that T-RFLP can be used as a rapid diagnostic to compare the heterotrophic bacteria present in PBR microbial communities.

Chapter 6. Effects of phosphate limitation on the production of soluble microbial products (SMP) in *Synechocystis*-based photobioreactors

In this chapter, I examined another strategy to manage PBR microbial communities: controlling the availability of SMP in the PBR. SMP probably are the major drivers of heterotrophic growth in *Synechocystis* PBRs. Thus, reducing the concentration of SMP should help to reduce heterotrophic bacteria in the PBR.

Towards this goal, I operated two semi-continuous PBRs with HRTs of 3 days and identical light and temperature profiles. The first (PBRP0) was operated with normal BG-11 medium, while the second (PBRP+) was operated with additional phosphate, added on a daily basis. In PBRP0, the soluble phosphate was completely removed after a few days of operation, inducing phosphate limitation. After the phosphate became limiting, the growth rate of *Synechocystis* in PBRP0 was lower than the dilution rate, and the culture density decreased. The soluble phosphate in PBRP+ was never depleted and the growth rate became roughly equal to the dilution rate after several days of operation.

PBRP0 had more soluble COD (SCOD) and dissolved organic carbon (DOC) than did PBRP+, indicating more SMP in PBRP0. Further analysis showed that the SMP in PBRP0 was dominated by carbohydrates that were probably derived from shearing and hydrolysis of EPS, which is rich in carbohydrates (Panoff et al., 1988). In PBRP+, carbohydrates represented a much smaller fraction of the SMP, suggesting that more of the SMP in this PBR was derived from non-EPS sources, such as cell lysis.

I then used 16S rRNA gene sequencing to analyze the microbial communities in both PBRs. PBRP0 had a much higher relative proportion of heterotrophic bacteria than did PBRP+, which was probably a result of the higher levels of SMP in PBR0. I concluded that, under phosphate-limited conditions, *Synechocystis* produced excess EPS in order to store photo-assimilated carbon and electrons. The EPS then acted as a substrate for heterotrophic bacteria. However, when phosphate was available, the carbon and electrons were used to produce *Synechocystis* biomass. Thus, maintaining phosphate availability in PBRs was key to maintaining biomass production and reducing heterotrophic bacteria.

Chapter 2

Characterization of heterotrophic bacteria isolated and enriched from photobioreactor

(PBR) cultures of *Synechocystis* sp. PCC6803[1]

2.1 Introduction

Interactions between *Cyanobacteria* and heterotrophic bacteria are well

documented for natural conditions (Eiler and Bertilsson, 2004; Li et al., 2011). Recently,

researchers have turned to *Cyanobacteria* as promising sources of renewable feedstock for

biofuel production, and they have begun growing *Cyanobacteria* in engineered

photobioreactor (PBR) systems (Ducat et al., 2011; Kim et al., 2010a). Sterilization and

aseptic maintenance of large-scale PBRs are neither technically nor economically feasible

for producing low-cost biofuels. Thus, heterotrophic bacteria will naturally colonize PBR

systems (Lakaniemi et al., 2012b). These heterotrophic bacteria can be beneficial to

Cyanobacteria by recycling macronutrients or by increasing the availability of

micronutrients, such as iron (Keshtacher-Liebson et al., 1995; Lakaniemi et al., 2012b).

Heterotrophic metabolism also lowers O_2 concentration in the culture medium, which may

help promote photosynthesis (Mouget et al., 1995). However, heterotrophic bacteria can

compete with *Cyanobacteria* for nutrients (Bratbak and Thingstad, 1985), consume

valuable organic products excreted by the *Cyanobacteria* (Liu et al., 2011b), and in some

cases induce lysis of *Cyanobacteria* (Radhidan and Bird, 2001). Therefore, it is important

_____

[1]This chapter is adapted from a manuscript submitted for publication.

to characterize the types of heterotrophic bacteria that commonly associate with *Cyanobacteria* in PBRs.

In the natural environment, one study reported that *Gammaproteobacteria* were the majority of heterotrophic bacteria associated with cyanobacterial blooms from several bodies of fresh and salt water (Berg et al., 2009). Another study reported a high proportion of *Bacteriodetes* in association with freshwater cyanobacterial blooms (Eiler and Bertilsson, 2004). Others have shown diverse consortia of heterotrophic bacteria associated with a cyanobacterial mat (Abed et al., 2007). Thus, the phylogeny of bacteria that associate with *Cyanobacteria* seems to vary greatly for different species of *Cyanobacteria* and in different environments. Only a few studies have addressed the phylogenetic diversity of heterotrophic bacteria that exist in engineered PBR settings (Lakaniemi et al., 2012a; Lakaniemi et al., 2012b), and none have done so for PBR cultures dominated by *Cyanobacteria*.

Heterotrophic bacteria in PBRs grow by oxidizing organic compounds produced and excreted by photoautotrophs, such as the model cyanobacterium *Synechocystis* sp. PCC6803. Important excreted organic compounds are extracellular polymeric substances (EPS) and soluble microbial products (SMP), which can be formed by shearing and hydrolysis of EPS (Laspidou and Rittmann, 2002; Li et al., 2009). EPS produced by *Synechocystis* sp. PCC6803 are mostly glucose-rich carbohydrates and protein (Panoff et al., 1988), indicating that glucose and dissolved free or combined amino acids likely represent the major carbon substrates utilized by heterotrophic bacteria in a PBR. Other SMP produced by *Cyanobacteria* may include fatty acids and alcohols (Abed et al., 2007).

Here, I isolated pure strains and enriched mixed consortia of heterotrophic bacteria from PBR cultures of *Synechocystis* sp. PCC6803 to assess the phylogenetic diversity and metabolic capability of the heterotrophic bacteria in these systems. I demonstrated that phylogenetically diverse heterotrophic bacteria can be isolated and enriched from PBR cultures of *Synechocystis* sp. PCC6803, but they are similar in terms of their abilities to grow well on a variety of carbon substrates.

2.2 Materials and Methods

Cyanobacteria cell cultures, strains and media

Stock cultures of *Synechocystis* sp. PCC 6803 (hereafter referred to as *Synechocystis*) were provided by the laboratory of Dr. Willem Vermaas (School of Life Sciences, Arizona State University). Stock cultures were grown in Erlenmeyer flasks at 30°C in BG-11 medium (Rippka et al., 1979) bubbled with air.

Isolation of heterotrophic bacteria

I isolated heterotrophic bacteria from several sources including 16-L bench top (BT) PBRs (Kim et al., 2010b), a 350-mL Photobioreactor FMT-150 (FMT) (Photon Systems Instruments, Czech Republic), and several flask cultures. All of the PBR cultures were *Synechocystis*-based and were grown with continuous light irradiation at a temperature of 30°C in BG-11 medium. To isolate the bacteria, I first diluted fresh PBR culture to 10^{-3} and 10^{-6} in BG-11. I then plated 100 µL of the diluted culture onto R2A agar (Teknova, Hollister, CA) or BG-11 agar plates supplemented with 0.1-mM laurate (Sigma Aldrich), 50-mM sodium acetate (Sigma Aldrich), or 100-mg/L glucose (Sigma

Aldrich); I incubated the plates at 30°C. After colonies formed (typically 1-3 days), I picked individual colonies, streaked them onto the same medium type, and allowed colonies to form again. I repeated this process three times to ensure purity of the isolated bacteria. Once the third set of plates showed growth, I picked colonies and used them to inoculate 5-mL cultures of the same liquid medium and grew them at 30°C. After the starter cultures grew to an appropriate density (1-3 days), I mixed 0.5 mL of the starter culture with 0.5 mL sterile 40% glycerol and stored these samples at -80°C as freezer stocks.

Growth on R2A

I selected one representative from each class of isolated heterotrophic bacteria to characterize further. The chosen representative bacteria were: *Pseudomonas stutzeri* PBR#6 (Acc no. KF539914), *Bacillus cereus* PBR#10 (Acc no. KF539915), *Sphingomonas adhaesiva* PBR#14 (Acc no. KF539916), *Corynebacterium amycolatum* PBR#21 (Acc no. KF539917), and *Ralstonia pickettii* PBR#24 (Acc no. KF539918). To determine growth rates of selected isolates on R2A medium, I inoculated 50 mL of R2A medium at a starting optical density at a wavelength of 600nm (OD_{600}) of approximately 0.1. I then incubated the cultures at 30˚C and removed 1-mL samples at regular intervals and measured the OD_{600} using a Cary-50-Bio UV-Visible spectrophotometer. I determined the specific growth rate (SGR) using Eq. 1, where *t* is time in days (Rittmann and McCarty, 2001).

Eq. 1) $\text{SGR} \left(\frac{1}{\text{day}} \right) = \frac{1}{OD_{600}} * \frac{dOD_{600}}{dt}$

Ecoplate Analysis

I used EcoPlates (BioLog, Hayward, CA), which are microwell plates that contain a panel of 31 unique carbon substrates and a negative control (water), to characterize the metabolic capacity of the five representative isolated bacteria. To do this, I first grew the heterotrophic bacteria on R2A medium and then centrifuged 1 mL of this culture at 13K RPM for 1 minute, removed the supernatant, and resuspended the cells in a final volume of 100 mL of fresh BG-11 medium without ferric ammonium citrate or calcium carbonate. I then added 150 µL of this to each well of the EcoPlates, incubated the EcoPlates at 30˚C in the dark, and measured the absorbance of each well at a wavelength of 590 nm (A_{590}) using a SpectraMax 190 (Molecular Devices, Sunnyvale, CA) at regular intervals for a total of 120 hours. I performed principal components analysis (PCA) using the R programming language.

Enrichment of consortia heterotrophic bacteria

I enriched consortia of heterotrophic bacteria from two *Synechocstis*-based PBRs that were separate from the PBRs from which I isolated heterotrophic bacteria. These PBRs will be referred to as PBR-1 and PBR-2. Both PBRs were operated as batch reactors and using BG-11 medium, constant light irradiation, constant temperature of 30˚C, and bubbling with filter-sterilized air (Pall). To enrich for heterotrophic bacteria, I added 200 µL of PBR culture to 50 mL of sterile BG-11 containing either 50 mM sodium acetate or 100 mg/L glucose. I then incubated these cultures at 30˚C for three days, or until bacterial growth was evident. I passaged these enrichment cultures into the same liquid medium two times before taking DNA samples.

23

DNA Extraction

For DNA extraction, 1 mL of the 5 -mL starter cultures was centrifuged to concentrate biomass, which was stored at -80°C prior to DNA extraction. I extracted total genomic DNA using the DNeasy Blood & Tissue Kit (Qiagen, Valencia, CA) with the following modifications designed to enhance lysis. I resuspended cell pellets in 200 μL lysis buffer (30 mM Tris·HCl, 10 mM EDTA, 200 mM sucrose, pH 8.2) and incubated the mixture at 65°C for 10 minutes. I then added chicken egg white lysozyme (Sigma Aldrich, St. Louis, MO) to a final concentration 10 mg/mL and incubated the samples for 1 hour at 37°C. Next, I added SDS at 1% (w/v) and incubated the samples at 56°C for 10 minutes. Finally, I added 25 μL proteinase K and 200μL buffer AL (Qiagen), incubated that mixture at 56°C for 30 minutes, and completed the DNA extraction according to the manufacturer's (Qiagen) instructions.

16S rRNA gene sequencing (Sanger) and phylogenetic assignment

I first PCR amplified the 16S rRNA genes from the genomic DNA extracted from each isolate using the universal bacterial primers 8F and 1525R (Torres et al., 2009) and purified the resulting PCR amplicons using a Qiaquick PCR Purificaiton Kit (Qiagen, Valencia, CA). I then sequenced the 16S rRNA genes from the isolates on an Applied Biosystems 3730 DNA Analyzer (Life Technologies, Grand Island, NY) using the universal bacterial primers 8F, 342F, 533F, and 1525R (Löffler et al., 2000; Weisburg et al., 1991). I assembled the partial 16S rRNA gene sequences using BioEdit v.7.0.9 (Ibis Biosciences, Carlsbad, CA) and assigned taxonomy to each isolate according to the closest match among cultured organisms from the NCBI BLAST tool. Only sequences with >1000

base pairs (bp) were used. I constructed maximum likelihood phylogenetic trees with the

MEGA V 5.2.2 (Tamura et al., 2011) software. The sequences of the heterotrophic bacteria

used in these studies were deposited in GenBank under accession numbers KF539914-

KF539918 and KJ806207-KJ806264.

High throughput 16S rRNA gene sequencing and data analysis

I sequenced 16S rRNA genes from the enriched consortia of heterotrophic bacteria

using previously described methods (Caporaso et al., 2012). I amplified the V4 region of

bacterial 16S rRNA genes using Golay barcoded primer set 515F/806R (Caporaso et al.,

2010a). I then pooled the triplicate PCR reactions and quantified them using the Quant-iT

PicoGreen dsDNA Assay Kit (Life Technologies). Next, I pooled 240 ng of each sample in

and cleaned the final pool using the QiaQuick PCR Cleanup Kit (Qiagen). For loading the

samples onto the Illumina MiSeq, I quantified the PCR library using the KAPA SYBR

FAST Universal qPCR Kit for Illumina (KAPA Biosystems). I then sent the prepared

library to the Microbiome Analysis Laboratory at Arizona State University for sequencing

on the Illumina MiSeq. I analyzed all 16S rRNA gene sequencing data using the QIIME

software using the default quality filters (Caporaso et al., 2010b). In order to examine only

the heterotrophic bacteria from the representative PBR experiment, I filtered all

cyanobacterial OTUS from the OTU table using the script filter_taxa_from_otu_table.py

prior to downstream analysis and removed any unassigned sequences. All analyses are of

150-bp forward reads. All sequence reads included in this work were uploaded to the

NCBI Sequence Read Archive under BioProject accession number SRP049557 with the

individual samples under accession numbers SRR1640754-SRR1640758 and

SRR1640762.

2.3 Results and Discussion

Heterotrophic bacteria isolated from *Synechocystis*-dominated PBRs belong to five

bacterial classes

I isolated 65 strains of heterotrophic bacteria from PBR cultures of *Synechocystis*.

The isolates belonged to five classes: *Alphaproteobacteria*, *Betaproteobacteria*,

Gammaproteobacteria, *Bacilli*, and *Actinobacteria*. **Figure 2.1** shows the distribution of

heterotrophic bacteria isolated from *Synechocystis*-based PBRs at the class level.

Gammaproteobacteria accounted for 52% of the bacteria isolated, *Betaproteobacteria*

accounted for 24%, and *Bacilli* accounted for 14%. *Actinobacteria* and

Alphaproteobacteria were less common, representing 8% and 3% of the isolates,

respectively.

34 of the bacterial isolates belonged to the class *Gammaproteobacteria*. *Of* the

isolated *Gammaproteobacteria*, 21 belonged to the genus *Pseudomonas*, 10 were

associated with the genus *Stenotrophomonas*, and two from *Pseudoxanthomonas*. The

species identified were closely related to *Pseudomonas aeruginosa*, *Pseudomonas*

alcaligenes, *Pseudomonas pseudoalcaligenes*, *Pseudomonas stutzeri*, *Stenotrophomonas*

maltophilia, Stenotrophomonas acidaminiphila, and *Pseudoxanthomonas mexicana*. A full

list of the isolated heterotrophic bacteria is provided in **Table 2.1**.

Comparative genomic studies have revealed that *Gammaproteobacteria* are able to

metabolize large carbon compounds, such as EPS or SMP (Livermore et al., 2013).

Consequently, *Gammaproteobacteria* may play a critical role in the PBR by breaking down

EPS produced by *Synechocystis* into smaller subunits. Additionally, some *S. maltophilia*

strains produce a variety of extracellular hydrolytic enzymes (Ryan et al., 2009), adding to

the notion that these bacteria are responsible for the biodegradation of large polymeric

materials in the PBR. G*ammaproteobacteria* typically display high growth rates compared

to other heterotrophic bacteria and may simply outcompete the other members of the PBR

microbial communities during isolation, an effect that has been previously observed

(Newton et al., 2011). Thus, high growth rate may be the reason that

Gammaproteobacteria accounted for the majority of the isolated heterotrophic bacteria and

the ability to metabolize EPS may be the reason that *Gammaproteobacteria* were present in

the PBR cultures.
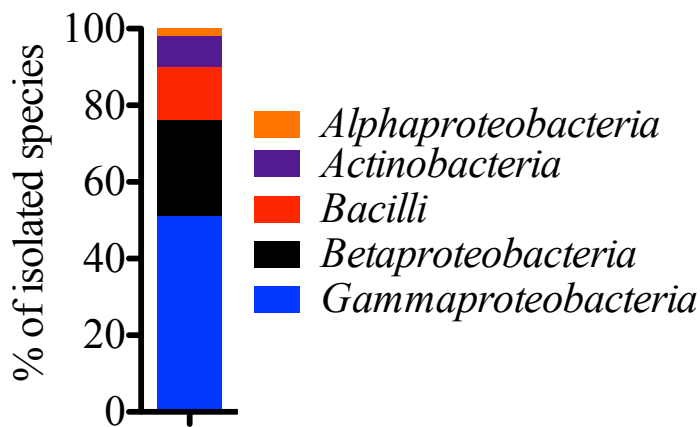
**Figure 2.1 Distribution of heterotrophic bacteria isolated
from *Synechocystis* PBRs at the class-level.** The majority
of the bacterial isolates belonged to the functionally diverse
Gammaproteobacteria.

Table 2.1 List of isolated heterotrophic bacteria. The heterotrophic bacteria were isolated from different *Synechocystis*-based PBR experiments. The isolates used in growth rate and EcoPlate studies are indicated in **bold font**.

PBR#	Class	Nearest BLAST hit species
	Isolated from BT-PBR	
1	*Gammaproteobacteria*	*Stenotrophomonas maltophilia*
2	*Betaproteobacteria*	*Comamonas acidovorans*
3	*Bacilli*	*Staphylococcus hominis*
4	*Gammaproteobacteria*	*Stenotrophomonas sp.*
6	***Gammaproteobacteria***	***Pseudomonas stutzeri***
7	*Gammaproteobacteria*	*Pseudomonas sp.*
8	*Gammaproteobacteria*	*Pseudomonas sp.*
9	*Bacilli*	*Staphylococcus epidermidis*
10	***Bacilli***	***Bacillus cereus***
11	*Betaproteobacteria*	*Achromobacter insolitus*
13	*Gammaproteobacteria*	*Pseudomonas sp.*
14	***Alphaproteobacteria***	***Sphingomonas adhaesiva***
15	*Gammaproteobacteria*	*Pseudomonas sp.*
16	*Gammaproteobacteria*	*Pseudomonas sp.*
17	*Gammaproteobacteria*	*Pseudomonas putida*
19	*Bacilli*	*Staphylococcus epidermidis*
20	*Bacilli*	*Staphylococcus hominis*
21	***Actinobacteria***	***Corynebacterium amycolatum***
23	*Bacilli*	*Staphylococcus sp.*
67	*Gammaproteobacteria*	*Pseudomonas sp.*
68	*Betaproteobacteria*	*Pigmentiphaga sp.*
69	*Gammaproteobacteria*	*Stenotrophomonas sp.*
72	*Gammaproteobacteria*	*Stenotrophomonas sp.*
74	*Gammaproteobacteria*	*Pseudomonas pseudoalcaligenes*
75	*Gammaproteobacteria*	*Stenotrophomonas maltophilia*
76	*Gammaproteobacteria*	*Stenotrophomonas maltophilia*
77	*Gammaproteobacteria*	*Stenotrophomonas maltophilia*
78	*Betaproteobacteria*	*Delftia tsuruhatensis*
79	*Gammaproteobacteria*	*Stenotrophomonas sp.*
81	*Actinobacteria*	*Rhodococcus sp.*
82	*Gammaproteobacteria*	*Stenotrophomonas maltophilia*
83	*Gammaproteobacteria*	*Pseudomonas sp.*
84	*Actinobacteria*	*Agromyces mediolanus*
88	*Betaproteobacteria*	*Delftia tsuruhatensis*

90	*Gammaproteobacteria*	*Stenotrophomonas maltophilia*
91	*Gammaproteobacteria*	*Pseudomonas pseudoalcaligenes*
92	*Gammaproteobacteria*	*Pseudomonas aeruginosa*
93	*Betaproteobacteria*	*Delftia sp.*
95	*Betaproteobacteria*	*Delftia tsuruhatensis*
Isolated from Flask Cultures		
25	*Betaproteobacteria*	*Cupravidius respiraculi*
26	*Betaproteobacteria*	*Cupravidius respiraculi*
27	*Betaproteobacteria*	*Cupravidius respiraculi*
28	*Betaproteobacteria*	*Hydrogenophaga pseudoflava*
29	*Betaproteobacteria*	*Cupravidius respiraculi*
30	*Bacilli*	*Staphylococcus epidermidis*
31	*Betaproteobacteria*	*Cupravidius respiraculi*
32	*Betaproteobacteria*	*Cupravidius respiraculi*
33	*Actinobacteria*	*Streptomyces rochei*
34	*Actinobacteria*	*Streptomyces rochei*
49	*Gammaproteobacteria*	*Pseudomonas alcaligenes*
50	*Gammaproteobacteria*	*Pseudomonas stutzeri*
51	*Gammaproteobacteria*	*Pseudomonas stutzeri*
Isolated from FMT-PBR		
24	**Betaproteobacteria**	**Ralstonia pickettii**
52	*Alphaproteobacteria*	*Sphingomonas sp.*
53	*Gammaproteobacteria*	*Pseudomonas stutzeri*
54	*Bacilli*	*Staphylococcus aureus*
55	*Actinobacteria*	*Acidovorax sp.*
56	*Gammaproteobacteria*	*Pseudoxanthomonas mexicana*
57	*Gammaproteobacteria*	*Pseudomonas stutzeri*
58	*Gammaproteobacteria*	*Pseudomonas stutzeri*
60	*Bacilli*	*Staphylococcus aureus*
61	*Gammaproteobacteria*	*Pseudoxanthomonas sp.*
62	*Gammaproteobacteria*	*Pseudomonas pseudoalcaligenes*
64	*Gammaproteobacteria*	*Pseudomonas stutzeri*
65	*Gammaproteobacteria*	*Pseudomonas stutzeri*

From the 65 isolates, 16 belonged to the class *Betaproteobacteria*. All of these

isolates were classified in the order *Burkholderiales* and had the most diversity at the

genus-level, including bacteria from the genera *Cupravidius, Ralstonia, Delftia,*

Achromobacter, Hydrogenophaga, Comamonas, Acidovorax, and *Pigmentiphaga*. Bacteria

from the order *Burkholderiales* are known to play a central role in bioremediation of

aromatic compounds such as benzene and toluene, especially members of the genera

Cupravidious and *Ralstonia* (Pérez-Pantoja et al., 2012). Thus, these heterotrophic bacteria

may occupy a special *niche* in the PBR setting, potentially catabolizing humic substances

or aromatic amino acids more rapidly than other members of the PBR microbial

communities (Weishaar et al., 2003).

Only two isolates were classified as *Alphaproteobacteria*, both associated with the

genus *Sphingomonas*. *Alphaproteobacteria* are common in freshwater systems, although

they do not account for a great proportion of the bacteria in these habitats. These bacteria

might also contribute to the biodegradation of humic substances (Newton et al., 2011).

Thus, the microbial ecology of the PBR appears to be similar to that of natural settings.

The isolated Gram-positive bacteria belonged to the classes *Actinobacteria* and *Bacilli* and

included species from the genera *Rhodococcus, Corynebacterium, Agromyces,*

Streptomyces, Bacillus, and *Staphylococcus*.

Because a high diversity of heterotrophic bacteria in association with

Cyanobacteria has been well documented, I expected to see similar diversity in the PBR

communities. All of the clades of bacteria isolated as a part of this study have been found

in association with natural cyanobacterial populations and commonly inhabit soil and

freshwater environments (Berg et al., 2009; Li et al., 2011). Thus, a wide variety of

heterotrophic bacteria probably possess the genes necessary to grow using EPS and SMP produced by *Synechocystis* as substrates.

Isolated heterotrophic bacteria demonstrate high specific growth rates and versatile metabolic capabilities

Figure 2.2 shows growth curves and associated SGR of the five representative isolates for growth on R2A medium. *B. cereus* and *P. stutzeri* showed the highest SGRs, while *C. amycolatum* and *R. pickettii* had the lowest. All of the isolates demonstrated SGRs that were in a range typical for heterotrophic bacteria (Kovárová-Kovar and Egli, 1998). The SGRs of all the tested heterotrophic bacteria were significantly higher than reported SGRs for *Synechocystis,* which have been reported in the range of 0.2-3.2/day (Kim et al., 2010a; Zavřel et al., 2015). Thus, provided with sufficient concentrations of substrate, the size of heterotrophic populations in PBRs could be significant compared to the size of the *Synechocystis* population. A substantial fraction of heterotrophic biomass would be detrimental to the performance of the PBR, since the goal is to produce lipid-rich cyanobacterial biomass.

Figure 2.3 shows the average well color development (AWCD) of the EcoPlate for each isolate. AWCD provides an indicator of when growth on the EcoPlates has ceased and also provides a comparison of the growth of the growth of the different isolates across the entire panel of substrates provided. The maximum AWCD for each isolate was achieved within 48-72 hours and remained relatively steady thereafter. In general, the isolates showed similar AWCD values indicating that they had similar growth kinetics. Thus, while *P. stutzeri* and *B. cereus* had the fastest growth rates under copiotrophic

conditions (R2A medium), their growth rates were more similar under more oligotrophic

conditions (EcoPlate minimal medium).
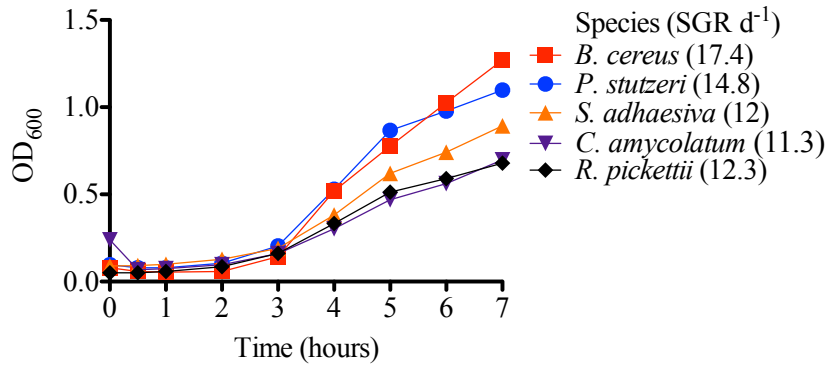
Figure 2.2 Growth of representative isolates on R2A medium.
The maximum measured SGR (1/day) of each isolate is noted in
the legend. All of the isolates demonstrated significantly higher
SGRs than the maximum reported SGR of *Synechocystis*
(3.2/day).
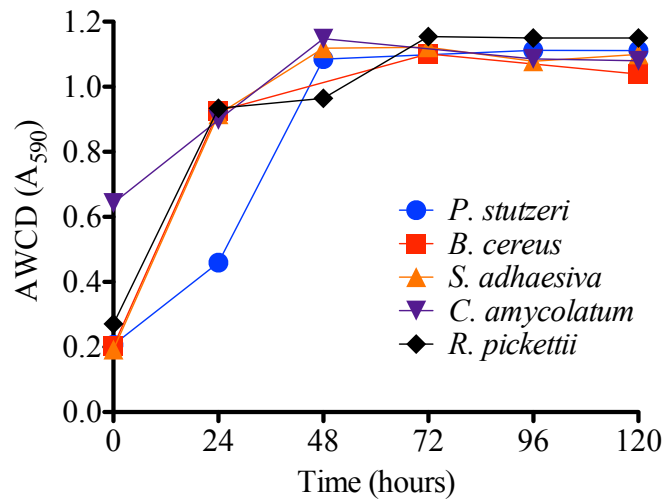
**Figure 2.3 AWCD of the EcoPlates for the five
representative isolates.** Maximum AWCD was
achieved in 48-72 hours

After the incubation period, all of the isolates tested showed A_{590} values above that of the negative control (water) for the 31 carbon substrates, meaning that the representative heterotrophic bacteria had the ability to metabolize a wide variety of carbon substrates. The measured A_{590} values for each carbon substrate after the 120-hour incubation are shown in **Figure 2.4**. In general, the A_{590} values for the carbohydrate substrates were lower than those of the organic nitrogen containing substrates. Thus, the heterotrophic bacteria in PBRs that grew on protein-derived substrates probably had faster growth kinetics than those that grow on EPS-derived substrates.

Figure 2.5 shows PCA of the EcoPlate data, which uses mathematical transformations of the EcoPlate data to explain the variability between the different isolates. Samples that cluster on PCA biplots are more similar, while those that do not cluster are less similar. For the EcoPlate analysis clustering on the PCA biplot was heavily positively correlated with A_{590} values. Thus, the substrates that showed the highest average A_{590} values are furthest to the right on PC1 while those that showed the lowest average A_{590} values are furthest to the left. The PCA indicates that the representative isolates tended to have similar metabolic capabilities, as shown by the arrows pointing to the right direction of PC1. The amino acids asparagine, arginine, and serine, as well as other compounds containing organic nitrogen (putrescine, phenylethylamine) showed the highest average A_{590} values. This is logical, as these compounds contain readily available carbon and nitrogen, and indicates that products resulting from the biodegradation of biomass may be the favored carbon source of heterotrophic bacteria in PBRs. This was especially true for *P. stutzeri*, which grouped most strongly with these substrates. The complex polymers, Tween 40 and Tween 80, were also heavily favored by all of the isolates.

33

No.	Substrate	Ps	Bc	Sa	Ca	Rp
1	L-Asparagine					
2	Tween 40					
3	Tween 80					
4	L-Arginine					
5	L-Serine					
6	Phenylethylamine					
7	D-Cellobiose					
8	Putrescine					
9	D-Mannitol					
10	D-Galacturonic Acid					
11	α-D-Lactose					
12	4-Hydroxybenzoic Acid					
13	Glycogen					
14	D-Malic Acid					
15	Itaconic Acid					
16	D-Xylose					
17	D,L-α-Glycerol Phosphate					
18	Glycyl-L-Glutamic Acid					
19	Phenylalanine					
20	α-Ketobutyric acid					
21	N-Acetyl-D-Glucosamine					
22	Glucose-1-phosphate					
23	L-Threonine					
24	i-Erythritol					
25	Pyruvic Acid Methyl Ester					
26	γ-Hydroxybutyric Acid					
27	β-Methyl-D Glucoside					
28	D-Glucosaminic Acid					
29	2-Hydroxybenzoic Acid					
30	α-cyclodextrin					
31	D-Galactonic Acid γ-Lactone					

A_{590}

2.2
1.8
1.1
0.7
0.5

Figure 2.4 Heatmap of EcoPlate results after 120-hour incubation period. The isolates tested were *P. stutzeri* (Ps), *B. cereus* (Bc), *S. adhaesiva* (Sa), *C. amycolatum* (Ca), and *R. pickettii* (Rp). All of the isolates showed greater A_{590} values for all of the carbon substrates than for the negative control, water (not shown).
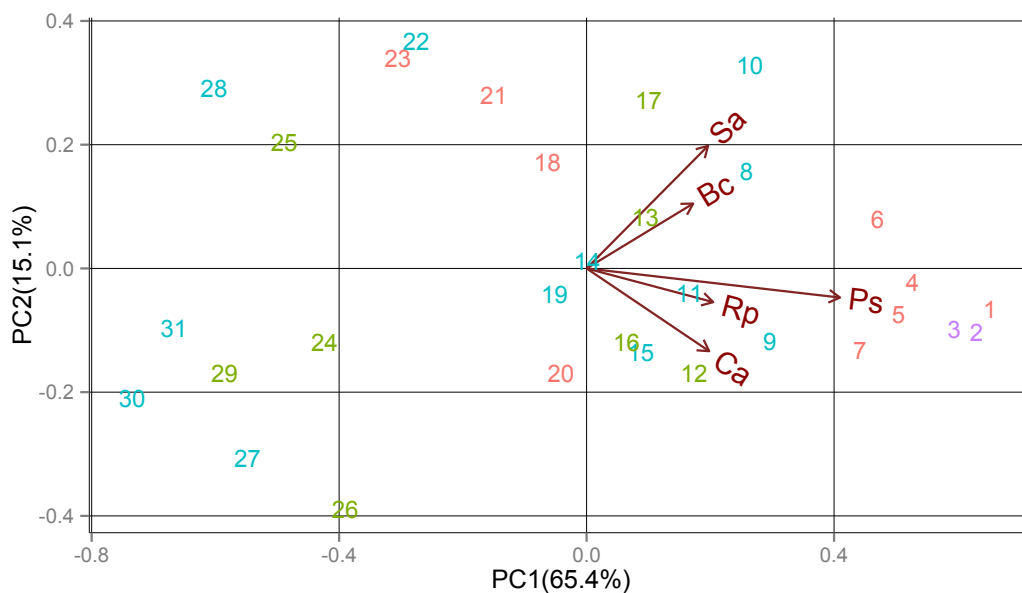
Figure 2.5 PCA of EcoPlate results. In general, the isolates showed similar metabolic profiles, indicated by clustering on PC1. However, each isolate showed preference for different types of substrates, indicated by clustering on PC2. *P. stutzeri* (Ps) heavily favored the amino acids and amine nitrogen-containing compounds (red) and Tween molecules (purple). *B. cereus* (Bc), *S. adhaesiva* (Sa), *C. amycolatum* (Ca), and *R. pickettii* (Rp) tended to show greater preference for carbohydrate (blue) and carboxylic acid (green) substrates. The substrates are numbered as shown in **Figure 2.4.**

The most favored carbohydrate compounds included cellobiose, galacturonic acid, mannitol, lactose, and glycerol phosphate. Cellobiose, galacturonic acid, and mannitoal can be derived from *Synechocystis* EPS (Panoff et al., 1988), and may be available in PBR settings. *B. cereus* and *S. adhaesiva* grouped more with mannitol and cellobiose while *C. amycolatum* and *R. pickettii* grouped more with galacturonic acid. Glycogen was metabolized to a similar extent by all of the isolates. *B. cereus, S. adhaesiva, C. amycolatum*, and *R. pickettii* grouped more with the carboxylic acid substrates, especially malic acid, itatonic acid, α-ketobutyric acid, and 4-hydoxybenzoic acid, than did *P. stutzeri*.

Even though each isolate showed slightly different substrate preferences, all could metabolize a wide variety of carbon substrates, and the most preferred substrates across all of the isolates were those that are most easily metabolized by the bacteria (e.g., amino acids and small carbohydrates). Thus, the heterotrophic bacteria in PBRs utilize simple substrates more rapidly than complex polymer substrates. Analysis of the metabolic potential of bacteria closely related to each of the tested isolates using the KEGG database (data not shown) demonstrated that, with few exceptions, the representative isolates showed a great amount of overlap in their metabolic pathways, especially in terms of their ability to metabolize carbohydrates and amino acids.

Heterotrophic bacteria enriched from PBRs are taxonomically similar to the isolated bacteria

I enriched consortia of heterotrophic bacteria from two different PBRs using acetate and glucose as organic substrates. **Figure 2.6** shows the distribution of the heterotrophic bacteria in the four enrichments based on high-throughput sequencing. The enrichments from PBR-1 (1-Ac and 1-Gluc) contained bacteria belonging to the orders *Rhizobiales*, *Burkholderiales*, *Cytophagales*, and *Actinomycetales*. *Sphingobacteriales* and *Opitutales* appeared in 1-Gluc, but not in 1-Ac. *Rhizobiales* are typically involved in nutrient cycling are often associated with plant roots (Newton et al., 2011; Rodríguez and Fraga, 1999). All of the isolated *Betaproteobacteria* were from the order *Burkholderiales*, and these were also the only *Betaproteobacteria* found in the enrichment cultures. Thus, *Burkholderiales* may be the major type of *Betaproteobacteria* that associate with *Synechocystis*-based PBRs. Bacteria from the order *Opitutales* have been shown to degrade polysaccharides

derived from algae (Sakai et al., 2003) and thus may have played a role in the degradation of *Synechocystis* EPS.
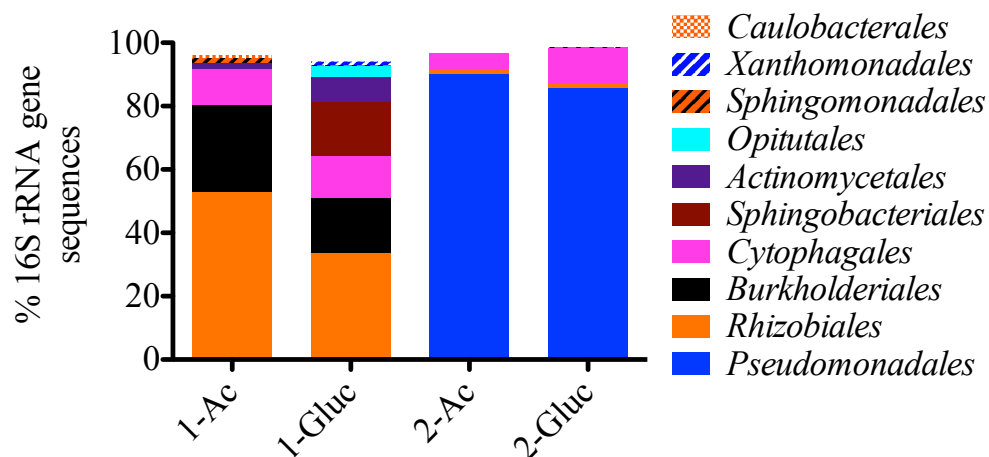
Figure 2.6 Consortia of heterotrophic bacteria enriched from two different PBRs using acetate or glucose as the sole carbon substrate at order-level classification. The enrichments from the first PBR (1-Ac, 1-Gluc) were dominated by bacteria mostly from the order *Rhizobiales* but also contained bacteria from *Burkholderiales*, and *Cytophagia*. *Pseudomonadales* heavily dominated the enrichments from the second PBR (2-Ac, 2-Gluc). In both cases, enrichment on glucose led to greater bacterial diversity than did enrichment on acetate.

Pseudomonadales dominated both enrichments from the second PBR (2-Ac and 2-Gluc) while a smaller proportion of *Cytophagales* was also present. This indicates that fast growing and metabolically diverse *Pseudomonas* spp. can outcompete other bacteria for carbon substrates in the PBR setting. *Cytophagales*, although not seen in the set of isolates, were the only bacteria to be identified in all of the enrichment cultures. *Cytophagales* are known degraders of polymers such as EPS and proteins (Koeck et al., 2014). Thus, many of the bacteria in the enrichment cultures appear to have the ability to grow on EPS, indicating that this and other polymers are probably important substrates for heterotrophic

bacteria in the PBR environment. This argument is strengthened by the EcoPlate data showing that all of the representative isolates could grow on complex polymers such as xylose, Tween 40, Tween 80, and glycogen.

In summary, I isolated and enriched heterotrophic bacteria from *Synechocystis*-based PBRs and showed that, in general, the same phylotypes of heterotrophic bacteria were present in the set of isolates and the enrichment cultures. *Gammaproteobacteria*, especially *Pseudomonas* spp., accounted for the majority of the isolated bacteria and also accounted for the majority of the bacteria in one of the enrichment cultures. Furthermore, a representative *P. stutzeri* showed a relatively higher growth rate compared to several of the other representative isolates. Isolates from each taxonomic class detected in the isolation study showed very diverse metabolic capabilities, although different isolates showed preferences for different types of substrates. Taken together, these data indicate that the ability to grow on a variety of carbon substrates is an important factor for the success of heterotrophic bacteria in *Synechocystis*-based PBRs, but that the simple substrates are the most favored. This, many different taxa of heterotrophic bacteria likely possess the genes necessary to grow in *Synechocystis*-based PBRs. In further studies, the heterotrophic bacteria isolated and enriched as a part of this study will be used to determine if they have differential effects on the growth of *Synechocystis*.

Chapter 3

Kinetic analysis and modeling of heterotrophic bacteria associated with photobioreactor

cultures of *Synechocystis* sp. PCC6803

3.1 Introduction

Mass culture of cyanobacterial biomass has attracted a great deal of attention as a

possible route towards production of renewable biofuels (Ducat et al., 2011; Kim et al.,

2010b) and other valuable bioproducts. Large-scale cultivation of *Cyanobacteria* presents

several key engineering challenges. One such challenge is, as in other biotechnologies,

management of microbial interactions in the system (Rittmann et al., 2006). Heterotrophic

bacteria are almost always associated with natural populations of cyanobacteria and, as

demonstrated in the literature and in the previous chapter, have also been shown to

associate with cyanobacteria in engineered settings, such as photobioreactor (PBR) cultures

(Berg et al., 2009). These heterotrophic bacteria could have positive or negative impacts in

the PBR. For example, heterotrophic bacteria can recycle organic carbon as carbon dioxide

and can reduce oxygen saturation in the PBR (Mouget et al., 1995). Heterotrophic bacteria

also can recycle macronutrients and increase the availability of micronutrients (Buchan et

al., 2014; Keshtacher-Liebson et al., 1995). However, heterotrophic bacteria may compete

with cyanobacteria for available nutrients in PBR settings. Furthermore, heterotrophic

bacteria can consume valuable organic products excreted by the *Cyanobacteria*, such as

fatty acids (Liu et al., 2011b). Thus, it is important to develop an understanding of the

heterotrophic bacteria that associate with PBR cultures.

As demonstrated in Chapter 2, taxonomically diverse and metabolically versatile

heterotrophic bacteria can be associated with PBR cultures of *Synechocystis*. In PBRs,

heterotrophic bacteria grow by oxidizing the organic matter produced by *Synechocystis*.

One major pool of these compounds includes soluble microbial products (SMP). SMP can be derived from several sources. Utilization-associated products (UAP) are produced as a direct result of electron donor oxidation, while biomass-associated products (BAP) are produced as a result of biomass decay or hydrolysis of extracellular polymeric substances (EPS) (Laspidou and Rittmann, 2002). *Synechocystis* EPS is composed of proteins and polymeric carbohydrates that contain up to 70% glucose monomers along with other monosaccharides (Panoff et al., 1988) that can be decorated with methyl or acetyl groups (Schmidt et al., 1980). Thus, compounds such as glucose, acetate, and free or combined amino acids could represent the most labile types of SMP available to the heterotrophic bacteria in the PBR.

Here, I examine the growth kinetics of heterotrophic bacteria associated with PBR cultures of *Synechocystis* on several model compounds, including SMP derived from *Synechocystis* PBRs (*S*-SMP) and compare the kinetic properties of a single pure strain of *P. stutzeri* to a mixed consortium of heterotrophic bacteria (*ENR1*). I then use simple mathematical models to explore the behavior of the heterotrophic bacteria in PBR settings. I demonstrate that the heterotrophic bacteria associated with *Synechocystis* PBRs display oligotrophic kinetic properties in that they have low Monod substrate half-maximum-rate concentrations (K_m) for labile substrates and low maximum specific growth rates ($\hat{\mu}$) (Kovárová-Kovar and Egli, 1998), especially when growing on *S*-SMP. The model results suggest that even relatively recalcitrant *S*-SMP can support the growth of heterotrophic bacteria at hydraulic retention times (HRTs) typical of *Synechocystis* PBRs (3-5 days) (Kim et al., 2010b), while the more labile substrates can support heterotrophic growth at

HRTs well below this range. This indicates that exclusion of heterotrophic bacteria from *Synechocystis* PBRs may be difficult with current PBR-operating strategies.

3.2 Materials and Methods

Bacterial strains, media, and substrates

The laboratory of Dr. Willem Vermaas (School of Life Sciences, Arizona State University) provided stock cultures of wild-type *Synechocystis* sp. PCC6803. *Pseudomonas stutzeri* strain PBR_B2 (GenBank Accession KF539914, hereafter referred to as *B2*) and PBR Enrichment Culture 1 – Acetate (BioSample Accession SAMN03165108, hereafter referred to as *ENR1*) came from our laboratory's strain collection. *B2* and *ENR1* were derived from *Synechocystis* PBR cultures as described in the previous chapter. I conducted all experiments with BG-11 medium (Rippka et al., 1979) to which I added simple organic substrates (1-100 mM sodium acetate (Sigma-Aldrich), 1-500 mg/L D-glucose (Sigma-Aldrich), or 1-50 mM sodium laurate (Fluka)), or *S*-SMP harvested from a PBR.

SMP harvest

To harvest the *S*-SMP, I removed cells from 1 L of *Synechocystis* culture by centrifuging them at 4,000 RPM for 30 minutes at 4°C. I then harvested the supernatant, which contained SMP, and removed residual particles by passing it across a membrane filter with a nominal pore size of 0.45µm (Whatman). It is critical to note that the *S*-SMP used in these experiments was harvested from PBRs in which heterotrophic bacteria were

41

present. Thus, the *S*-SMP used here represents the relatively recalcitrant substrates

available to heterotrophic bacteria in *Synechocystis*-based PBRs.

Experimental setup and derivation of kinetic constants

To determine the growth kinetic constants of maximum specific growth rate on

compound m ($\hat{\mu}_m$), the Monod half-maximum-rate concentration for substrate *m* (K_m), and

yield for growth on each substrate (*Y*), I conducted a series of batch growth tests using the

different bacterial cultures. I grew the bacteria on various concentrations of each substrate

and monitored the growth of the bacteria and consumption of the substrate.

For each substrate, I calculated the observed specific growth rate (μ_{obs}) using **Eq.**

1, in which X_a is the measured concentration of biomass as chemical oxygen demand (mg

COD/L), and t is time in days. I then calculated the specific growth rate due to synthesis

(μ_{syn}) using **Eq. 2**, wherein *b* is the endogenous-decay coefficient having a value of *b* =

0.1 d^{-1}, which is a typical value for aerobic heterotrophs (Rittmann and McCarty, 2001). I

then plotted the μ_{syn} values versus substrate concentration (*S*) measured in mg COD/L and

determined the values of $\hat{\mu}$ and K_m by fitting the data points to the Monod Equation (**Eq. 3**)

using non-linear regression analysis. I then calculated *Y* using **Eq. 4.**

Eq. 1) $\mu_{obs} = \dfrac{1}{X_a} * \dfrac{dX_a}{dt}$

Eq. 2) $\mu_{syn} = \mu_{obs} + b$

Eq. 3) $\mu_{syn} = \hat{\mu}_m \dfrac{S_m}{K_m + S_m}$

Eq. 4) $Y = \dfrac{\mu_{syn} * X_a}{dS/dt}$

$[\theta_x{}^{min}]_{lim}$ is the absolute minimum HRT and the maximum μ_{syn} value necessary to have steady-state biomass in a chemostat bioreactor. Thus, any HRT lower than $[\theta_x{}^{min}]_{lim}$ will cause washout of the bacteria. I calculated the value of $[\theta_x{}^{min}]_{lim}$ using **Eq. 5.**, in which $\hat{q}$ is equal to $\hat{\mu}_m$ divided by Y. S_{min} represents the minimum input substrate concentration required to sustain steady-state biomass. Thus, if S is less than S_{min}, the μ_{syn} value is negative and biomass cannot accumulate. I calculated S_{min} using **Eq. 6**. All calculations were carried out in Microsoft Excel and GraphPad Prism. All equations were adapted from Rittmann and McCarty, (2001).

Eq. 5) $[\theta_x^{min}]_{lim} = \left(Y\hat{q}-b\right)^{-1}$

Eq. 6) $S_{min} = K\dfrac{b}{Y\hat{q}-b}$

Measurement of microbial biomass

I measured biomass by directly measuring optical density at a wavelength of 600 nm (OD_{600}) using a Cary-50-Bio UV-Visible spectrophotometer and converting that value to the dry biomass Iight (DW) using a calibration curve determined for each bacterial culture. For the calibration, I determined DW using the total suspended solids (Method 2540D) in *Standard Methods* (American Public Health Association, American Water Works Association, 1998). I then converted dry biomass to chemical oxygen demand (COD) using a conversion factor of 1.29 mg COD/mg dry biomass and that biomass was 53% carbon based on the empirical formula $C_5H_7O_2N$ (Rittmann and McCarty, 2001).

There were two instances in which there was interference with OD_{600} measurements. The first was when sodium laurate, which precipitated in BG-11 medium at concentrations greater than ~20 mg/L, was used as an electron donor and carbon source. The second was when S-SMP was used as an electron donor and carbon source, In this case, biomass concentrations often were too low to be measured reliably by OD_{600}. In these two instances, I estimated the biomass by measuring cellular protein. To do this, I centrifuged a 1-mL sample (13K RPM, 3 min) to pellet the cells, removed the supernatant, resuspended the cell pellet in 1 mL deionized water, and stored these samples at -20˚C for at least 24 hours. Later, I thawed the cell pellets at room temperature and quantified protein in the samples using a QuantiPro BCA Kit (Qiagen) according to the manufacturer's protocol. Finally, I converted from protein to biomass by assuming that the protein comprised 55% of total dry weight biomass (Rittmann and McCarty, 2001; Ziv-El et al., 2012).

Analytical techniques

To quantify acetate, I used an HPLC (Waters) equipped with an Aminex HPX-87H column (Bio-Rad) and a photodiode array detector (PDA) (Waters). The operational parameters were 10 µL injection volume, flow rate of 0.6 mL/min for 35 minutes, column temperature of 50˚C, and PDA wavelength set to 210 nm. I used sodium acetate (Sigma Aldrich) as a reference compound and converted acetate concentration to COD using a conversion factor of 1.07 mg COD/mg acetate. To quantify laurate, I used a GC-FID (Shimadzu) equipped with an Rxi-1HT column (Restek). The operational parameters were 4-µL injection volume, linear velocity of 60.3 cm/sec, split ratio of 2, injector temperature

of 240˚C, the column temperature starting at 110˚C and rising at a rate of 20˚C/min to 240˚C and then at a rate of 50˚C/min to 320˚C, detector temperature of 340˚C, makeup gas of H_2 supplied at a rate of 10 mL/min. The carrier gas was H_2 and was supplied at a rate of 32 mL/min; and the air flow was 400 mL/min. I used dodecanoic acid (Sigma Aldrich) as a reference standard and converted the laurate concentration to COD using a conversion factor of 2.67 mg COD/mg laurate. To quantify glucose, I used a Dionex ICS3000 equipped with a CarboPac PA10 and an electrochemical detector (Dionex). The operational parameters were 20 μL injection volume, flow rate of 1 mL/min with a gradient elution which began at 90% H_2O and 10% 200 mM NaOH (Thermo Fisher) for 15 minutes, then 100% 200 mM NaOH for 15 minutes, and finally 90% H_2O and 10% 200 mM NaOH for 15 minutes. The column temperature was 30˚C. I used high-purity D-glucose (Sigma Aldrich) as a reference standard and converted the glucose concentration to COD using a conversion factor of 1.07 mg COD/mg glucose. I measured total organic carbon (TOC) and inorganic carbon (C_i) using a TOC-V Analyzer (Shimadzu) using potassium hydrogen phthalate (Sigma Aldrich) as a reference standard. Dissolved organic carbon (DOC) was equal to the difference of TOC and C_i. To convert from mg DOC to mg COD, I assumed that the DOC could be represented as glucose and used a conversion factor of 2.67 mg COD/mg C.

Modeling approach

I used a chemostat model to examine and compare the growth of *B2* and *ENR1* at different HRTs and with different substrates in steady-state conditions (Rittmann and McCarty, 2001). For growth on a single substrate, I calculated X_a using **Eq. 7** and *S* using

Eq. 8, solving both equations with the kinetic parameters I determined for the different

substrates tested.

Eq.7) $X_a = Y(S^0 - S)\frac{1}{1+b\theta}$

Eq.8) $S = K_m \dfrac{1+b\theta}{Y\hat{q}\theta - (1+b\theta)}$

It is likely that very labile substrates such as fatty acids and monosaccharides are

present in a true PBR setting, even if their presence is only transient prior to their rapid

utilization by heterotrophic bacteria. Thus, I modeled growth of *ENR1* when other, more

labile, substrates were available in addition to *S*-SMP. To achieve this, I first derived the

equations for the steady-state mass balances for X_a growing on *S*-SMP with one (**Eq. 9**)

additional substrate, wherein *m* is the substrate that is more labile than *S*-SMP (acetate,

laurate, or glucose). In this equation, I included a switch function $\left(\frac{K_m}{K_m+S_m}\right)$ to control the

utilization of *S*-SMP. Thus, *S*-SMP is used only when the concentration of more labile

substrate is low.

Eq.9) $0 = \left[Y_{SMP}\dfrac{\hat{q}_{SMP}*S_{SMP}}{K_{SMP}+S_{SMP}}X_a\theta*\left(\dfrac{K_m}{K_m+S_m}\right) \right] + Y_m\dfrac{\hat{q}_m*S_m}{K_m+S_m}X_a\theta - bX_a\theta - X_a$

To calculate steady-state substrate concentrations for the labile substrates, I used

Eq. 10, the steady-state mass balance on substrate *m*. The steady-state mass balance for

S_{SMP} in the presence of one additional substrate is **Eq. 11**.

Eq. 10) $0 = -\dfrac{\hat{q}_m*S_m}{K_m+S_m}X_a\theta + (S^0 - S)$

Eq. 11) $0 = \left[-\dfrac{\hat{q}_{SMP}*S_{SMP}}{K_{SMP}+S_{SMP}}X_a\theta*\left(\dfrac{K_m}{K_m+S_m}\right) \right] + (S^0 - S)$

I simultaneously solved the equations for steady-state values of X_a, S_{SMP}, and S_m using the Solver function of Microsoft Excel.

3.3 Results and Discussion

Heterotrophic bacteria from PBRs demonstrate rapid growth on labile organic compounds compared to *S*-SMP

Table 3.1 shows a comparison of the empirically derived growth kinetic parameters for *B2* and *ENR1* when acetate, laurate, glucose, or *S*-SMP was provided as single substrates. In general, *B2* and *ENR1* displayed similar $\hat{\mu}$ values for growth on acetate, laurate, and glucose as sole carbon substrates, although those for *B2* were typically slightly higher. The $\hat{\mu}$ values for *B2* and *ENR1* were between 5.7 and 8.8/d, which is lower than those of some *E. coli* strains that demonstrated $\hat{\mu}$ values up to 29/d when grown on glucose as a sole carbon source (Kovárová-Kovar and Egli, 1998). However, they were higher than reported growth rates of some heterotrophic bacteria isolated from oligotrophic environments, which demonstrated specific growth rates around 2/d when grown on a low nutrient medium (Cho and Giovannoni, 2004). *B2* and *ENR1* had K_m values for glucose similar to characterized strains of *E. coli* (Kovárová-Kovar and Egli, 1998). The K_m value of *ENR1* for growth on glucose was much lower than that of *B2*, while *B2* had lower K_m values for growth on acetate and laurate. In general, the measured K_m values were typical for heterotrophic bacteria in general, but tended to be higher than those of heterotrophic bacteria grown in truly oligotrophic conditions (Button, 1985).   Representative growth curves and Monod fits are presented in **Appendix A**.

Compared to growth on the labile substrates, *ENR1* demonstrated a much lower $\hat{\mu}$ value and a much higher K_m value when utilizing S-SMP.   Thus, S-SMP was comparatively recalcitrant. *B2* did not show significant growth or substrate consumption when *S*-SMP was provided as a sole carbon substrate. One reason for this might be that *B2* does not possess the enzymes necessary to degrade the polymers present in *S*-SMP, while the bacteria in *ENR1* do. This is often the case when comparing single bacterial strains to mixed consortia of bacteria (Sutherland, 1999).

Table 3.1 Kinetic parameters for growth of *B2* and *ENR1* on acetate, laurate, glucose, and *S*-SMP.

Constant	Units	Acetate/Laurate		Glucose		SMP
		B2	*ENR1*	*B2*	*ENR1*	*ENR1*
Y	mg COD/mg COD	0.51/0.5	0.37/0.52	0.53	0.51	0.3
K_m	mg COD/L	2.4/8.8	18.8/34.5	44.1	0.17	187.3
$\hat{\mu}$	1/d	6.0/8.8	7.2/5.7	7.3	6.5	1.7
$\hat{q}$	mg COD/mg COD*d	11.8/17.6	19.5/11.0	13.9	12.7	5.7
S_{min}	mg COD/L	0.04/0.1	0.7/0.62	0.62	0.003	11.7
$[\theta_x^{min}]_{lim}$	d	0.17/0.11	0.14/0.18	0.14	0.16	0.63
K_{Pi}	mg P/L	0.045	0.18			

Because the measured $\hat{\mu}$ and K_m values tended to be higher than reported values for bacteria in oligotrophic environments, it is reasonable to conclude that PBR environments have characteristics similar to eutrophic lakes. This assessment is reasonable, as some eutrophic lakes may only have DOC concentrations in the range of 1-10 mg C L^{-1} (Biddanda et al., 2001; Imai et al., 2001), which is considerably lower than DOC concentrations of >1 g C L^{-1} measured in photobioreactor cultures (Lakaniemi et al., 2012b). Furthermore, nutrient concentrations in BG-11 medium are significantly higher

than those in eutrophic lakes (Huang et al., 2003; Rippka et al., 1979), indicating that PBRs will have more primary productivity and, thus, more release of DOC than their natural counterparts.

However, the K_{Pi} values measured for *B2* and *ENR1* when acetate was provided in excess indicate that both can grow at phosphate concentrations <1 mg P/L and can drive P concentrations very low. These values are in the range of those reported for both heterotrophic bacteria and *Cyanobacteria* (~0.031-0.31 mg P/L) (Button, 1985), indicating that competition between *Synechocystis* and heterotrophic for phosphate may be an important consideration in PBR operations. Thus, the heterotrophic bacteria in *Synechocystis*-based PBRs demonstrate copiotrophic growth kinetics, but have the ability to grow even at very low concentrations of DOC and phosphate, suggesting that they can also display oligotrophic properties.

The calculated $[\theta_x^{min}]_{lim}$ values for growth on the labile substrates range from 0.14-0.38 d. PBRs would have to achieve a minimum *Synechocystis* specific growth rate of 2.7/d in order to wash out the heterotrophic bacteria. The $[\theta_x^{min}]_{lim}$ for *S*-SMP was 0.63 d, requiring a *Synechocystis* specific growth rate of at least 1.6/d. These values are significantly higher than reported growth rates of *Synechocystis* in continuously operated PBRs (Kim et al., 2010a; Kim et al., 2010b; Sheng et al., 2011a). This means that, once introduced, heterotrophic bacteria probably will not be washed out of the PBR, provided that sufficient quantities of carbon substrates are available.

The S_{min} values for the labile substrates ranged from 0.003 to 0.7 mg COD/L, and it was 11.7 mg COD/L for *S*-SMP. To limit the growth of heterotrophic bacteria, the carbon substrates, especially the most labile ones, must be effectively removed from the culture

49

medium. However, in continuously operated PBRs, *Synechocystis* biomass concentrations can reach concentrations of up to 1200 mg/L. Thus, if *Synechocystis* biomass itself is considered to be a potential substrate for heterotrophic bacteria, then sufficient concentrations of substrate will always be available to heterotrophic bacteria.

Figure 3.1 shows the average result of two batch growth experiments of *ENR1* using *S*-SMP as a carbon substrate. The average net biomass production was 47 mg COD/L, which corresponds to 36.4 mg biomass dry weight/L. Thus, the biomass contained about 20 mg C/L. The *S*-SMP concentration decreased rapidly from 60 to 23 mg C/L and never dropped below 18 mg C/L, indicating that a certain fraction of *S*-SMP was resistant to biodegradation by the heterotrophic bacteria. Biodegradation of *S*-SMP was linked to an increase in C_i by 23 mg C/L, reaching a maximum of 40 mg C/L.
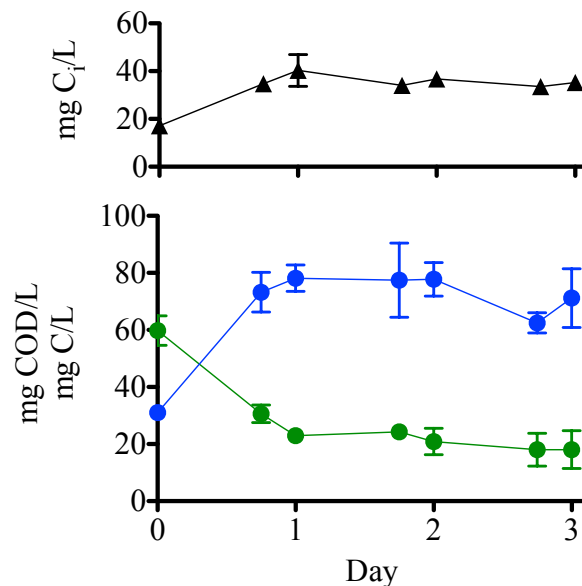
Figure 3.1 Growth of *ENR1* on *S*-SMP. *ENR1* biomass (blue) grew by utilizing *S*-SMP (green). The growth of *ENR1* was tied to an increase in C_i (black).

Figure 3.2 shows a mass balance for the carbon in the system along with the pH. The estimated total carbon was calculated as the sum of the measured DOC, C_i, and the calculated C in biomass at the beginning of the experiment. Throughout the experiment, the sum of measured DOC, C_i, and calculated C in biomass was close to the estimated total C. This demonstrated that all the organic C that was consumed was conserved within the system. Some of the organic carbon was returned as C_i, the carbon source for *Synechocystis*. The decrease in pH from 10.3 to 8.5 indicates that the partitioning of C_i was driven from mostly carbonate to mostly bicarbonate. This is also beneficial for *Synechocystis*-based PBRs, as bicarbonate is a form of C_i available to *Synechocystis* while carbonate is not (Kim et al., 2010a).
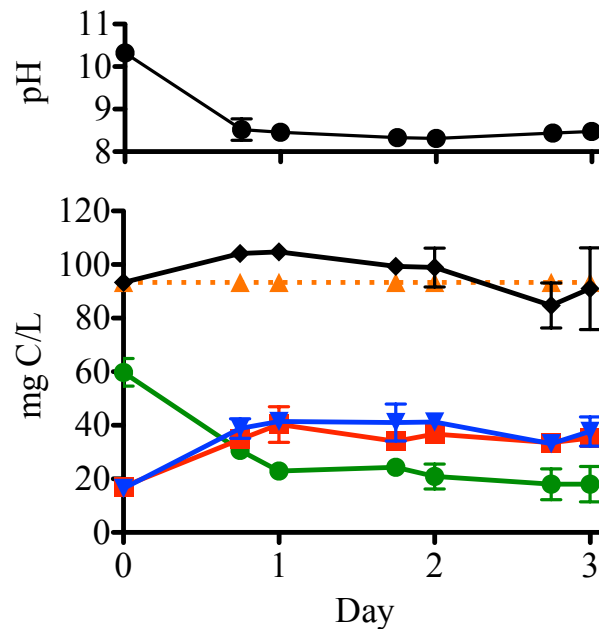
Figure 3.2 Carbon balance for growth of *ENR1* on *S*-SMP. The top panel shows pH. The bottom panel shows DOC (green), C_i (red), C in biomass (blue), estimated total C (orange), and sum of DOC, C_i, and C in biomass (black).

Modeling analysis reveals trends of heterotrophic growth in continuous *Synechocystis*-based PBRs

I used the kinetic parameters in **Table 3.1** to predict the concentration of heterotrophic biomass in continuous *Synechocystis*-based PBRs. I assumed a constant *Synechocystis* biomass concentration of 400 mg COD/L and that *Synechocystis* diverted 20% of fixed COD to SMP, including labile and recalcitrant substances; thus, the influent concentration of organic substrate was 100 mg COD/L, or 20% of the total of 500 mg COD/L. **Figure 3.3** shows the modeled X_a for growth of *B2* and *ENR1* on 100 mg COD/L of acetate, laurate, glucose, or *S*-SMP as a sole carbon substrate and for HRTs from 0.25 to 10 days. Because most of the $[\theta_x{}^{min}]_{lim}$ values were around 0.2 days, I decided to only model the system at HRTs longer than this. *B2* displayed similar biomass concentrations for growth on the three labile substrates. *ENR1* demonstrated the most biomass production with glucose and laurate as a sole carbon sources, but slightly less with acetate.

Figure 3.4 shows growth of *ENR1* at various input *S*-SMP concentrations for HRTs up to 10 days (*B2* did not grow on S-SMP.) Lower input concentration of *S*-SMP caused E*NR1* to washout at a larger HRTs. For example, 100 mg COD/L input showed washout at HRTs < 2 days, while the washout HRT was < 1 day for 500 mg COD/L. Achieving washout for and HRTs of 5 days would require that the input *S*-SMP concentration be lower than 40 mg COD/L. Thus, achieving a low input of *S*-SMP can be a strategy to minimize heterotrophic growth in *Synechocystis*-based PBRs.
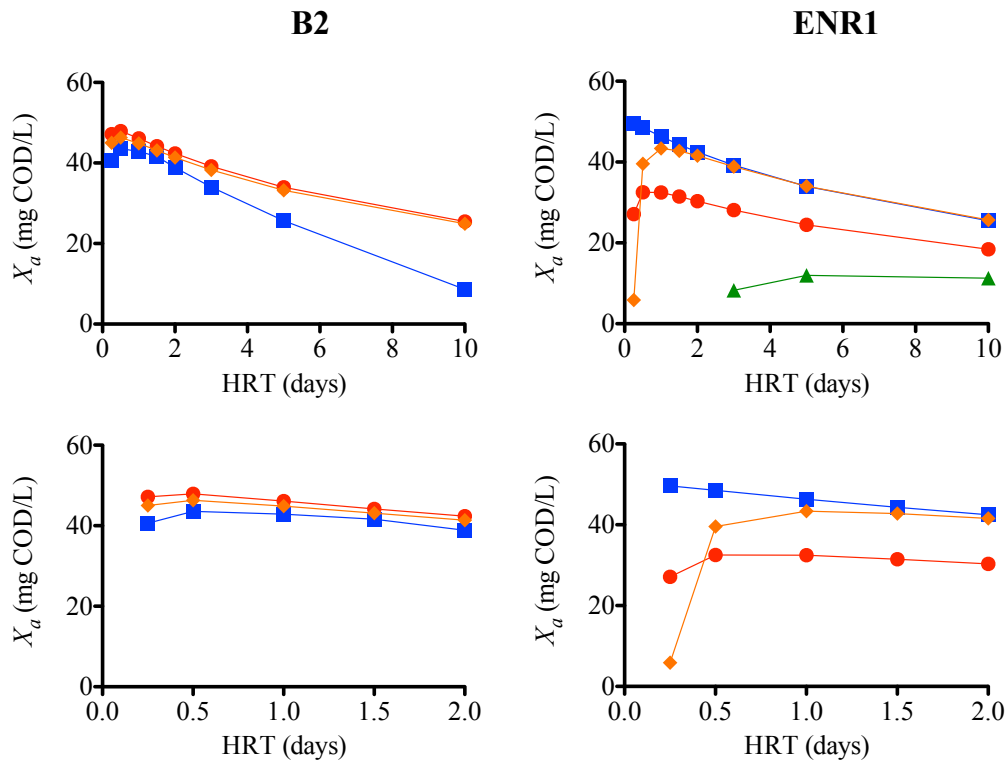
Figure 3.3 Modeled X_a values for *B2* and *ENR1* for growth on acetate (red), laurate (orange), glucose (blue), or *S*-SMP (green). The top panels show the modeled values for HRTs up to 10 days, while the bottom panels expand the horizontal scale for the same data for HRTs up to 2 days. *B2* showed similar trends for all the labile substrates, while *ENR1* showed greater biomass production on glucose than on the other substrates.
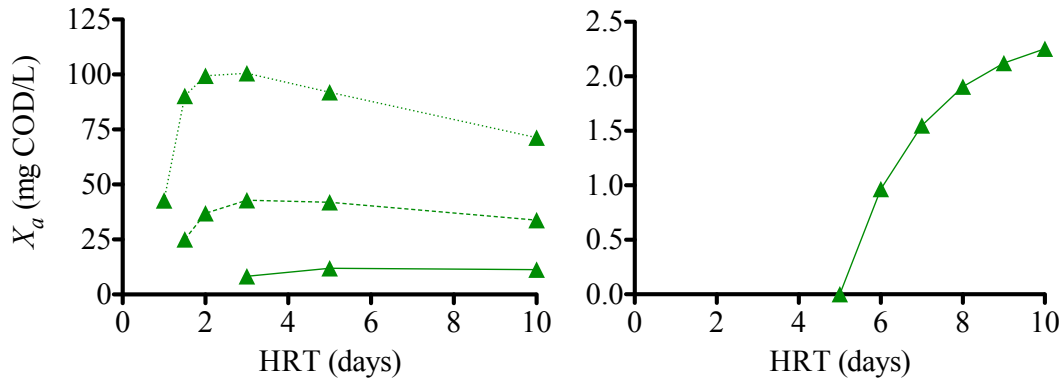
Figure 3.4 Modeled X_a values for growth of *ENR1* on different input concentrations of *S*-SMP. In the panel on the left, the values used were: 100 mg COD/L (solid line), 250 mg COD/L (dashed line), and 500 mg COD/L (dotted line). As the input *S*-SMP concentrations increased, the HRT required for washout decreased. The panel on the right shows the modeled X_a values for a system with an input *S*-SMP concentration of 40 mg COD/L. In this instance, washout occurred at all HRTs<5 days.

Figure 3.5 shows the modeled X_a values for growth of *ENR1* on equal-COD mixtures of *S*-SMP with acetate, *S*-SMP with glucose, or *S*-SMP with laurate; the total substrate loading was set at an initial concentration of 100 mg COD/L (50 mg COD/L of each substrate). The glucose and *S*-SMP mixture showed the most biomass at HRTs <3 days. At HRTs >3 days, the laurate and *S*-SMP mixture showed similar biomass concentrations to the glucose and *S*-SMP mixture. The acetate and *S*-SMP mixture showed the least growth at all HRTs, because *ENR1* had a lower *Y* value for growth on acetate compared to glucose and laurate.

54
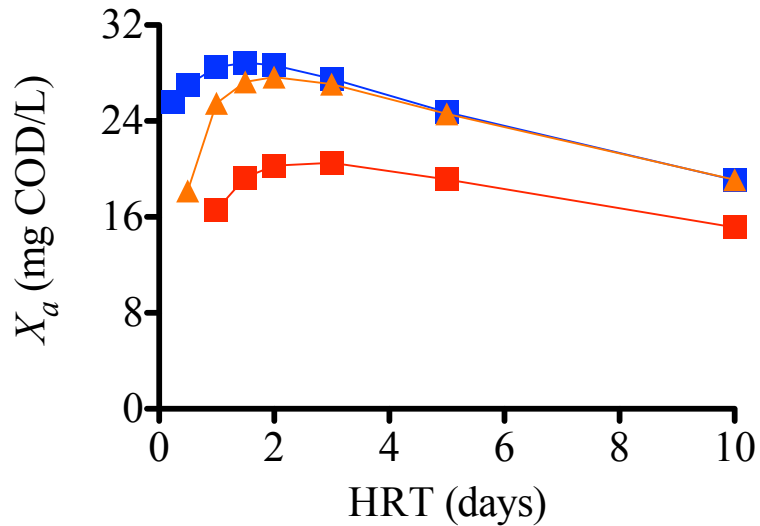
Figure 3.5 Modeled X_a for growth of *ENR1* on *S*-SMP with acetate (red), glucose (blue), or laurate (orange) with a total COD loading of 100 mg COD/L. The mixture of glucose and *S*-SMP showed the most growth at all HRTs while acetate showed the least.

Figure 3.6 shows modeled X_a values for mixtures of glucose and *S*-SMP in which the two substrates were added in different ratios, but the total substrate loading was always 100 mg COD/L. As expected, the scenarios with higher initial ratios of glucose showed overall higher X_a values. However, as the ratio of S-SMP increased, the highest X_a values were achieved at longer HRTs. This demonstrates that the presence of labile substrates drives growth of heterotrophic bacteria at low HRTs and that that excluding labile substrates is a key if the goal is to minimize heterotrophic bacteria from *Synechocystis*-based PBRs.
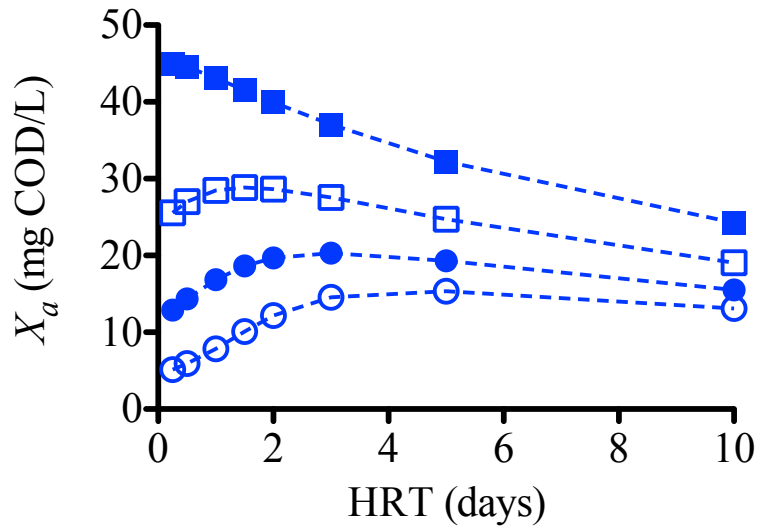
Figure 3.6 Modeled X_a for growth of *ENR1* on different mixtures of *S*-SMP and glucose. In all cases, the total substrate loading was 100 mg COD/L. The ratios (Glucose:S-SMP) used were 90:10 (closed squares), 50:50 (open squares), 25:75 (closed circles), and 10:90 (open circles). The highest biomass concentrations were achieved with higher glucose loadings. As the ratio of *S*-SMP increased, the highest biomass concentrations were achieved at longer HRTs.

However, this may not be achievable if fatty acids and monosaccharides are derived directly from *Synechocystis* biomass by cell lysis or through the hydrolysis of EPS. This presents an important challenge in systems where the goal is to recover excreted biomolecules, such as laurate (Liu et al., 2011b). To examine this, I modeled a system with 100 mg COD/L input laurate concentration with no additional substrate, 10 mg COD/L *S*-SMP, or 10 mg COD/L glucose. **Figure 3.7** shows that at an HRT of 0.25 days, the addition of 10 mg COD/L *S*-SMP did not greatly affect the effluent laurate concentration, while addition of 10 mg COD/L glucose reduced the effluent laurate concentration by nearly 50%. At HRTs >1 day, all effluent laurate concentrations were below 8.25 mg

COD/L, which corresponds to 3.1 mg laurate/L. Thus, if the goal of the PBR is to recover

laurate, then the PBR must be operated at HRTs < 0.25 days, which corresponds to a

Synechocystis growth rate of at least 4/day. This growth rate is much higher than typically

reported *Synechocystis* growth rates in PBR operations, which range from 0.22-3.4/day

(Kim et al., 2010a; Zavřel et al., 2015).
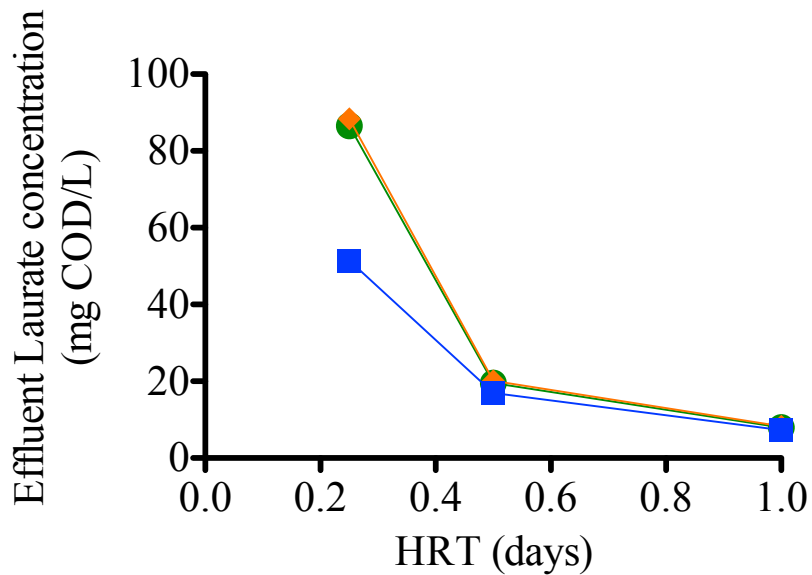
Figure 3.7 Modeled effluent laurate concentrations for a chemostat culture of *ENR1*. The modeled input substrate concentration was 100 mg COD/L laurate (orange) with an addition of 10 mg COD/L *S*-SMP (green), or 10 mg COD/L glucose (blue). At HRTs longer than 1 day, the effluent laurate concentration was always below 10 mg COD/L.

Three routes may be useful to suppress heterotrophic bacteria in *Synechocystis*-

based PBRs. The first is to prevent the introduction of any heterotrophic bacteria to the

system. At very large scales, however, this represents a significant practical challenge.

The second is to rapidly and thoroughly remove the available labile substrates while

driving the concentration of *S*-SMP as low as possible in the PBR. SMP can be reliably removed from PBRs by contacting the culture medium with granular activated carbon, which will adsorb the SMP (Gur-Reznik et al., 2008). However, active and inactive *Synechocystis* biomass can act as a substrate for heterotrophic growth. The third option is to operate the PBR in a way that achieves the highest μ value for *Synechocystis* while minimizing the concentration of *Synechocystis* biomass in the PBR. This will allow the PBR to be operated at low HRTs, which will drive the system more towards washout of the heterotrophic bacteria by maintaining low concentrations of both labile and recalcitrant *Synechocystis*-derived substrates in the PBR. If the goal is to operate *Synechocystis*-based PBRs at HRTs shorter than 5 days, the *S*-SMP concentration should be maintained below 40 mg COD/L, meaning that the *Synechocystis* biomass concentration should be maintained below 200 mg COD/L.

Here, I demonstrated that heterotrophic bacteria isolated or enriched from *Synechocystis*-based PBRs could grow on a variety of simple carbon substrates, such as short and long-chain fatty acids and monosaccharides. In general, the pure isolated strain of *P. stutzeri* (*B2*) and the enriched culture (*ENR1*) displayed similar kinetic properties for growth on the simple substrates. In contrast, *ENR1* could grow on more recalcitrant carbon substrates harvested directly from *Synechocystis*-based PBRs (*S*-SMP). I used empirically determined kinetic parameters to predict the concentration of heterotrophic biomass in continuous *Synechocystis*-based PBRs and demonstrated that heterotrophic bacteria can grow at HRTs well below the typical operating range of *Synechocystis*-based PBRs (3-5 days) (Kim et al., 2010a).

Chapter 4

Removal of *Synechocystis* sp. PCC6803 16S rRNA genes does not significantly improve

resolution of heterotrophic bacteria in 16S rRNA-based microbial community analysis

4.1 Introduction

The work in Chapters 2 and 3 focused on developing an understanding of the

heterotrophic bacteria associated with *Synechocystis*-based PBRs using culture dependent

methods. However, culture independent methods, especially 16S rRNA gene sequencing,

offer a greater ability to assay the structure of microbial communities. The work in this

chapter presents the first step towards developing 16S rRNA gene sequencing techniques to

analyze the microbial diversity in *Synechocystis*-based PBRs.

Cyanobacteria are a diverse group of photoautotrophic microorganisms that can be

used to produce renewable fuels and replace traditional fossil fuel resources (Rittmann,

2008). The cyanobacterium *Synechocystis* provides an excellent platform for biofuel

production due to its fast growth rate and tolerance of a wide range of environmental

factors (Sheng et al., 2011a). Additionally, *Synechocystis* is naturally transformable and

has a fully sequenced genome, opening the door for large-scale production of many

valuable products (Ducat et al., 2011; Vermaas, 1998).

Closed photobioreactors (PBRs) are more productive per unit area, offer greater

protection from environmental factors, and provide increased control over culturing

conditions when compared to traditional open ponds or raceways (Chisti, 2007). However,

maintaining axenic culturing conditions in closed PBRs can be difficult because

sterilization of the culture vessel and media is neither economically feasible or technically

practical at large scale (Lakaniemi et al., 2012b). In natural settings, diverse communities

59

of heterotrophic bacteria associate with *Cyanobacteria* (Eiler and Bertilsson, 2004; Hube et al., 2009; Li et al., 2011), and heterotrophs have been found in PBR cultures as well (Carney et al., 2014; Lakaniemi et al., 2012a; Lakaniemi et al., 2012b). Heterotroph-*Cyanobacteria* interactions are ubiquitous, because heterotrophic bacteria grow by catabolizing organic compounds that the *Cyanobacteria* produce and release. The *Cyanobacteria* can benefit when the heterotrophs recycle nutrients (Abed et al., 2007; Berg et al., 2009; Eiler and Bertilsson, 2004), but the heterotrophic bacteria could be harmful by causing lysis of cyanobacterial cells (Radhidan and Bird, 2001) or by competing for nutrients (Bratbak and Thingstad, 1985).

Since heterotrophic bacteria are intrinsic in PBR technologies, determining which heterotrophic bacteria are commonly associated with the cyanobacteria is essential for the effective management of PBR systems. Studies on microbial communities associated with *Cyanobacteria* are so far limited in number and focus solely on natural settings such as freshwater cyanobacterial blooms (Berg et al., 2009; Eiler and Bertilsson, 2004; Li et al., 2011). Heterotrophic-community analysis of PBR cultures is made difficult because *Synechocystis* normally is by far dominant in terms of cell numbers and biomass, as it is the primary producer of the system. This dominance often is amplified when using genomics approaches, since *Synechocystis* is highly polypoid (Chisholm and Binder, 1995; Griese et al., 2011; Labarre et al., 1989). Thus, *Synechocystis* usually is overwhelmingly dominant when the assay is based on the abundance of 16S rRNA genes. Eliminating the *Synechocystis* 16S rRNA genes prior to analysis should be a means to amplify the signal from the less abundant species in the PBR.

Streptavadin-coated magnetic beads coupled with biotin-tagged oligonucleotide probes are routinely used to isolate and purify nucleic acids on the basis of sequence similarity (Rodriguez et al., 2012). The technique, termed magnetic capture hybridization (MCH), is usually employed to concentrate low-abundance bacterial or viral DNA from complex pools of DNA (Böni et al., 2004; Parham et al., 2007). Here, I use MCH to specifically remove high-abundance *Synechocystis* 16S rRNA genes from a pool of genomic DNA (gDNA) extracted from PBR cultures in order to enrich the low-abundance 16S rRNA genes from the heterotrophic population of the PBR. This novel application of a classical technology stands to greatly improve our understanding of the heterotrophic bacteria associated with *Synechocystis* in PBR cultures and can be adapted to almost any system. I then compare the microbial community profiles before and after MCH removal of *Synechocystis* 16S rRNA genes by high-throughput sequencing of PCR amplified 16S rRNA gene libraries using an Ion Torrent Personal Genome Machine (PGM).

I found that the MCH treatment did not significantly improve the resolution of heterotrophic bacteria in 16S rRNA gene-based assays and that, in some cases, the MCH treated samples showed lower abundances of certain groups of heterotrophic bacteria. I then determined that this was because the oligonucleotide probe shared at least nine base pairs of sequence similarity with a number of non-*Synechocystis* 16S rRNA gene sequences and also shared this degree of sequence similarity with a number of non-16S rRNA genes from *Synechocystis* and other bacteria and was likely cross-reactive with these other sequences and probably removed them along with the *Synechocystis* 16S rRNA genes.

4.2 Materials and Methods

Cell cultures, growth and sampling

The laboratory of Dr. Willem Vermaas (School of Life Sciences, Arizona State University) provided stock cultures of wild type (WT) *Synechocystis* sp. PCC 6803 (hereafter abbreviated as *Synechocystis*) and a genetically modified strain designed to produce and excrete the fatty acid laurate. Stock cultures of both strains were grown in Erlenmeyer flasks at 30°C in BG-11 medium bubbled with air. I obtained a stock of *Pseudomonas stutzeri* strain PBR_B2 (GenBank Acc. No. KF539914) from our laboratory's culture collection.

DNA Extraction

I took 1-mL samples from each PBR daily and centrifuged them (13K RCF, 3 min) to remove the biomass. I removed the supernatant and stored the samples at -80˚C prior to DNA extraction. I extracted total genomic DNA from PBR samples using the DNeasy Blood & Tissue Kit (Qiagen, Valencia, CA) with the following modifications designed to enhance lysis. I resuspended cell pellets in 200μL lysis buffer (30 mM Tris·HCl, 10 mM EDTA, 200 mM sucrose, pH 8.2) and incubated the mixture at 65°C for 10 minutes. I then added chicken egg white lysozyme (Sigma Aldrich, St. Louis, MO) to a final concentration 10 mg/mL and incubated the samples for 1 hour at 37°C. Next, I added SDS at 1% (w/v) and incubated the samples at 56°C for 10 minutes. Finally, I added 25μL proteinase K and 200μL buffer AL (Qiagen) and incubated that mixture at 56°C for 30 minutes and completed the DNA extraction according to the manufacturer's (Qiagen) instructions.

Capture/TaqMan probe design

I performed a Basic Local Alignment Search Tool (BLAST) search against the

Synechocystis 16S rRNA gene sequence (accession no. BA000022.2) and generated a list

of highly similar 16S rRNA gene sequences from other cyanobacteria. I selected four

closely related 16S rRNA gene sequences from *Synechocystis* spp. (accession nos.

AB041938, AB041937, AB039001, and AB041936), as well as the more distantly related

Microcystis aeruginosa and *Anabaena* sp. PCC 7120. I then used ClustalW to generate a

pairwise sequence alignment to identify the conserved and variable regions within the 16S

rRNA gene. A hyper-variable region near nucleotide position 560 on the *Synechocystis*

16S rRNA gene was identified as a target for probe annealing. The sequence of the probe

was (5'-CTCCTATGGAGTTAAGCTC-3').

qPCR for specific detection of *Synechocystis* 16S rRNA genes

I determined that the SynMCH probe was appropriate for use as a TaqMan qPCR

probe (when labeled with the appropriate fluorescent dye and quencher molecule) when

combined with the forward primer SYN522F (5'- CGTCCGTAGGTGGTTATGC-3') and

reverse primer SYN620R (5'-CCTGCTACCCCTACTGT-3'). Control templates for the

16S rRNA gene were generated by PCR amplifying the entire 16S rRNA gene from

Synechocystis using the universal bacterial primers 8F and 1525R (Löffler et al., 2000).

PCR products were purified using the QiaQuick PCR Purification Kit (Qiagen) and cloned

using the TOPO-TA cloning kit for sequencing (Life Techonolgies). I extracted plasmid

DNA from transformants with the expected insert length using a Qiaprep Spin Minprep Kit

(Qiagen). I used a similar approach to generate control templates for the other

cyanobacterial species. qPCR conditions were as follows: 1x 5PRIME RealMasterMix

probe and 300 nM each of SYN522F and SYN620R and the SynMCH probe (labeled with

a 5'FAM and 3' BHQ1 quencher) in a total volume of 10 μL. Reactions were denatured at

95°C for 2 minutes, followed by 40 cycles of 95°C for 10 seconds, 56°C for 20 seconds,

68°C for 20 seconds. I performed qPCR reactions in a Realplex 4 epGradient S

Mastercycler (Eppendorf) and ran all reactions in triplicate. To measure total bacterial 16S

rRNA gene sequences, I prepared qPCRs exactly as described above, but using forward

primer Bac1055yf (Ritalahti et al., 2006), reverse primer 1392r, and probe 16STaq1115

(Dionisi et al., 2003) carrying a 5' FAM fluorescent dye and 3' BHQ1 quencher. I

generated a calibration curve using serial dilutions of the plasmid harboring the 16S rRNA

gene from *Synechocystis* described above which ranged from 72.492 to 7.2492e7 16S

rRNA gene copies/μL.

To test the quantitative capacity of the total bacterial (TBac) and *Synechocystis*

specific qPCR (Syn) primer sets, I performed qPCR on mixtures of the plasmid carrying

the *Synechocystis* 16S rRNA gene (described above) and genomic DNA (gDNA) extracted

from a pure culture of *P. stutzeri* strain PBR_B2. I first quantified 16S rRNA gene copies

in each separate gDNA stock using the TBac primer set. I then made mixtures targeting a

total of 10^6 16S rRNA gene copies/μL. The mixtures were composed of 100, 99, 90, 75,

50, 25, 10, and 1% *Synechocystis* 16S rRNA genes with the remainder (i.e. 0, 1, 10, 25, 50,

75, 90, and 99%) composed of 16S rRNA genes from the *P. stutzeri* strain PBR_B2.

Specific removal of *Synechocystis* 16S rRNA genes by MCH

I based the conditions for the MCH on previous work (Parham et al., 2007; Rodriguez et al., 2012; Thompson et al., 2006). I selected a hybridization temperature of 47°C based on the predicted T_m of the SynMCH probe (49°C). I used a biotin-tagged oligonucleotide probe SynMCH (5'-Biotin-CTCCTATGGAGTTAAGCTC-3', Integrated DNA Technologies) to specifically target and remove *Synechocystis* 16S rRNA genes from gDNA extracted from PBR cultures. First, I normalized all samples of gDNA to 20 ng/μL and placed 10μL of this into a clean microcentrifuge tube (200 ng gDNA total). To test the effect of different concentrations of the SynMCH probe, I added the SynMCH to the normalized gDNA at concentrations of 0.5 μM or 1 μM. I incubated this mixture at 90°C for 10 minutes to denature the DNA and then incubated the samples at 47°C for 1 hour to allow the SynMCH probe to anneal to the gDNA. I washed and prepared fresh Streptavadin-coated Dynabeads (Life Technologies) for DNA manipulations as described by the manufacturer. To test the effect of different concentrations of the magnetic beads, I added 5, 10, or 15 μL of the prepared beads to the reaction mixtures and incubated these mixtures at 47°C and 800 RPM for 30 minutes on a Thermomixer R (Eppendorf). I then separated the beads magnetically and moved the supernatant, which contained non-*Synechocystis* 16S rDNA, to a fresh tube. Finally, I recovered the non-*Synechocystis* DNA by purifying the reactions using a QiaQuick PCR Cleanup Kit (Qiagen). I repeated this experiment using gDNA extracted from a separate PBR. **Table 4.1** shows the different MCH conditions used in this study. In all instances, the concentrations of the SynMCH probe and streptavidin coated beads were above the dissociation for the biotin-streptavidin interaction (0.04 pM) (Holmberg et al., 2005).

Reaction Number	Probe Concentration (µM)	Bead concentration (mg/mL)	Theoretical total binding capacity of beads* (µg dsDNA)
	Table 4.1 MCH conditions. The SynMCH probe was used in two different concentrations and the magnetic beads were used in three different concentrations.		
1		0.3	0.2
2	0.5	3.0	2
3		4.5	3
4		0.3	0.2
5	1	3.0	2
6		4.5	3
* Based on binding capacity of 20 µg dsDNA/mg Beads			

High-throughput sequencing and data analysis

  I sequenced 16S rRNA genes from the different samples using previously described methods (Caporaso et al., 2012). I amplified the V4 region of bacterial 16S rRNA genes using Golay barcoded primer set 515F/806R (Caporaso et al., 2010a). I then pooled the triplicate PCR reactions and quantified them using the Quant-iT PicoGreen dsDNA Assay Kit (Life Technologies). Next, I pooled 240 ng of each sample in and cleaned the final pool using the QiaQuick PCR Cleanup Kit (Qiagen). For loading the samples onto the Illumina MiSeq, I quantified the PCR library using the KAPA SYBR FAST Universal qPCR Kit for Illumina (KAPA Biosystems). I then sent the prepared libraries to the Microbiome Analysis Laboratory at Arizona State University for sequencing on the Illumina MiSeq. I analyzed all 16S rRNA gene sequencing data using the QIIME software using the default quality filters (Caporaso et al., 2010b; Zhou et al., 2014). All sequences that were not assigned a specific taxonomic classification and taxa that represented less

than 1% of the microbial community were removed from the analyses. All analyses are of

150 bp reads in the forward direction. I computed rarefaction curves using the PD Whole

Tree index.

Terminal-restriction fragment length polymorphism (T-RFLP) analysis

I amplified 16S rRNA genes using the universal bacterial primers 8F (5'-

AGAGTTTGATCCTGGCTCAG-3') and 1392R (5'-ACACACCGCCCGT-3') (Fortuna et

al., 2011; Liu et al., 1997). The 8F primer carried a 5'-HEX fluorescent dye (Integrated

DNA Technologies), while the 1392R primer was unlabeled. PCR conditions were as

follows: 1x *Taq* PCR Master Mix (Qiagen), 250 nM each primer, 1 mM Mg^{2+}, and 10 ng

template DNA in a total of 50 μL. PCR reactions were denatured at 94°C for 6 minutes,

followed by 30 cycles of 94°C for 45 seconds, 55°C for 45 seconds, 72°C for 2 minutes

and a final extension period at 72°C for 10 minutes. Following PCR, I checked for

amplicons of the proper size on a 1% (w/v) agarose gel. I then digested the amplified 16S

rRNA genes using the restriction enzymes *Hha*I or *Mse*I (New England Biolabs, Ipswich,

MA). Next, I analyzed the sizes of the T-RFs produced on an ABI 3730 DNA Analyzer

using the GeneScan500 ROX Size Standard (Applied Biosystems). I gathered raw T-RFLP

data using the Peak Scanner Software v1.0 (Applied Biosystems) and analyzed the data

using previously described methods (Rees et al., 2004). I determined total fluorescence

intensity within each individual sample by summing the fluorescence intensity of all

detected T-RFs for that sample. I normalized T-RFLP data by removing peaks that

contained less than 1% of the total fluorescence intensity and calculated a new total

fluorescence intensity using only T-RFs detected as above background. I then determined

true T-RFs as any T-RF that contained more than 5% of the new total fluorescence

intensity (Rees et al., 2004). To compensate for T-RF drift, all T-RFs were aligned

manually by assuming that T-RFs within ±1 bp were the same size (Smith et al., 2005). T-

RFs smaller than 50 base pairs (bp) and larger than 600 bp were omitted from the analyses,

as fragments of these sizes are not supported by the size standard I used. I performed all

manipulation of raw T-RFLP data using original Perl scripts and Microsoft Excel

spreadsheets.

BLAST analysis for alternative hybridization sites for SynMCH probe

To test for cross-reactivity between the SynMCH probe and 16S rRNA genes from

other bacterial species, I used the NCBI BLAST tool with the megablast algorithm to find

sites in other bacterial 16S rRNA gene sequences that had at least 9 bp of sequence

similarity with the SynMCH probe sequence. I also used the BLAST tool to find other

sites within the genome of *Synechocystis* sp. PCC6803 and within the genomes of

heterotrophic bacteria including *Pseudomonas* and *Bacillus* spp. that had at least 9 bp of

sequence similarity with the SynMCH probe. To determine if a longer probe would have

less cross-reactivity, I performed a BLAST analysis similar to above, but with a probe

sequence that was 40 bp long. I generated this sequence by extending the original

SynMCH probe sequence 10 bp in the 5' direction and 11 bp in the 3' direction along the

Synechocystis 16S rRNA gene. This sequence was 5'-

GAGCTTAACTCCATAGGAGCGGTGGAAACTGCAAGACTAG-3'.

4.3 Results and Discussion

qPCR for specific detection of *Synechocystis* 16S rRNA genes

Figure 4.1 shows amplification plots for qPCR reactions performed using the SYN522F/SYN620R/SynMCH primer and TaqMan qPCR probe set (hereafter referred to as SynTaq). *Synechocystis* 16S rRNA gene templates showed amplification, while the 16S rRNA genes of the four other *Cyanobacteria* did not show amplification. Therefore, the SynTaq probe set demonstrated high specificity for *Synechocystis* 16S rRNA genes.

The results of the test of the quantitative ability of the two probe sets are shown in **Figure 4.2**. Except for the 99%, 90%, and 75% mixtures, the TBac probe set returned around 10^6 16S rRNA gene copies/μL. The 50%, 25%, 10%, and 1% mixtures returned the greatest concentrations of 16S rRNA gene copies, indicating that the TBac probe set had greater quantitative accuracy for systems dominated by heterotrophic bacteria. However, for the 100% and 99% mixtures, the SynTaq probe set showed more 16S rRNA gene copies/μL than did the TBac probe set. Thus, for systems that are highly enriched in *Synechocystis*, the TBac probe set may underestimate the true concentration of 16S rRNA genes.
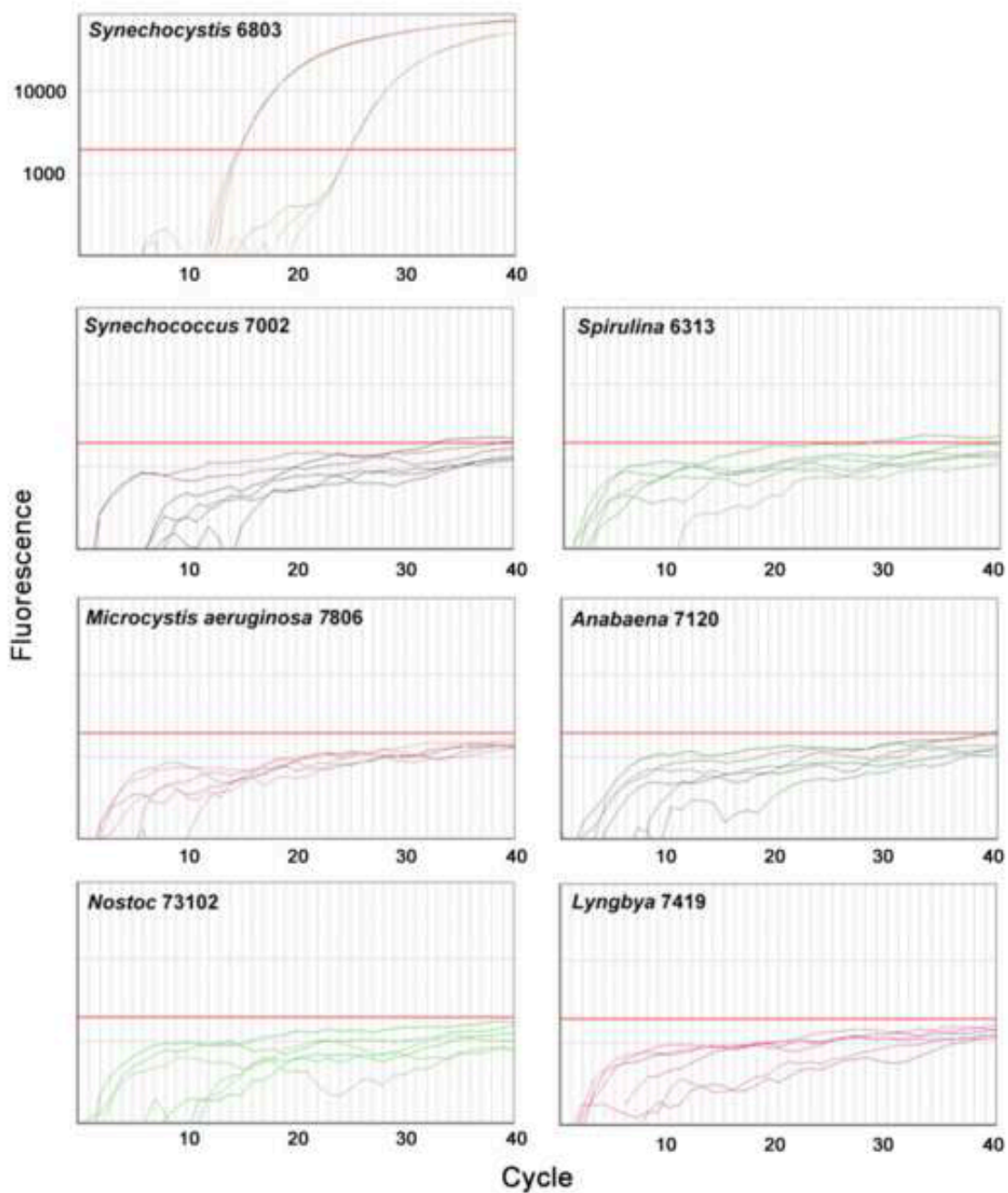
Figure 4.1 Amplification plots of cloned cyanobacterial 16S rRNA genes.
Templates were present in qPCRs in triplicate at either 40 pg (concentrated) or 40 fg
(dilute) per reaction. The y-axes are scaled identically in each plot. The red line is
shown at the same fluorescence threshold on each plot and was determined as the
noiseband value from the *Synechocystis* amplification plot. Amplification was only
detected for *Synechocystis*.

70
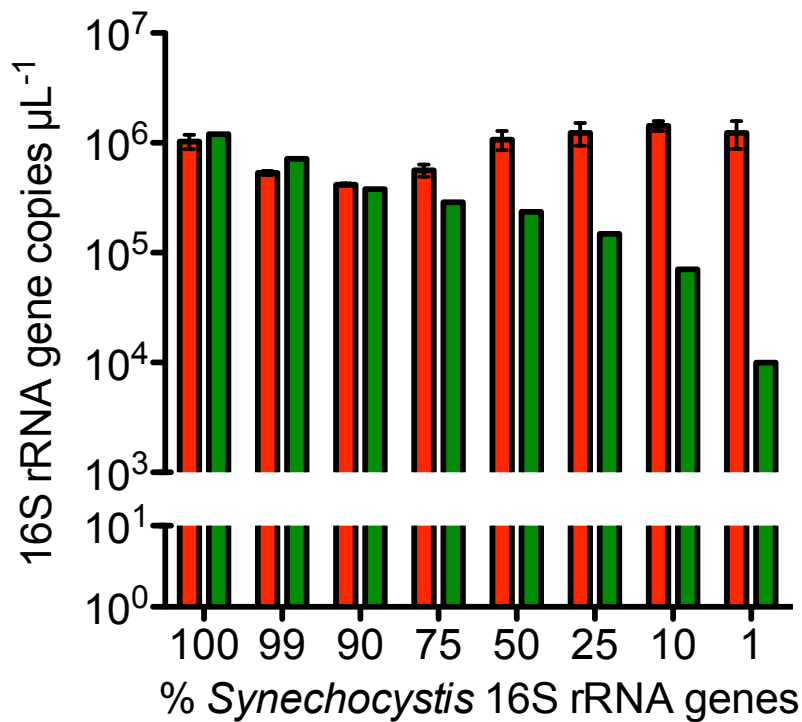
Figure 4.2 qPCR analysis of mixtures of a plasmid carrying the *Synechocystis* 16S rRNA gene and *P. stutzeri* gDNA. The TBac probe set (red) detected more 16S rRNA gene copies at higher concentrations of *P. stutzeri*, but was near the target 10^6 copies/μL in all cases. The SynTaq agreed well with the TBac probe set in most cases and demonstrated reasonable quantitative capability.

qPCR shows a reduction in 16S rRNA gene copy concentration after MCH treatment

Figure 4.3 shows qPCR results from the original, untreated sample of gDNA extracted from each PBR (Pool) and from the six different treated samples. For the first sample set (A), the Pool sample showed more 16S rRNA gene copies/μL for the TBac probe set than for the SynTaq probe set, while the Pool sample for the second sample set

(B) showed more 16S rRNA gene copies/µL for the SynTaq probe set. This indicates that sample set B was initially more enriched for *Synechocystis* than was sample set A.
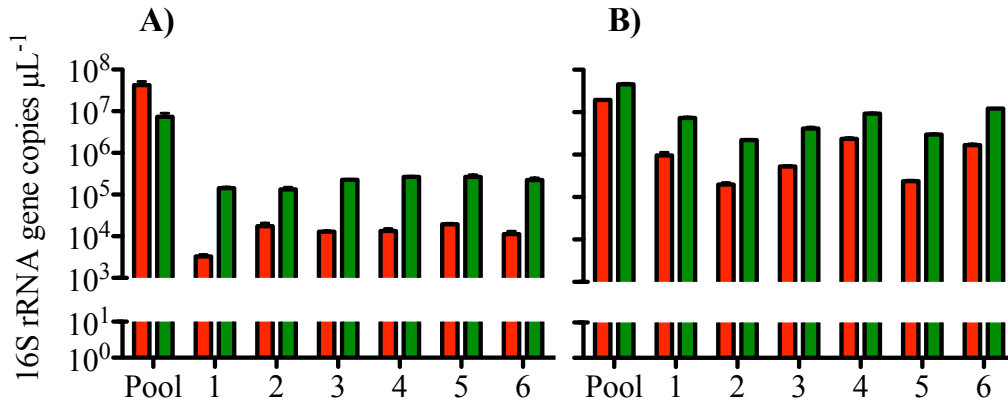
Figure 4.3 qPCR analysis of the two MCH sample sets. The Pool from sample set A showed more 16S rRNA gene copies/µL for the TBac probe set (red) than for the SynTaq probe set (green) while the opposite was true for the Pool sample set B, indicating that sample set B was more enriched for *Synechocystis* than sample set A. For both sample sets, the MCH treatment reduced the 16S rRNA gene copies/µL detected with both probe sets. The probe and bead concentrations did not affect the efficiency of the MCH.

All of the treated samples in both sample sets showed more 16S rRNA gene copies/µL with the SynTaq probe set than for the TBac probe set. This result was unexpected, as the specific removal of *Synechocystis* 16S rRNA genes ought to have enriched for 16S rRNA genes from heterotrophic bacteria, which should have increased the ratio of 16S rRNA gene copies detected with the TBac probe set compared to those detected with the SynTaq probe set. Nevertheless, both qPCR probe sets showed a reduction in the 16S rRNA gene copies/µL for all of the treated samples in both sample

sets. Thus, it is reasonable to conclude that the MCH technique successfully removed 16S

rRNA genes from the two samples.

High-throughput 16S rRNA gene sequencing reveals minimal removal of

***Synechocystis* 16S rRNA genes**

High-throughput sequencing results presented at the order-level are summarized in

Figure 4.4 For sample set A, sequences assigned to the order *Chroococcales*, to which

Synechocystis belongs, comprised only around 10% of the 16S rRNA gene sequences in the

Pool sample, while the remaining sequences were assigned to orders of heterotrophic

bacteria. All of the MCH-treated samples from sample set A showed similar abundances of

sequences from the order *Chroococcales*, indicating that the MCH failed to remove any of

the 16S rRNA genes from *Synechocystis*. Interestingly, the treated samples showed a

decrease in the relative proportion of sequences assigned to the order *Bacillales* compared

to the Pool sample. Thus, the SynMCH probe may have some cross-reactivity with 16S

rRNA genes from non-*Synechocystis* bacterial species. All of the other bacterial orders

detected showed increased relative abundance in the MCH treated samples compared to the

Pool sample.

For sample set B, the relative abundance of 16S rRNA genes assigned to the order

Chroococcales was slightly reduced (5-10%) in the MCH treated samples compared to the

Pool sample. In this sample set, sequences assigned to the order *Saprospirales* also

decreased slightly (1-2%) in the MCH treated samples as compared to the Pool sample. As

in sample set A, all of the other bacterial orders detected showed increased relative

abundance in the MCH treated samples compared to the Pool sample. In both sample sets,

all of the bacterial orders detected in the Pool samples also were detected in the MCH treated samples, but the MCH treatment did not lead to the detection of bacterial orders that were not detected in the Pool samples. Thus, the MCH treated samples may more closely represent the actual structure of the heterotrophic communities in the different PBRs. Both the qPCR and high-throughput sequencing results suggest that neither the amount of probe nor the amount of magnetic beads used had a great effect on the removal of *Synechocystis* 16S rRNA genes.
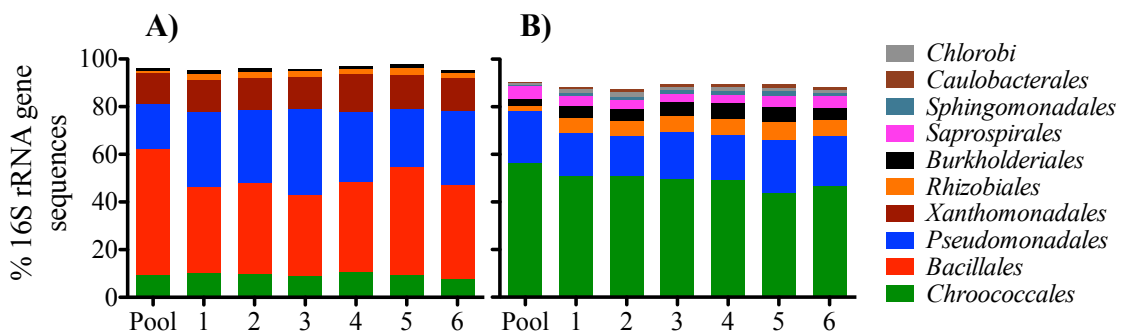
Figure 4.4 High-throughput 16S rRNA gene sequencing analysis of the two MCH sample sets at order-level definition. Sample set A did not show any reduction, while sample set B showed only minor reduction in the relative abundance of sequences assigned to the order *Chroococcales* (*Synechocystis*). In general, the relative abundance of the different orders of heterotrophic bacteria increased following the MCH treatment.

Tables 4.2 and 4.3 show whether or not the MCH treatment increased or decreased the relative abundance of each taxonomic order detected compared to the untreated "Pool" sample in sample set A and sample set B, respectively. In sample set A, the relative abundance of *Chroococcales* increased in some of the MCH-treated samples, while the relative abundance of *Bacillales* decreased. In sample set B, the relative abundance of

74

Chroococcales and *Saprospirales* decreased in all of the MCH treated samples, while the

relative abundance of *Pseudomonadales* decreased in all but one of the MCH-treated

samples. For both sample sets, the relative abundance of the other taxonomic orders

increased following the MCH treatment. This demonstrated that the SynMCH probe may

have had some cross-reactivity with the 16S rRNA genes of several other species.

Furthermore, this showed that the MCH treatment was most effective in reducing the

relative abundance of *Synechocystis* (*Chroococcales*) in systems with a greater initial

proportion of *Synechocystis* 16S rRNA genes, as was the case for sample set B.

Table 4.2 Change in abundance of each taxonomic order detected in sample set A.
Compared to the "Pool" sample, red indicates a decrease in the relative abundance of
each taxonomic order detected, while green indicates an increase in the relative
abundance. The relative abundance of *Chroococcales* increased in three of the MCH
reactions while the relative abundance of *Bacillales* decreased in all of the MCH
reactions. The abundance of all the other detected taxa increased following the MCH
treatment.

	Chroococcales	*Bacillales*	*Pseudomonadales*	*Xanthomonadales*	*Rhizobiales*	*Burkholderiales*
Pool	9.37	52.52	18.92	13.37	0.84	1.17
1	10.29	35.92	31.47	13.46	2.44	1.61
2	9.73	38.16	30.64	13.36	2.86	1.46
3	8.67	34.3	35.71	13.82	2.2	1.24
4	10.68	37.59	29.35	16.02	2.04	1.26
5	9.36	45.28	24.4	14.15	2.9	1.68
6	7.67	39.38	31.01	13.92	2.15	1.23

Table 4.3 Change in abundance of each taxonomic order detected in sample set B. Compared to the "Pool" sample, red indicates a decrease in the relative abundance abundance of each taxonomic order detected while green indicates an increase in the relative abundance. In all of the treated samples, the relative abundance of *Chroococcales* and *Saprospirales* decreased in all of the MCH treated samples while the relative abundance of *Pseudomonadales* decreased in all but one of the MCH treated samples. All of the other taxonomic orders detected increased in relative abundance following the MCH treatment.

	Chroococcales	*Pseudomonadales*	*Rhizobiales*	*Burkholderiales*	*Saprospirales*	*Sphingomonadales*
Pool	56.2	22.3	2.1	2.6	5.4	0.6
1	50.7	18.4	6.1	5.2	4	1.6
2	50.7	17.2	6.1	4.8	3.9	1.6
3	49.6	19.7	6.9	5.7	3.6	1.6
4	49	19.1	6.8	6.6	3.4	1.8
5	43.5	22.6	7.2	6.7	4.5	2
6	46.5	21.2	6.5	5.4	4.6	1.7

	Chlorobi	*Caulobacterales*
Pool	0.8	0.4
1	1.3	1.2
2	1.7	1.3
3	1.3	1.4
4	1.5	1.3
5	1.5	1.4
6	1.2	1.2

Alpha rarefaction curves for the two samples sets are shown in **Figure 4.5**. In general, the rarefaction curves for the MCH-treated samples plateaued at lower sequences per sample than did the Pool samples, indicating that more of the operational taxonomic unit (OTU) diversity in the MCH-treated samples were detected with fewer sequences per sample. Compared to the Pool samples, the MCH-treated samples showed very similar community profiles with fewer sequences per sample. Thus, the MCH treatment may have removed redundant OTUs that would have been assigned to the order *Chroococcales*.
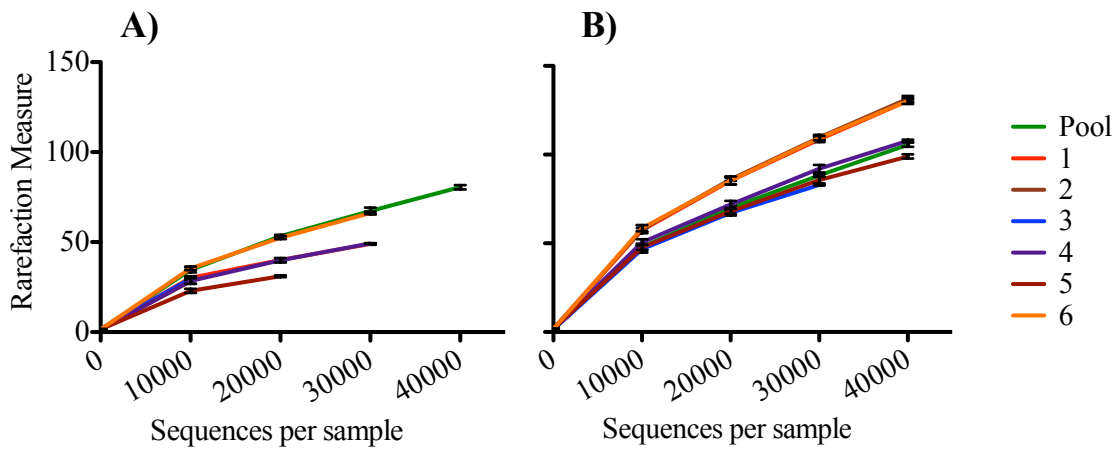
Figure 4.5 Rarefaction plots of the 16S rRNA gene sequencing data. The MCH-treated samples from sample set A showed fewer sequences per sample and did not detect as many unique OTUs as compared to the Pool sample. Most of the MCH treated samples from sample set B showed similar rarefaction measures as compared to the Pool sample.

These data indicate that the MCH technique for specific removal of *Synechocystis* 16S rRNA genes was most effective in systems with high ratios of *Synechocystis* 16S rRNA genes to total bacterial 16S rRNA genes. Even in such systems, the MCH may be unnecessary for high-throughput sequencing techniques, as they are sensitive enough to detect 16S rRNA gene sequences that are present in very low abundances.

MCH improves detection of heterotrophic bacteria in T-RFLP assays

Table 4.4 shows the number of T-RFs detected for each sample with the restriction enzyme *Hha*I and *Mse*I. Importantly, the T-RF generated by digesting the *Synechocystis* 16S rRNA gene with *Hha*I is too large to be detected in these T-RFLP assays. Thus, *Synechocystis* is excluded from the analysis of the microbial community (this is examined

in greater detail in the following chapter). For sample set A, the Pool sample showed more

T-RFs than did any of the MCH treated samples. In contrast, for sample set B, all but one

of the MCH treated samples (condition 6) showed more T-RFs than the Pool sample.

Synechocystis produces a T-RF in the detectable range for T-RFLP assays using *Mse*I. For

sample set A, only one of the MCH treated samples showed more non-*Synechocystis* T-RFs

than did the Pool sample. For sample set B, all of the MCH-treated samples showed as

many or more non-*Synechocystis* T-RFs than the Pool sample. Thus, the MCH treatment

showed some improvement in detection of non-*Synechocystis* species in sample set B for

both *Hha*I and *Mse*I. However, the MCH treatment tended to reduce the number of non-

Synechocystis T-RFs detected in sample set A for both restriction enzymes. These results

also show that the MCH treatment is most effective in systems with a higher initial

proportion of *Synechocystis* 16S rRNA genes.

Table 4.4 Number of non-*Synechocystis* T-RFs detected in the two sample sets with the *Hha*I restriction enzyme digest. For sample set A, the most T-RFs were detected in the Pool sample. For sample set B, the most T-RFs were detected in the MCH treated samples.

	*Hha*I		*Mse*I	
	A	**B**	**A**	**B**
Pool	8	6	5	2
1	3	7	4	2
2	5	8	4	3
3	3	7	8	4
4	2	8	4	3
5	4	7	4	4
6	1	3	2	2

In summary, I developed a qPCR assay targeted towards detecting *Synechocystis* 16S rRNA genes in diverse backgrounds. The qPCR assayed was highly specific to *Synechocystis* 16S rRNA genes and quantitative, although it may have slightly overestimated the concentration of *Synechocystis* 16S rRNA genes in systems that are highly enriched for *Synechocystis*. I also developed a novel MCH strategy specifically to remove *Synechocystis* 16S rRNA genes from pools of gDNA extracted from *Synechocystis*-based PBRs so that I could detect non-*Synechocystis* bacteria. Analysis by qPCR showed that the MCH method successfully removed *Synechocystis* 16S rRNA genes. However, this removal ability has only small impacts on the outcome of high-throughput sequencing analysis of the microbial community. The MCH method improved the resolution of non-*Synechocystis* bacteria in T-RFLP analyses, but this effect was limited to systems that had a relatively high abundance of *Synechocystis*. Thus, the current MCH method may only be useful for the analysis of heterotrophic bacteria in PBRs that are highly dominated by *Synechocystis*. Since I conducted the MCH using pools of gDNA, it was more thermodynamically favorable for large fragments of gDNA to hybridize to one another than to the MCH probe, which provides a likely explanation for the low removal efficiencies. A future approach may be to increase the fragmentation of the gDNA prior to the MCH treatment using physical or enzymatic processes, which may help to increase the favorability of the probe-gDNA binding. Another approach could be to perform the MCH on very dilute samples of 16S rRNA gene libraries prepared by PCR amplifying 16S rRNA genes using the universal bacterial primers described above.

Cross-reactivity between SynMCH probe and non-*Synechocystis* 16S rRNA gene sequences

The reason that MCH did not have a large impact on the resolution of high-throughput sequencing and T-RFLP was probably in part due to the probes' cross-reactivity with non-*Synechocystis* 16S rRNA genes, as well as with non-16S rRNA genes in the genomes of heterotrophic bacteria. BLAST results showed that the short and long probes had at least 9 bp of sequence similarity with more than 900 non-*Synechocystis* 16S rRNA gene sequences. Thus, neither probe was wholly specific to *Synechocystis* 16S rRNA genes. The short probe had at least 9 bp of sequence similarity with 251 unique non-16S rRNA gene regions within the *Synechocystis* genome, while the long probe shared at least 9 bp of sequence similarity with 293 unique non-16S rRNA regions within the *Synechocystis* genome. Similarly, the short and long probes showed more than 9 bp of sequence similarity with the genomes of a number of unique *Pseudomonas* and *Bacillus* species and it is likely that this is the case for many other heterotrophic bacteria. From this, I conclude that the SynMCH probe used in the MCH treatments bound to some alternative sites either within the 16S rRNA genes or in non-16S rRNA gene regions of the genomes of the heterotrophic bacteria. These data also explain why the MCH technique worked best in systems with high proportions of *Synechocystis,* as they had lower proportions of non-*Synechocystis* 16S rRNA gene targets.

In this chapter, I demonstrated a novel MCH technique to remove *Synechocystis* 16S rRNA genes from pools of DNA from *Synechocystis*-based PBRs. I found that, while the MCH was successful in removing 16S rRNA gene sequences, it did not affect the final outcome of 16S rRNA gene sequencing. This was due to the extremely high throughput of

the 16S rRNA gene sequencing technique. I also found that the capture probe used for the

MCH treatment was cross-reactive with non-*Synechocystis* 16S rRNA genes and non-16S

rRNA genes in the genome of *Synechocystis* and other bacteria. From this I conclude that

high-throughput sequencing is sufficient to detect the true diversity of heterotrophic

bacteria in *Synechocystis*-based PBRs. Thus, in the following chapters, I do not employ

this technique for any of the 16S rRNA gene sequencing-based analyses.

Chapter 5

Effects of inoculum source on the structure of microbial communities in *Synechocystis* sp.

PCC6803-based photobioreactors[1]

5.1 Introduction

In Chapter 4, I demonstrated that high-throughput 16S rRNA gene sequencing

techniques are sensitive enough to uncover the microbial diversity in *Synechocystis*-based

PBRs despite the polyploidy of *Synechocystis*. In this chapter, I continue to develop

techniques to specifically interrogate the heterotrophic communities in *Synechocystis*-based

PBRs and begin to focus on developing strategies to manage PBR microbial communities.

Cyanobacteria are promising candidates for large-scale production of renewable

biofuels to replace petroleum resources, including biodiesel made from lipids extracted

from biomass (Chisti, 2007; Ortiz-Marquez et al., 2013). *Cyanobacteria* perform oxygenic

photosynthesis, gaining energy from sunlight and carbon from carbon dioxide. Thus, they

can produce carbon-neutral, non-fossil fuel feedstock. *Cyanobacteria* have many

advantages over terrestrial plants, including higher areal yields, superior photosynthetic

efficiencies, faster growth rates, and no requirement for arable land for cultivation (Chisti,

2008; Ducat et al., 2011; Kim et al., 2010b).

Heterotrophic bacteria grow by oxidizing organic molecules produced by

Cyanobacteria, including proteins, lipids, nucleic acids, and sugars (Abed, 2010).

_____

[1]This chapter is adapted from a manuscript submitted for publication.

Although associations between cyanobacteria and heterotrophic bacteria are normal, studies of the communities of heterotrophic bacteria that associate with *Cyanobacteria* in natural settings are rare (Berg et al., 2009; Lakaniemi et al., 2012b; Li et al., 2011). No study to date has addressed the presence of heterotrophic communities in photobioreactor (PBR) cultures of *Cyanobacteria*. In large-scale PBRs, sterilizing the culture medium and maintaining axenic culture conditions are economically and practically prohibitive (Lakaniemi et al., 2012b). Thus, a complete understanding of the properties and performance of a PBR demands knowledge of the structure and dynamics of the microbial community, including the heterotrophic bacteria.

While the functions of the heterotrophic bacteria that associate with *Cyanobacteria* are not fully understood, several important beneficial interactions have been documented. Primarily, heterotrophic bacteria can provide CO_2 to the *Cyanobacteria* by oxidizing organic compounds released by the *Cyanobacteria*. Additionally, heterotrophic bacteria can recycle macronutrients, such as nitrogen (N) and phosphorus (P), or increase the availability of micronutrients, such as iron, to the *Cyanobacteria* with which they associate (Keshtacher-Liebson et al., 1995). Heterotrophic metabolism also may reduce O_2 super-saturation in cyanobacterial cultures (Mouget et al., 1995). Heterotrophic bacteria also can be detrimental to PBR operations by causing lysis of cyanobacterial cells (Radhidan and Bird, 2001), competing for key macronutrients, or consuming a desired product produced by the *Cyanobacteria* such as excreted fatty acids (Liu et al., 2011b). Since the purpose of the PBR is to produce cyanobacterial biomass, exclusion of specific heterotrophic bacteria may be difficult, as the best growth conditions for the *Cyanobacteria* also will be suitable

83

for an array of heterotrophic bacteria. Thus, elucidating the common heterotrophs and key microbial interactions is critical for successful photobioreactor operation.

Molecular methods targeting the 16S rRNA gene are useful to uncover the structure of these microbial communities (Rittmann et al., 2008). Terminal-restriction fragment length polymorphism (T-RFLP) is a rapid, robust, and cost-effective method that is widely used to analyze microbial communities (Fortuna et al., 2011; Liu et al., 1997; Schütte et al., 2008). T-RFLP provides a useful avenue to compare and contrast the structures of different PBR microbial communities. Similarly, high-throughput sequencing of 16S rRNA gene libraries can be used to assess the structures of microbial communities (Ontiveros-Valencia et al., 2013). High-throughput sequencing is beneficial because it is highly sensitive and provides phylogenetic information not afforded by T-RFLP; however, it is not accessible to every researcher and involves a significant time for sequencing and data analysis.

Synechocystis sp. PCC6803 (hereafter referred to as *Synechocystis*) is one of the most extensively studied *Cyanobacteria* and was the first phototrophic organism to have a completely sequenced genome, making it an ideal model organism for further studies leading to large-scale use of *Cyanobacteria* to produce renewable feedstock (Kim et al., 2010b; Sheng et al., 2011b; Vermaas, 1998). Here, I used T-RFLP and high-throughput sequencing of 16S rRNA gene libraries to monitor the microbial communities in PBR cultures of *Synechocystis*. To improve the resolution of the heterotrophic bacteria, I applied a strategy to remove *Synechocystis* from the T-RFLP analyses. I achieve this goal by choosing a primer and restriction enzyme combination that produces a *Synechocystis* terminal-restriction fragment (T-RF) that is outside of the detectable range of the assay,

thereby excluding the *Synechocystis* signal from the analysis and increasing sensitivity towards 16S rRNA gene fragments belonging to other bacteria present in the PBR. I demonstrate that communities of heterotrophic bacteria exist in the PBRs and show that the structure of the PBR microbial communities can be different for each PBR. I also provide evidence that the starter cultures used to inoculate the various PBR experiments play an important role in determining the structure of the resulting PBR microbial communities. Finally, I demonstrate strong agreement between T-RFLP and high-throughput sequencing data, showing that these techniques can be used in tandem or separately to provide a detailed understanding of PBR microbial communities.

5.2 Materials and Methods

Cell cultures, strains, media and preparation of inocula

The laboratory of Dr. Willem Vermaas (School of Life Sciences, Arizona State University) provided stock cultures of *Synechocystis* sp. PCC6803, which were maintained in BG-11 medium (Rippka et al., 1979). 0.5 mL of a stock culture was mixed with 0.5 mL of sterile 40% glycerol and stored as a freezer stock at -80°C. To prepare fresh PBR inoculum, I spread a small amount of the freezer stock on a sterile BG-11 plate with 1.5% Bacto Agar (BD, Sparks, MD) using a sterile inoculation loop. I grew the inoculated plates at 30°C under 200 $\mu E/m^2$*sec constant incident light intensity until cells grew to sufficient density (5-7 days). I then transferred a small amount of the cells from the agar plate into 100 mL sterile liquid BG-11 medium in a 250 mL Erlenmeyer flask bubbled with air filtered through a 0.2 μm filter (Pall). I grew this starter culture at 30°C under 200 $\mu E/m^2$*sec constant incident light intensity until cells grew to sufficient density (3-5 days).

For the purposes of this work, each separate starter culture can be considered as originating from a separate BG-11 agar plate.

PBR operational parameters

I used a Photobioreactor FMT-150 (Photon Systems Instruments, Czech Republic) equipped with a temperature/pH probe and bubble interrupter for all experiments. I autoclaved the cultivation chamber to ensure that it was sterile prior to inoculation. All PBR experiments were operated with a constant incident light intensity of 200 $\mu E/m^2*sec$, maintained at 30°C, and bubbled with air that was humidified by passing through sterile water and filtered through a 0.2 μm filter (Pall, Ann Arbor, MI). I measured optical density (OD) at a wavelength of 730 nm using a Cary-50-Bio UV-Visible spectrophotometer (Varian, Palo Alto, CA) and pH directly using a pH probe integrated with the Photobioreactor FMT-150 and calibrated according to the manufacturer's directions. I inoculated four PBRs at a starting OD_{730} of 0.6 and ran each experiment for a total of 168 hours (7 days). Two of the PBRs (PBR-A and PBR-A2) were inoculated from the same starter culture, and the other two PBRs (PBR-B and PBR-C) were inoculated using different starter cultures.

Light Microscopy

For light microscopy, I took 1-mL samples of PBR cultures daily, added 0.2 mL 37.5% formaldehyde (Sigma Aldrich) to fix the cells, and stored these samples at 4°C. Cells were imaged later by light microscopy using an Olympus BX61 light microscope (Olympus Inc., Center Valley, PA) equipped with differential interference contrast (DIC)

using a 100X oil-immersion objective. Images were captured with an Olympus DP72 color camera.

DNA extraction

For DNA extraction I used a previously described method (Sheng et al., 2011a). Briefly, 1-mL samples of the PBR culture were taken daily with a sterile syringe and transferred to a sterile microcentrifuge tube and centrifuged (13 g, 3 minutes) to concentrate the biomass, which was stored at -80°C prior to DNA extraction. I extracted total genomic DNA from PBR samples using the DNeasy Blood and Tissue Kit (Qiagen, Valencia, CA) with the following modifications to enhance lysis. I resuspended cell pellets in 200 μL lysis buffer (30 mM Tris·HCl, 10 mM EDTA, 200 mM sucrose, pH 8.2) and incubated the mixture at 65°C for 10 minutes. I then added chicken egg white lysozyme (Sigma Aldrich, St. Louis, MO) to a final concentration 10 mg/mL and incubated the samples for 1 hour at 37°C. Next, I added SDS at 1% (w/v) and incubated the samples at 56°C for 10 minutes. Finally, I added 25 μL proteinase K and 200 μL buffer AL (Qiagen) and incubated that mixture at 56°C for 30 minutes. After these additional lysis steps, I completed the DNA extraction according to the manufacturer's (Qiagen) instructions.

Terminal restriction fragment length polymorphism (T-RFLP)

I performed T-RFLP analysis using a previously described method (Sheng et al., 2011a). Briefly, I amplified 16S rRNA genes using the universal bacterial primers 8F (5'-AGAGTTTGATCCTGGCTCAG-3') with a 5'-HEX fluorescent dye and 1392R (5'-ACACACCGCCCGT-3') (Fortuna et al., 2011; Liu et al., 1997; Sheng et al., 2011a). PCR

conditions were as follows: 1x *Taq* PCR Master Mix (Qiagen), 250 nM each primer, 1 mM

Mg^{2+}, and 10 ng template DNA in a total of 50 μL. PCR reaction temperature profiles

were the following: 94°C for 6 minutes, followed by 30 cycles of 94°C for 45 seconds,

55°C for 45 seconds, 72°C for 2 minutes and a final extension period at 72°C for 10

minutes. Following PCR, I checked for amplicons of the proper size on a 1% (w/v)

agarose gel. I then digested the amplified 16S rRNA genes using the restriction enzymes

HhaI, *MseI*, *HaeIII*, or *HpaII* (New England Biolabs, Ipswich, MA). Next, I analyzed the

sizes of the T-RFs produced on an ABI 3730 DNA Analyzer using the GeneScan500 ROX

Size Standard (Applied Biosystems).

Analysis of T-RFLP data

I gathered raw T-RFLP data using the free Peak Scanner Software v1.0 (Applied

Biosystems) and analyzed the data using previously described methods (Rees et al., 2004).

I determined total fluorescence intensity within each individual sample by summing the

fluorescence intensity of all detected T-RFs for that sample. I normalized T-RFLP data by

removing peaks that contained less than 1% of the total fluorescence intensity and

calculated a new total fluorescence intensity using only T-RFs detected as above

background. I then determined true T-RFs as any T-RF that contained more than 5% of the

new total fluorescence intensity. To compensate for T-RF drift, all T-RFs were aligned

manually. T-RFs smaller than 50 base pairs (bp) and larger than 600 bp were omitted from

the analyses, as fragments of these sizes are not supported by the size standard I used. I

performed all manipulation of raw T-RFLP data using original Perl scripts and Microsoft

Excel spreadsheets. When appropriate, I removed the *Synechocystis* T-RFs from the raw

data prior to downstream analyses. I used the QIIME software (Caporaso et al., 2010b) for principal coordinate analysis (PCoA) of T-RFLP data.

To analyze T-RFLP data, I used original Perl scripts in combination with Microsoft Excel. First, raw T-RFLP data was gathered from the free Peak Scanner Software v1.0 (Applied Biosystems). I then exported all data to a .txt file using the "Export Combined Table" command. Next, I imported this table into Microsoft Excel, and trimmed away all columns except for "Dye/Sample Peak", "Sample File Name", "Size", and "Height" (I analyzed T-RFLP data using both T-RF peak height or peak area and no difference in the data after analysis, and chose to use peak height for all data). I exported the trimmed T-RFLP data from Microsoft Excel as a .txt file. I then used an original Perl script to parse the T-RFLP data by enzyme and dye color. The Perl script (named TRFdata.pl, shown below) produced four output files: one file for each enzyme used. The output files contained data from only the green channel, which corresponds to the color of the HEX dye used to label the 8F primer. TRFdata.pl requires useres to add in their own file paths for input and output files, which can be achieved using any text editor. I then imported the individual .txt files (with data corresponding to each restriction enzyme) to Microsoft Excel. In Excel, I used simple Excel commands to sum the peak heights within each sample, and determined which peaks were above background. To compensate for T-RF drift, I manually aligned all T-RFs across all samples by assuming that T-RFs within ±1 base pair (bp) were the same T-RF.

Importing T-RFLP data to QIIME software

I imported the T-RFLP data into the QIIME software package using the QIIME script trflp_file_to_otu_table.py. For each experiment, I generated one .txt file per restriction enzyme. The .txt were organized as shown in **Table 5.1**. The intensity of each T-RF was then entered into the table when appropriate. Unless otherwise noted, the values entered for each T-RF were the percent of fluorescence intensity occupied by the T-RF.

Table 5.1 **Example of formatted table for loading T-RFLP data into QIIME software.** Each sample name is placed into a row while the T-RF sizes are placed into columns. Then, the relative fluorescence intensity for each T-RF detected within each sample is entered. If a T-RF was not detected in a sample, it is assigned a value of 0.			
	100	200	300
Sample1	0	50	30
Sample2	25	10	0
Sample3	15	75	0

Prediction of *Synechocystis* T-RF sizes

Ideally, each species generates a unique T-RF size. I predicted the size of the *Synechocystis* T-RF generated with each enzyme used by submitting the *Synechocystis* 16S rRNA gene sequence (NCBI accession number NR_074311.1) to *in silico* restriction digests. I determined T-RF sizes of 1048, 546, 293, and 490 bp for the enzymes *HhaI*, *MseI*, *HaeIII*, and *HpaII*, respectively. I validated the predictions by performing T-RFLP on pure cultures of *Synechocystis* shown in **Figure 5.1**.
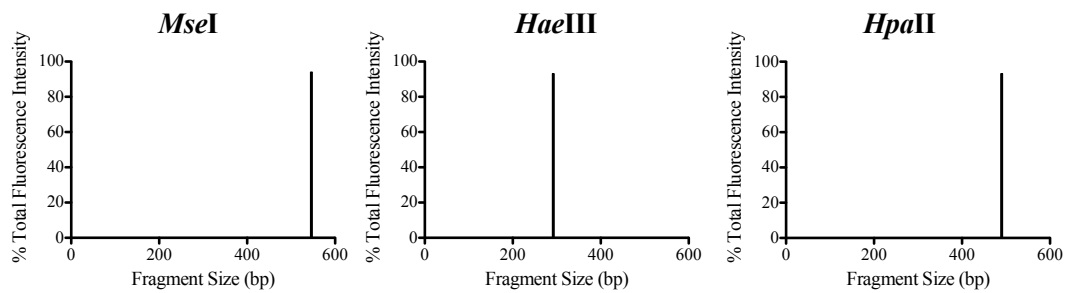
Figure 5.1 T-RFLP data from a pure culture of *Synechocystis* sp. PCC6803. I predicted T-RF sizes of 546, 292 and 490 bp for digests using the *MseI, HaeIII*, and *HpaII* restriction enzymes and confirmed the predicted sizes by performing T-RFLP on a pure culture of *Synechocystis* sp. PCC6803. *Synechocystis* sp. PCC6803 T-RFs are indicated with a black dot. No T-RFs were detected above background for the *Hha*I restriction digest. No other T-RFs were detected as above background for any of the restriction digests.

High-throughput 16S rRNA gene sequencing and data analysis

I sequenced 16S rRNA genes from the enriched consortia of heterotrophic bacteria and from representative PBR experiments using previously described methods (Caporaso et al., 2012). I amplified the V4 region of bacterial 16S rRNA genes using Golay barcoded primer set 515F/806R (Caporaso et al., 2010a). I then pooled the triplicate PCR reactions and quantified them using the Quant-iT PicoGreen dsDNA Assay Kit (Life Technologies). Next, I pooled 240 ng of each sample in and cleaned the final pool using the QiaQuick PCR Cleanup Kit (Qiagen). For loading the samples onto the Illumina MiSeq, I quantified the PCR library using the KAPA SYBR FAST Universal qPCR Kit for Illumina (KAPA Biosystems). I then sent the prepared library to the Microbiome Analysis Laboratory at Arizona State University for sequencing on the Illumina MiSeq. I analyzed all 16S rRNA gene sequencing data using the QIIME software using the default quality filters (Caporaso et al., 2010b; Ontiveros-Valencia et al., 2013). In order to examine only the heterotrophic

91

bacteria from the representative PBR experiment, I filtered all cyanobacterial operational

taxonomic units (OTUs) from the OTU table using the script filter_taxa_from_otu_table.py

prior to downstream analysis and removed any unassigned sequences. All analyses are of

150 bp forward reads.

Inoculum effect experiments

To determine the impact of the inoculum on the structure of PBR microbial

communities, I conducted a series of batch tests. I collected three different *Synechocystis*

cultures, each of which was grown in a different building on the Tempe campus of Arizona

State University. I then used these flasks to inoculate three identical experimental flasks,

giving a total of nine experimental flasks. All experimental flasks were grown in the same

light incubator under identical conditions (30˚C, 85 $\mu E/m^2*sec$) for 96 hours and were

bubbled with air filtered through a 0.2 μm filter (Pall). Samples were collected from each

inoculum at the time of inoculation and from the experimental flasks after the 96-hour

incubation period. For these experiments, I performed T-RFLP using all four enzymes and

evaluated the structure of the microbial communities based on the presence or absence of

the different T-RFs detected. If a T-RF was detected in a specific sample, it was assigned a

value of 1, and if it was not detected in that sample, it was assigned a value of 0.

5.3 Results and Discussion

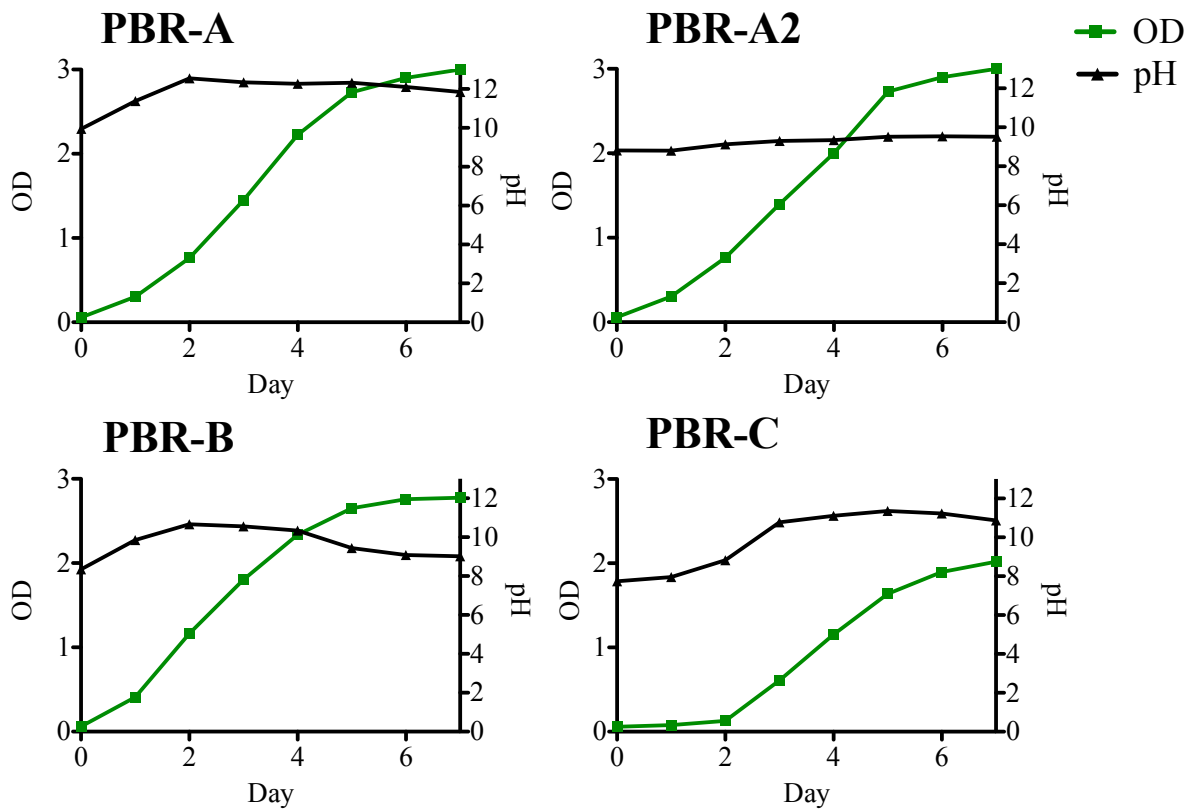**PBRs operated under identical conditions show different performances**

Figure 5.2 shows the OD_{730} and pH for the four PBR experiments. PBR-A and

PBR-A2 (inoculated from the same starter culture) reached the highest OD_{730} values of 3.0

and had an average pH of 11.8 and 9.2, respectively. PBR-B and PBR-C (different starter cultures) attained OD_{730} and pH values of at least 2.0 and 9.7, respectively. The lower OD_{730} for PBR-C correlated with a 2-day lag period not seen in the other experiments. The high pH values in all the PBR experiments indicated that *Synechocystis* was photosynthetically active and utilized available inorganic carbon efficiently (Kim et al. 2010a). Thus, despite being operated under identical conditions with the same culture medium, each PBR produced a different amount of biomass and had different final pH values.

Figure 5.3 shows light microscopy images from PBR-A, which showed similar patterns to the other PBR experiments shown in **Figure 5.4**. On Day 0 (inoculation), only green *Synechocystis* cocci were detected in the PBR culture after counting at least 200 cells total. Rod-shaped heterotrophic bacteria became detectable by microscopy in PBR-A starting on Day 4. For the other PBR experiments, rod-shaped heterotrophic bacteria were detectable by light microscopy starting on or around Day 4. Once the heterotrophic bacteria became detectable in the PBR, they persisted for the duration of the experiment (Day 7). This was expected, as the association of heterotrophic bacteria with cyanobacterial blooms and cultures is ubiquitous in natural conditions (Li et al., 2011) and has been observed and predicted to have impacts in other engineered PBR systems (Lakaniemi et al., 2012a; Unnithan et al., 2013).

Figure 5.2 OD$_{730}$ and pH from four PBRs operated under identical conditions. All PBRs were inoculated at OD$_{730}$ = 0.6 with 200 μE/m^2*sec constant light intensity, held at 30°C, and bubbled with filter-sterilized air. A, B, or C indicates inoculation with different starter cultures; PBR-A and PBR-A2 were inoculated with the same starter culture. Despite identical operating parameters, each PBR had unique OD$_{730}$ and pH profiles, and PBR-C did not grow as well as the others.

Day 0

Day 4

Day 7
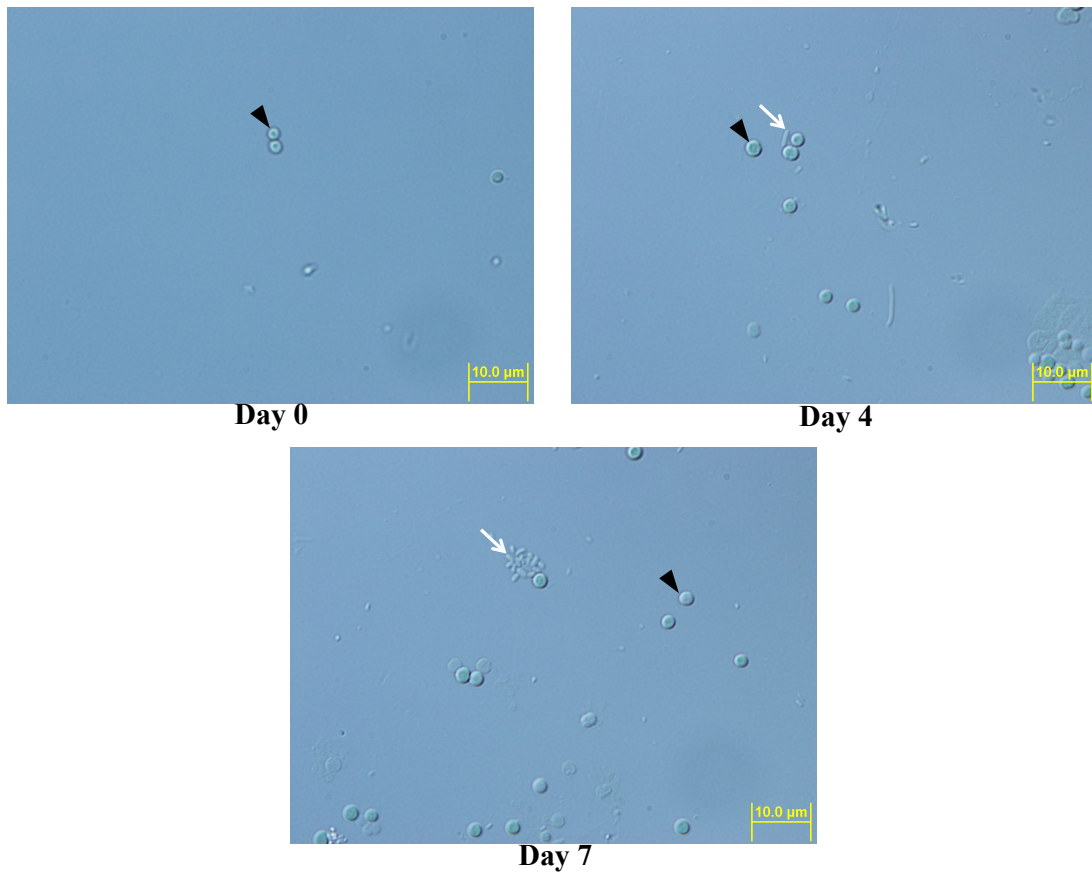
Figure 5.3 Light microscopy images from PBR-A. All images were taken with a 100X oil-immersion DIC objective. Upon inoculation (Day 0), only *Synechocystis* (black arrowheads) was detected after counting at least 200 total cells. By Day 4, rod-shaped heterotrophic bacteria (white arrows) were detectable in the PBR. Heterotrophic bacteria grew in the PBR until the end of the experiment (Day 7). Scale bars are 10 μm.
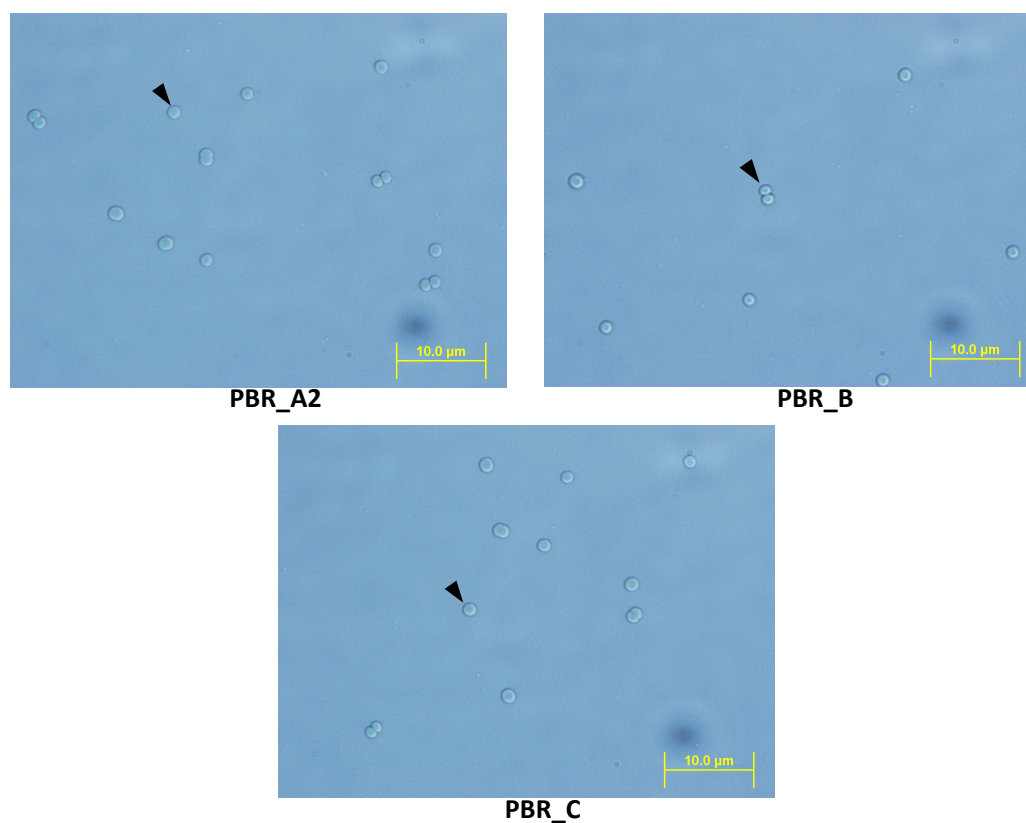
Figure 5.4 Light microscopy of PBR inocula. *Synechocystis* is indicated with a black arrowhead. No heterotrophic bacteria were detected in any of the inocula used in this study after counting at least 200 total cells. All images were taken using a 100X oil-immersion differential interference contrast objectives. Scale bars are 10 μm.

Removal of *Synechocystis* signal improves detection of heterotrophic bacteria with T-RFLP analyses

Table 5.2 shows the number of unique T-RFs detected using the restriction enzymes *Mse*I, *Hae*III, *Hpa*II, or *Hha*I for the PBR-A, PBR-A2, PBR-B, and PBR-C at the end of each experiment. As predicted, eliminating the *Synechocystis* T-RF via the *Hha*I digest increased the resolution of the rest of the PBR microbial community.

96

Table 5.2 **Number of unique T-RFs detected with each restriction enzyme.** *Synechocystis* T-RFs were detected for all restriction enzymes except for *Hha*I, where the *Synechocystis* T-RF is too large and is excluded from the analysis. In all of the PBRs, the number of non-*Synechocystis* T-RFs detected with *Hha*I was greater than the number of non-*Synechocystis* T-RFs detected with any of the other restriction enzymes.				
	PBR-A	PBR-A2	PBR-B	PBR-C
*Mse*I	1	2	1	2
*Hae*III	2	2	1	1
*Hpa*II	2	2	1	2
*Hha*I	2	2	2	3

This was especially evident for PBR-B, where the *Hha*I digest yielded one unique non-*Synechocystis* T-RF even though no non-*Synechocystis* T-RFs were detected in any of the other digests. Even for PBR-A and PBR-C, where one non-*Synechocystis* T-RF was detected with the *Mse*I, *Hae*III, and *Hpa*II digests, the *Hha*I digest still improved the resolution of the non-*Synechocystis* members of the PBR microbial communities. This shows that using the *Hha*I restriction enzyme provided best resolution of the heterotrophic bacteria in the PBRs.

T-RFLP and high-throughput sequencing analysis of PBR microbial communities showed similar trends

In order to understand better the heterotrophic bacteria present in our PBR, I employed T-RFLP using the *Hha*I restriction enzyme to target the heterotrophic bacteria in the microbial communities and high-throughput sequencing. **Table 5.3** shows the results of T-RFLP analysis of the microbial communities from PBR-A, PBR-A2, PBR-B, and PBR-C using the *Hha*I restriction enzyme on Day 0, Day 3, and Day 7 of each experiment.

Table 5.3 T-RFs detected in each PBR using the *Hha*I restriction enzyme. PBR-A and PBR-A2 had nearly identical T-RF patterns while PBR-B and PBR-C had unique T-RF patterns.						
	Day 0		**Day 3**		**Day 7**	
	T-RF Size (bp)	**% Total Area**	**T-RF Size (bp)**	**% Total Area**	**T-RF Size (bp)**	**% Total Area**
PBR-A	ND	ND	242, 582	81.6, 5.9	242, 582	87, 11.6
PBR-A2	ND	ND	242, 582	79.3 11.9	242, 582	68.7, 12.1
PBR-B	204, 570	56, 38.5	135, 204	31.9, 17.8	135, 240	28.2, 71.8
PBR-C	212, 365, 372	65.8, 19.1, 6.6	212, 342, 372	75.1, 5.5, 9.4	212, 342, 372	74.8, 8, 9.1

Figure 5.5 shows order-level taxonomic classification determined by high-throughput sequencing of 16S rRNA gene libraries from PBR-A, PBR-A2, PBR-B, and PBR-C from Day 0, Day 3, and Day 7 of each experiment, and **Figure 5.6** shows genus-level taxonomic classification of the heterotrophic bacteria from the first and last days of each PBR experiment.
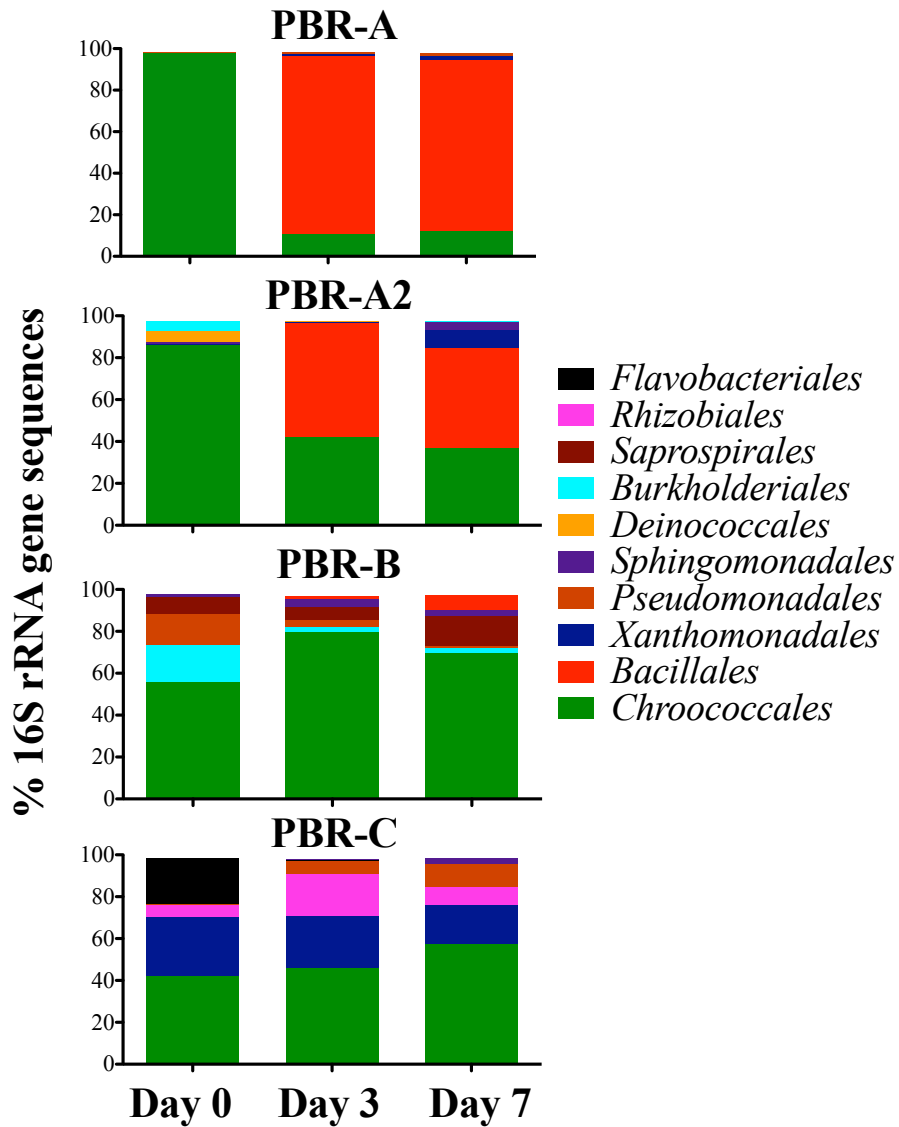
Figure 5.5 Microbial community structure in the four PBR experiments through high-throughput 16S rRNA gene sequencing. All taxa are classified at the order level definition.
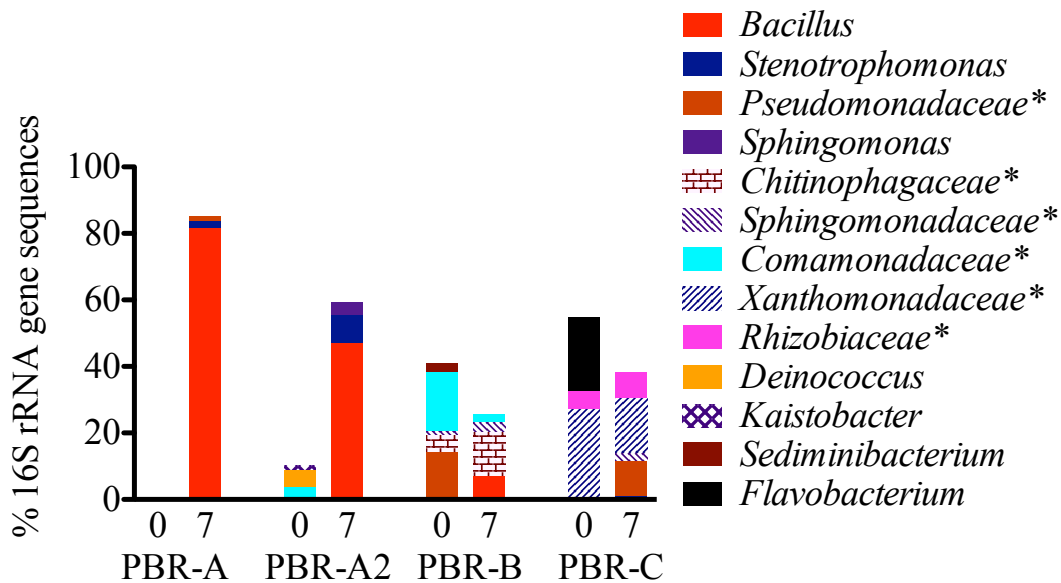
Figure 5.6 Heterotrophic bacteria detected in the four PBR experiments through high-throughput 16S rRNA gene sequencing. All taxa are classified at the genus level unless otherwise indicated.

*Not classified below the family level

On Day 0, PBR-A and PBR-A2 had very high abundances of *Chroococcales,* the order to which *Synechocystis* belongs, and only small proportions of heterotrophic bacteria. However, no non-*Synechocystis* T-RFs were detected for these PBRs on that day. Thus, high-throughput 16S rRNA gene sequencing was more sensitive to the presence of heterotrophic bacteria than was the *Hha*I T-RFLP. On Days 3 and 7, PBR-A and PBR-A2 showed a large proportion of heterotrophic bacterial phylotypes from the order *Bacillales,* which was a single *Bacillus* sp. that corresponded to a large 242-bp T-RF detected in both PBRs. The smaller 582-bp T-RF may correspond to the bacterial species from the order *Xanthomonadales*, which was a single *Stenotrophomonas* sp. These data demonstrate that

the same species of heterotrophic bacteria were present in the microbial communities of PBR-A and PBR-A2. In these PBRs, the *Bacillus* sp. was the most dominant bacterial species by the end of the experiments.

On Day 0 of PBR-B, I detected heterotrophic bacterial phylotypes belonging to the orders *Burkholderiales*, *Pseudomonadales*, and *Saprospirales*. By Day 7, *Saprospirales* and *Bacillales* became the most dominant phylotypes. This shift in the structure of the microbial community also was seen with the *Hha*I T-RFLP, in which a 570-bp T-RF disappeared, while 135-bp T-RF appeared.

Heterotrophic bacteria assigned to the orders *Xanthomonadales* and *Flavobacteriales* were most abundant on Day 0 of PBR-C. The lag period at the beginning of this PBR was correlated with the presence of a bacterium from the order *Flavobacteriales*, which was a single *Flavobacterium* sp. *Flavobacteria* associated with marine phytoplankton typically are most abundant during the decay phase (Buchan et al., 2014). Thus, the inoculum for PBR-C may have been in decay, which inhibited the growth at the beginning of the experiment. As the culture entered exponential growth, the *Flavobacterium* sp. was no longer detected, and the relative proportion of *Chroococcales* increased. By Day 7, the most predominant non-*Synechocystis* phylotypes were *Xanthomonadales*, *Pseudomonales,* and *Rhizobiales*. As with PBR-B, T-RFLP also detected the shift that occurred in microbial community of PBR-C between Day 0 and Day 3: the disappearance of the 365-bp T-RF and the appearance of a 342-bp T-RF.

Our data demonstrated strong agreement between the high-throughput sequencing and T-RFLP analysis of the different PBR microbial communities. While high-throughput sequencing usually detected more unique taxa of heterotrophic bacteria (more non-

Synechocystis OTUs) than did the *Hha*I T-RFLP, T-RFLP usually detected the major

heterotrophic phylotypes in the PBRs. Thus, high-throughput sequencing was more

informative than T-RFLP for determining microbial community structure, but T-RFLP was

more suitable for routine monitoring of the structures of different PBR microbial

communities due to its low cost and rapid turnaround time.

Inoculum source strongly influences PBR microbial community structure

The two PBRs inoculated with the same starter culture (PBR-A and PBR-A2) had

similar microbial communities, while the two PBRs inoculated with different starter

cultures (PBR-B and PBR-C) had unique microbial communities. I conducted a separate

set of experiments to examine more closely the effects of using different inocula on the

structure of PBR microbial communities. Here, three unique inocula (labeled 1, 2, and 3)

were used to inoculate three experimental flasks (nine flasks in total), which were then

grown under identical conditions. **Figure 5.7** shows high-throughput sequencing data from

the microbial communities from the three unique *Synechocystis* inocula and from the

experimental cultures derived from the inocula. The microbial communities in the

respective experimental flasks were most similar to the microbial community from that

inoculum, even though the culture conditions were identical. The microbial communities

within a set of experimental flasks also were more similar to one another than to any of the

other experimental or inoculum flasks. The heterotrophic bacteria in the first set of flasks

(1Inoc, 1A, 1B, and 1C) contained mostly phylotypes from the order *Cytophagales*, while

those in the second set (2Inoc, 2A, 2B, and 2C) mostly contained phylotypes from the

orders *Burkholderiales* and *Sphingobacteriales*. All of the flasks in the third set (3Inoc,

3A, 3B, and 3C) were composed almost entirely of *Synechocystis*. However, the microbial communities exhibited slight difference between the flasks within each set. Most notable was the second set (2Inoc, 2A, 2B, and 2C), where each of the experimental flasks contained bacteria from the order *Sphingobacteriales*, even though those bacteria were not detected in the inoculum flask.
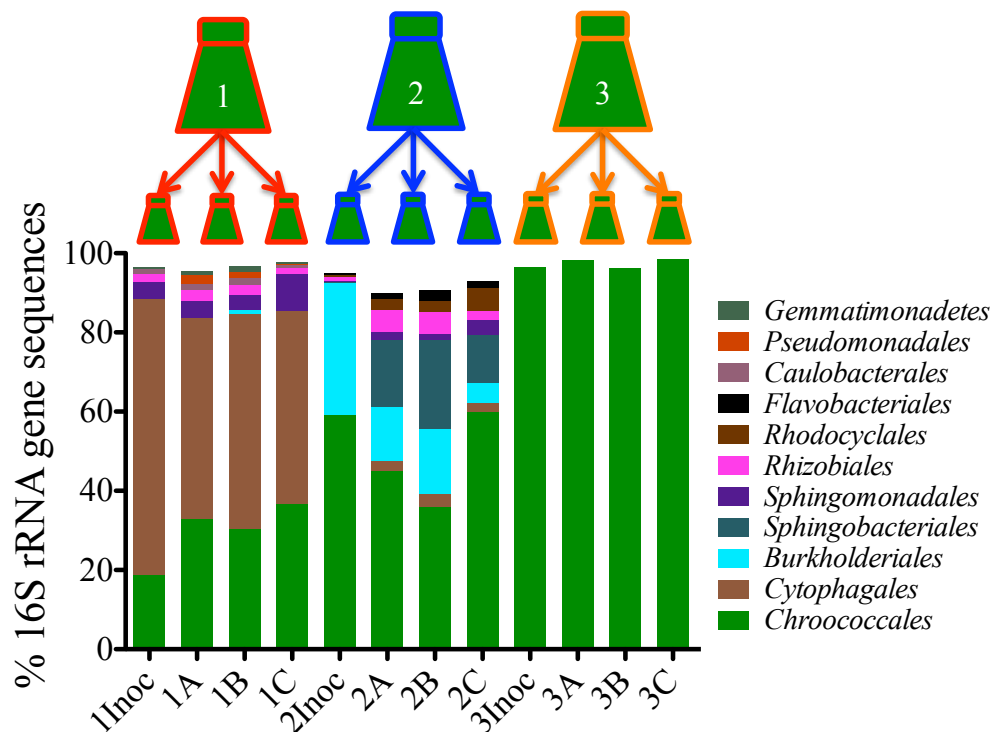
Figure 5.7 Microbial communities in experimental flasks are similar to the microbial communities in inocula. For each different inoculum (1, 2, 3), the microbial communities in the experimental flasks (A, B, C) were similar to the microbial communities in the respective inoculum (Inoc) flasks.

Figure 5.8 shows PCoA biplots of the high-throughput 16S rRNA gene sequencing data and T-RFLP data generated using the *Mse*I, *Hae*III, *Hpa*II, or *Hha*I restriction enzymes. As expected from the 16S rRNA gene sequencing taxonomic data, PCoA showed that the microbial communities in each set of experimental flasks grouped with the inoculum flask from that set, indicating that those microbial communities were more similar to one another than they were to the microbial communities in the other sets of flasks. PCoA generated from the T-RFLP showed the same trends as the PCoA generated from the high-throughput sequencing data in terms of the grouping of the different microbial communities.
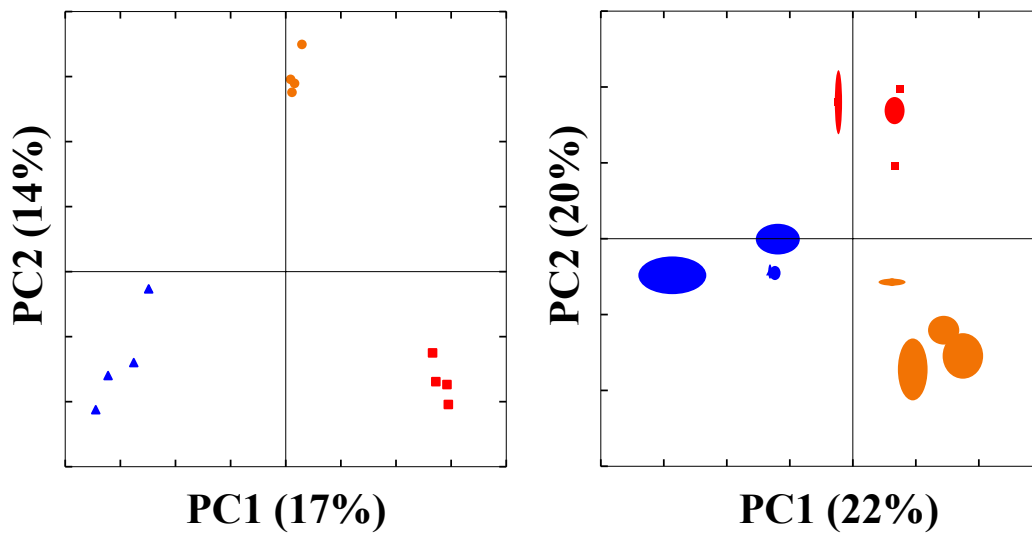
Figure 5.8 PCoA of high-throughput 16S rRNA gene sequencing (left) and T-RFLP (right) data. The T-RFLP data represent a jackknifed PCoA analysis of data from the four restriction enzymes used. Each set of four flasks (inoculum and three experimental flasks) is shown in a different color. Both techniques show that the microbial community in each flask was more similar to those in the flasks within that set than to the microbial communities in the flasks from the other sets.

These data show that the inoculum source strongly influenced the structure of microbial communities of the PBRs, an effect that has been demonstrated in other biotechnological applications (Ruiz et al., 2014). This further explains the similar structure of the microbial communities in PBR-A and PBR-A2, for which I also showed strong agreement between the T-RFLP and high-throughput sequencing data.

Because heterotrophic bacteria will be ubiquitously associated with large-scale PBR cultures, it is critical to develop rapid and sensitive techniques to track the structure of PBR microbial communities. In all of the PBRs, I detected heterotrophic bacteria in the inoculum cultures with either T-RFLP, high-throughput sequencing, or both techniques, even though light microscopy indicated that these cultures were free of heterotrophic bacteria. This finding points out the value of using sensitive genome-based methods to assess the purity of starter cultures, which seem to control the heterotrophic community structure. I demonstrated that T-RFLP (a quick and inexpensive method) was valuable for comparing and tracking the structures of different PBR microbial communities. Furthermore, I showed that using the same inoculum source preserved PBR microbial communities. Thus, in order to truly appreciate the effects of different operational or culturing conditions on the performance of PBRs and on the structure of the PBR microbial communities, it is important to use the same inoculum source. This would remove the need to account for effects of different phylotypes of heterotrophic bacteria and allow for direct comparisons between different PBR conditions.

Chapter 6

Effects of phosphate limitation on soluble microbial products and microbial community structure in semi-continuous *Synechocystis*-based photobioreactors[1]

6.1 Introduction

In the previous chapters, I developed methods to interrogate the structure of microbial communities associated with *Synechocystis*-based PBRs. Here, I demonstrate a method to manage PBR microbial communities and drive the system towards the production of *Synechocystis* biomass.

Cyanobacteria provide a potential avenue for large-scale production of biomass feedstock, as they require only sunlight, carbon dioxide, water, and stoichiometric amounts of nutrients for growth (Chisti, 2007). *Cyanobacteria* achieve higher areal yields than land plants and do not compete with human food sources (Chisti, 2008). Closed photobioreactor (PBR) systems are an effective means to cultivate large quantities of cyanobacterial biomass in small areas and offer more control over culturing conditions such as temperature and mixing when compared to open-pond PBRs (Pulz, 2001).

Recently, attention has been paid to the importance of interactions between heterotrophic bacteria and microalgae in PBRs, especially in terms of the types of heterotrophic bacteria present (Carney et al., 2014; Lakaniemi et al., 2012a; Lakaniemi et al., 2012b; Unnithan et al., 2013).

---

[1]This chapter is adapted from a manuscript accepted for publication in *Biotechnology and Bioengineering*

106

Heterotrophic bacteria can have beneficial or harmful impacts in PBR settings. On the one hand, heterotrophic metabolism recycles organic carbon produced by the *Cyanobacteria* as inorganic carbon and can reduce oxygen saturation in the PBR culture (Mouget et al., 1995). Furthermore, heterotrophic bacteria can remineralize important macronutrients, particularly nitrogen and phosphate, and can increase the availability of micronutrients, such as iron (Keshtacher-Liebson et al., 1995). On the other hand, some heterotrophic bacteria can cause lysis of cyanobacterial cells through enzymatic or antibiotic action, an obvious detriment to PBR technologies (Radhidan and Bird, 2001). Additionally, heterotrophic bacteria can consume valuable organic products if they are excreted by the *Cyanobacteria*.

Soluble microbial products (SMP) are released by all bacteria as part of their normal metabolism, and they can have deleterious impacts in many industrial biotechnological applications (Fenu et al., 2011; Jarusutthirak and Amy, 2006; Jiang et al., 2010; Ni et al., 2011a). SMP are classified as either utilization associated products (UAP) that result directly from substrate oxidation or biomass associated products (BAP) that result from hydrolysis of extracellular polymeric substances (EPS) and decay of biomass (Laspidou and Rittmann, 2002). Previous research showed that heterotrophic bacteria grew solely by utilizing SMP produced by autotrophic bacteria in nitrifying biofilms (Merkey et al., 2009; Ni et al., 2011b). Therefore, SMP produced by autotrophic *Cyanobacteria* in PBRs are likely to support the growth of heterotrophic populations. This has been demonstrated to some extent in natural settings, where heterotrophic bacteria were grown on EPS produced by *Cyanobacteria* (Giroldo et al., 2003; Li et al., 2009). Although one study examined the production of general dissolved organic carbon in microalgal PBRs

(Hulatt and Thomas, 2010), no studies have linked the dynamics of SMP to the dynamics of heterotrophic bacteria in PBRs, even though SMP represent a major pool of dissolved organic carbon in the PBR and are important drivers for the growth of heterotrophic bacteria in PBRs.

Because associations between *Cyanobacteria* and consortia of heterotrophic bacteria are ubiquitous in natural and PBR settings (Lakaniemi et al., 2012a; Lakaniemi et al., 2012b), understanding the composition of SMP produced by *Cyanobacteria* is a critical step towards the goal of managing PBR microbial communities. Here, I examine SMP in axenic PBR cultures of *Synechocystis*, a well characterized cyanobacterium that has been used as a model organism in a variety of molecular and engineering studies (Ikeuchi and Tabata, 2001; Kim et al., 2010b; Sheng et al., 2011a). I show that phosphate-limited conditions in the PBR led to increased amount of SMP derived from EPS produced by *Synechocystis*.

6.2 Materials and Methods

Synechocystis sp. PCC6803 cultures

The laboratory of Dr. Willem Vermaas (School of Life Sciences, Arizona State University) provided stock cultures of *Synechocystis* sp. PCC6803. I maintained the stock cultures in Erlenmeyer flasks with BG-11 medium (Rippka et al., 1979) bubbled with air filtered through a 0.2-μm air filter (Pall). This flask culture was used to inoculate the PBR to a starting optical density (OD) of 0.2.

PBR experiments

The PBR was a Photobioreactor FMT-150 (Photon Systems Instruments, Czech Republic), which has a volume of 350 mL and is equipped with a temperature/pH probe and bubble interrupter for all experiments. I autoclaved the cultivation chamber to ensure that it was sterile prior to inoculation and sterilized BG-11 medium prior to all experiments. The first experiment (PBRP0) used only BG-11 medium. The second experiment (PBRP+) used BG-11 medium with an addition of 350 µL of 30.5 g L^{-1} KH_2PO_4 each day beginning on Day 2 of operation. I operated each PBR at a constant temperature of 30˚C, in semi-continuous mode with a hydraulic retention time (HRT) of three days, and with constant illumination of 200 µmol PAR photons m^{-2} s^{-1}. The PBRs were bubbled with humidified air filtered through a 0.2-µm air filter (Pall). I measured optical density (OD) of the culture at a wavelength of 730 nm using a Cary-50-Bio UV-Visible spectrophotometer (Varian, Palo Alto, CA) and converted the OD_{730} value to dry weight (DW) using calibration curves for *Synechocystis*. For the calibration, DW was determined using the total suspended solids (Method 2540D) (American Public Health Association, American Water Works Association, 1998), and DW was converted to COD using 1.4 mg COD/mg DW (Rittmann and McCarty, 2001). I measured pH directly using a pH probe integrated with the Photobioreactor FMT-150 and calibrated according to the manufacturer's directions.

SMP collection

To collect SMP, I centrifuged the samples at 4,000 RPM for 20 minutes at 4˚C, collected the supernatant (containing the SMP), and stored it at 4˚C. Prior to all analyses,

SMP samples were placed into microcentrifuge tubes and centrifuged at 13,000 RPM for 5 minutes to further remove particles.

Chemical Analyses

I measured total chemical oxygen demand (TCOD) and soluble chemical oxygen demand (SCOD) using HACH TNT822 (HACH, Loveland, CO). For TCOD, 1 mL of the whole culture (biomass and SMP) and 1 mL of deionized water were added to the test vial. For SCOD, 2 mL of SMP were added to the test vials. I calculated particulate chemical oxygen demand (PCOD) as the difference between TCOD and SCOD. I measured total and reactive phosphate using the HACH TNT843 kit and Total Nitrogen and NO_3^-/NO_2^- using the HACH TNT880 kit. All HACH test vials were treated according to the manufacturer's instruction and analyzed in a HACH DR 2800 Spectrophotometer (HACH, Loveland, CO). I measured the carbohydrate fraction of the SMP with the phenol-sulfuric acid method using glucose as a standard and report values as glucose equivalents (Dubois et al., 1956). I converted glucose equivalents to COD using a conversion factor of 1.07 mg COD/mg glucose (Rittmann and McCarty, 2001). I measured the protein fraction of the SMP with a QuantiPro BCA Assay Kit (Sigma-Aldrich, St. Louis, MO) using bovine serum albumin (BSA) as a standard and converted BSA equivalents to COD using a conversion factor of 1.4 mg COD/mg BSA (Rittmann and McCarty, 2001). I measured the absorbance at 254 nm (A_{254}) using a Cary-50-Bio UV-Visible spectrophotometer (Varian, Palo Alto, CA), dissolved organic carbon (DOC) using a HACH TNT Plus 810 TOC Kit (HACH, Loveland, CO), inorganic carbon (C_i) using a TOC-V Carbon Analyzer

(Shimadzu), and chlorophyll fluorescence in the SMP (Ex. 342 nm, Em. 684 nm) using a

Cary Eclipse Spectrofluorometer (Varian, Palo Alto, CA).

Calculations

I estimated the carbon in *Synechocystis* biomass by assuming that 49.8% of dry

Synechocystis biomass is carbon (Kim et al., 2010a). I calculated the mean oxidation

number of carbon (MOC) in the SMP using the equation: $MOC = 4-1.5*(SCOD/DOC)$

(Vogel et al., 2000) and the Specific UV Absorbance at 254 nm ($SUVA_{254}$) using the

equation: $SUVA_{254} = (A_{254}/DOC)*100$ (Weishaar et al., 2003). I calculated the average

internal light intensity (AILI) in the photobioreactors from the incident light intensity and

the dry weight concentration data using the Beer-Lambert law with previously described

equations and constants (Kim et al., 2010a).

DNA extraction

For DNA extraction, 1-mL samples of the PBR culture were taken daily with a

sterile syringe and transferred to a sterile microcentrifuge tube and centrifuged (13 *g*, 3

minutes) to concentrate the biomass, which was stored at -80°C prior to DNA extraction. I

extracted total genomic DNA from PBR samples using the DNeasy Blood and Tissue Kit

(Qiagen, Valencia, CA) with the following modifications to enhance lysis: Cell pellets

were resuspended in 200 μL of lysis buffer (30 mM Tris·HCl, 10 mM EDTA, 200 mM

sucrose, pH 8.2) and incubated the mixture at 65°C for 10 minutes. I then added chicken

egg white lysozyme (Sigma Aldrich, St. Louis, MO) to a final concentration 10 mg/mL and

incubated the samples for 1 hour at 37°C. Next, I added SDS at 1% (w/v) and incubated

the samples at 56°C for 10 minutes. Finally, I added 25 μL proteinase K and 200 μL buffer AL (Qiagen) and incubated that mixture at 56°C for 30 minutes. After these additional lysis steps, I completed the DNA extraction according to the manufacturer's (Qiagen) instructions.

Quantitative Polymerase Chain Reaction (qPCR)

For specific quantification of 16S rRNA genes from *Synechocystis*, I prepared triplicate qPCR reactions containing 1X 5 PRIME RealMasterMix probe (4 U HotMaster Taq DNA polymerase, 1 mM magnesium acetate, 0.4 mM each deoxynucleotide triphosphate [dNTP] final concentration; 5 PRIME Inc., Gaithersburg, Maryland) and 300 nM each of forward primer CYAN 108F, reverse primer CYAN 377R, and probe CYAN328R carrying a 5' FAM fluorescent dye and a 3' BHQ1 quencher (Rinta-Kanto et al., 2005). I generated 16S rRNA gene control templates by PCR amplifying the entire 16S rRNA gene from *Synechocystis* using the universal bacterial primers 8F and 1525R (Löffler et al., 2000). PCR products were purified using the QiaQuick PCR Purification Kit (Qiagen) and cloned using the TOPO-TA cloning kit for sequencing (Life Techonolgies). I extracted plasmid DNA from transformants with the expected insert length using a Qiaprep Spin Minprep Kit (Qiagen) and used these plasmids to generate calibration curves with precise concentrations. For the qPCR reactions, I used the following cycling program: initial denaturation at 95°C for 2 minutes, followed by 40 cycles of 95°C for 10 seconds, 56°C for 20 seconds, 68°C for 20 seconds. I performed qPCR reactions in a Realplex 4 epGradient S Mastercycler (Eppendorf).

**High-throughput 16S rRNA gene sequencing and data analysis**

I sequenced 16S rRNA genes from the enriched consortia of heterotrophic bacteria and from representative PBR experiments using previously described methods (Caporaso et al., 2012). I amplified the V4 region of bacterial 16S rRNA genes using Golay barcoded primer set 515F/806R (Caporaso et al., 2010a). I then pooled the triplicate PCR reactions and quantified them using the Quant-iT PicoGreen dsDNA Assay Kit (Life Technologies). Next, I pooled 240 ng of each sample in and cleaned the final pool using the QiaQuick PCR Cleanup Kit (Qiagen). For loading the samples onto the Illumina MiSeq, I quantified the PCR library using the KAPA SYBR FAST Universal qPCR Kit for Illumina (KAPA Biosystems). I then sent the prepared libraries to the Microbiome Analysis Laboratory at Arizona State University for sequencing on the Illumina MiSeq. I analyzed all 16S rRNA gene sequencing data using the QIIME software using the default quality filters (Caporaso et al., 2010b; Zhou et al., 2014). All sequences that were not assigned a specific taxonomic classification and taxa that represented less than 1% of the microbial community were removed from the analyses. All analyses are of 150 bp reads in the forward direction. The sequence reads associated with this study have been uploaded to the NCBI SRA under the BioProject with accession number PRJNA266438. The accession numbers for the individual BioSamples are SAMN03283295-SAMN03283304.

6.3 Results and Discussion

**Growth of biomass and utilization of PO_4^{3-} in the PBR experiments**

Figure 6.1 shows the concentrations of soluble PO_4^{3-}-P, NO_3^--N, SO_4^{2-}-S, and C_i, as well as pH values from both PBR experiments. The soluble PO_4^{3-} in PBRP0 was rapidly

depleted and was driven below detection by Day 4, indicating severe limitation of soluble PO_4^{3-}. NO_3^- and SO_4^{2-} sulfate were amply available at all times in PBRP0. The measured pH and C_i indicated no limitation in the availability of C_i to *Synechocystis* (Kim et al., 2010a) in PBRP0. Therefore, the specific growth rate of *Synechocystis* was determined by the dilution rate (0.3 d^{-1}) from Day 5 until the end of the experiment.
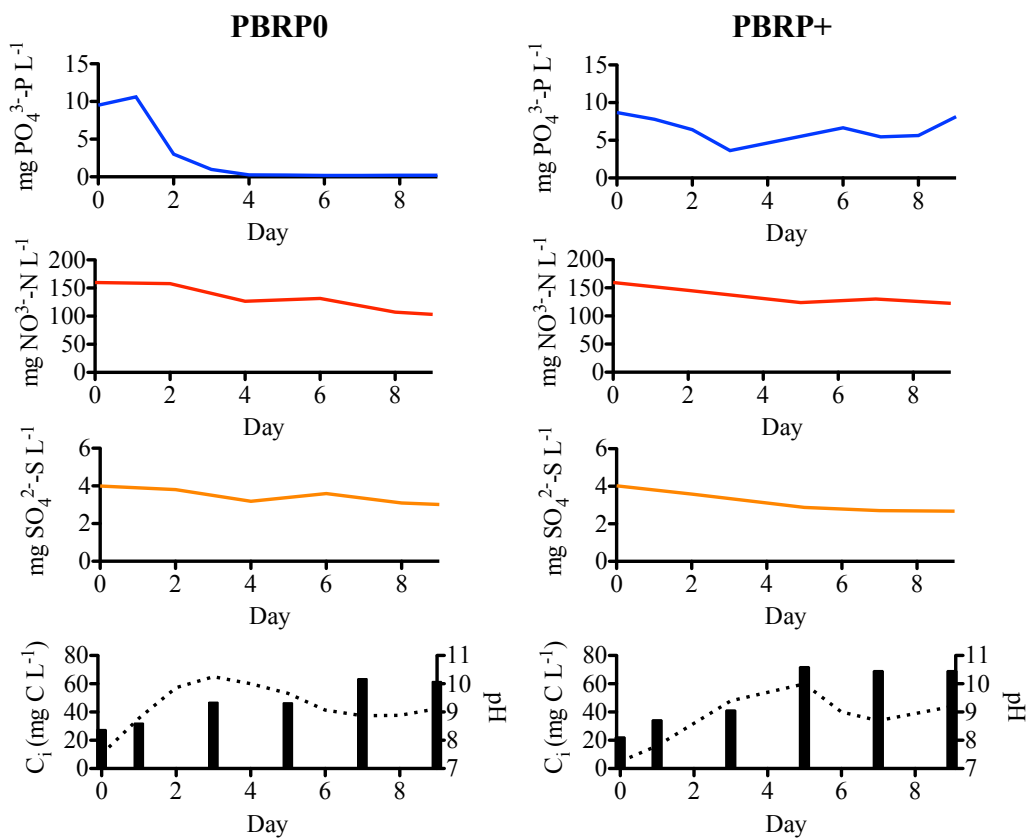
Figure 6.1 Macronutrient profiles in the two PBRs. The soluble phosphate in PBRP0 was completely depleted by Day 4, while all other macronutrients were available. PBRP+ had no nutrient limitation.

Furthermore, the average internal light irradiance (AILI) demonstrated that light also was not limiting the growth of *Synechocystis* as shown in **Figure 6.2**. Thus, the sole factor limiting the growth of *Synechocystis* in PBRP0 was PO_4^{3-}. In PBRP+, the PO_4^{3-} concentration was never depleted and began to increase after Day 3. As in PBRP0, PBRP+ had no limitations in NO_3^-, SO_4^{2-}, C_i, or light.
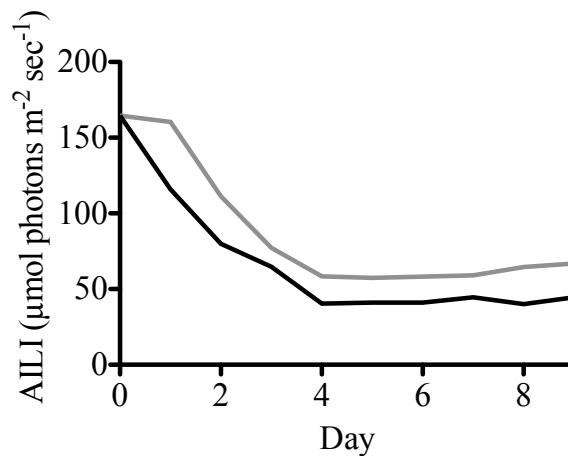
Figure 6.2 AILI in the two PBRs. PBRP0 (grey line) and PBRP+ (black line) both had available light for the entire experiment, indicating that there was no light limitation in either PBR.

Figure 6.3 shows the OD_{730} and daily concentrations of TCOD and PCOD from both PBR experiments. PBRP0 achieved a maximum OD_{730} of 1.7 on Day 4 and decayed slightly in the following days. PBRP+ achieved a maximum OD_{730} of 2.4 on Day 5, and the OD_{730} remained stable for the rest of the experiment. The TCOD in PBRP0 reached 850 mg COD L^{-1}, and the TCOD in PBRP+ reached around 1100 mg COD L^{-1}; these results are consistent with previously reported TCOD and biomass concentrations in

Synechocystis PBRs operated under similar conditions (Kim et al., 2010b). The greatest difference between the TCOD and PCOD values occurred in PBRP0 during the period of decay following the depletion of PO_4^{3-} (Day 4 to Day 9). The PCOD values from both PBRs mirror the OD_{730} measurements making PCOD a good representation of the energy stored in biomass in each PBR.
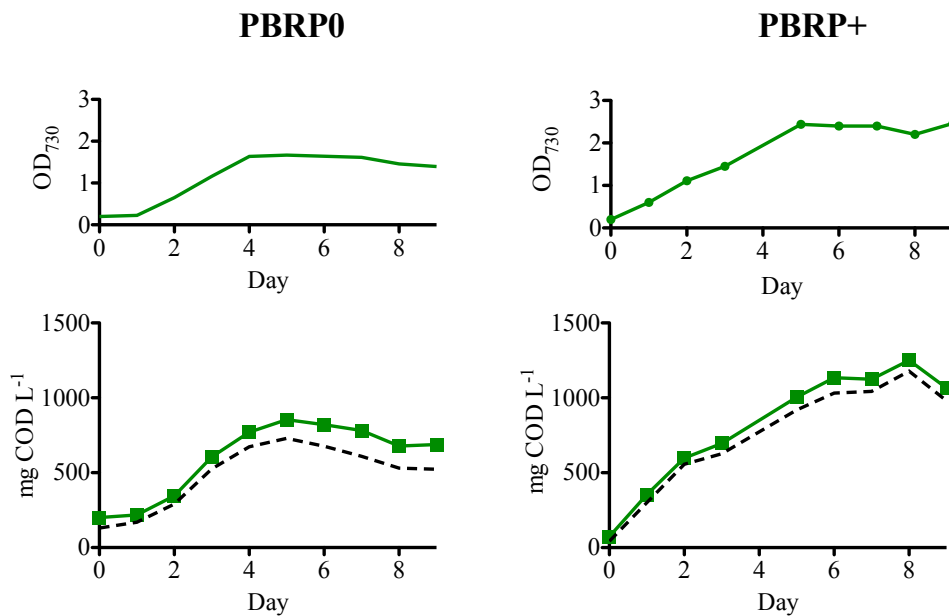

Figure 6.3 OD_{730} (above), TCOD (below squares), and PCOD (below dashed lines) from the two PBR experiments. PBRP+ had a much higher OD_{730} value than did PBRP0. PBRP0 produced around 800 mg TCOD L^{-1} while PBRP+ produced 1200 mg TCOD L^{-1}. TCOD was substantially greater than PCOD only in PBRP0. The OD_{730} values track well with the PCOD values.

SMP Analysis

SMP quantity can be gauged by concentrations of SCOD and DOC. **Figure 6.4** shows that the SCOD and DOC values were higher in PBRP0 than in PBRP+. The greatest difference occurred from Day 5 to Day 9, which is when PBRP0 had severe PO_4^{3-} limitation. From Day 4 until the end of the experiment, the SCOD in PBRP0 averaged 150 mg COD L^{-1}. In PBRP+, the SCOD averaged only 82 mg COD L^{-1} from Day 4 until the end of the experiment. Thus, despite the increased production of PCOD in PBRP+, the SCOD was significantly lower than in PBRP0. The DOC in PBRP0 rose to concentrations of over 60 mg C L^{-1}, while the DOC in PBRP+ stayed relatively steady at 40 mg C L^{-1} during this period.
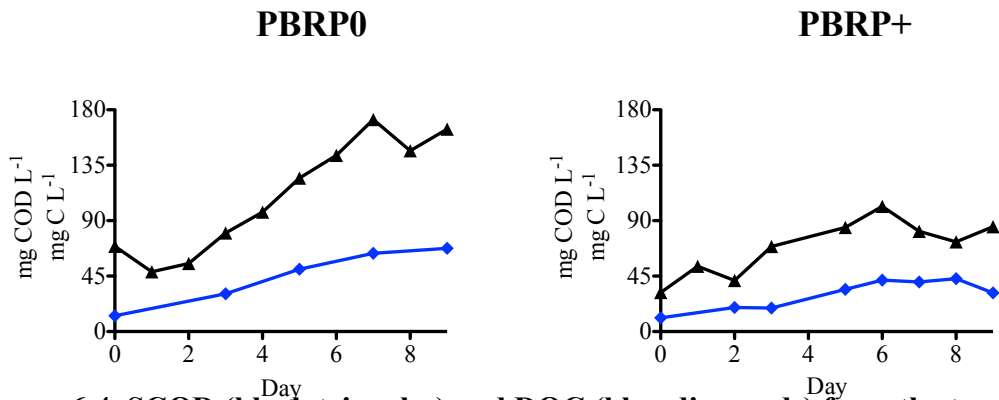
PBRP0   **PBRP+**

Figure 6.4 SCOD (black triangles) and DOC (blue diamonds) from the two PBR experiments. PBRP0 produced more SCOD and DOC than PBRP+ indicating higher SMP concentrations in PBRP0.

117

Table 6.1 shows important values and ratios from the final day of operation from both PBRs. The MOC of the SMP in PBRP0 was much lower than in PBRP+, meaning that the C in the SMP in PBRP0 was more reduced and energy dense than the SMP-C in PBRP+. SCOD represented 31% of the PCOD in PBRP0, but only 7% of the PCOD in PBRP+.

Table 6.1 Important ratios and values from the final day of PBR operation. PBRP0 had a lower MOC value and a higher ratio of SCOD:PCOD and DOC:Biomass C			
	MOC	**SCOD:PCOD**	**DOC:Biomass C**
PBRP0	0.35	0.31	0.31
PBRP+	1.6	0.078	0.13

Likewise, the DOC represented 31% of the calculated carbon in *Synechocystis* biomass in PBRP0; again, this is much more than the 13% in PBRP+. Thus, much more of the light energy captured by *Synechocystis* photosynthesis was diverted to SMP in PBRP0 than in PBRP+.

Figure 6.5 shows concentrations of total carbohydrates (glucose equivalents converted to COD) and protein (BSA equivalents converted to COD) in the SMP. In PBRP0, carbohydrates accounted for the majority (>70%) of the SCOD, especially during the period in which no net growth was observed (Day 4 to Day 9), and the concentration of total carbohydrates continued to rise even after biomass production had ceased. The MOC values from PBRP0 (0.35) also support the claim that the SMP in this PBR was mostly composed of carbohydrates (an MOC of 0). The concentration of soluble protein remained relatively stable for the entire experiment, accounting for ~20% of the SCOD. The

majority of soluble carbohydrates probably were derived from shearing and hydrolysis of *Synechocystis*-generated EPS, which is rich in polysaccharides (Panoff et al., 1988). Therefore, *Synechocystis* may have used EPS as a sink for electrons and photosynthetically assimilated carbon during the period when phosphate limitation halted the production of active biomass. This type of mechanism for the disbursal of excess electrons and carbon under nutrient stresses has been observed and proposed in many different algal and cyanobacterial systems (Bratbak and Thingstad, 1985; Huang et al., 2007; Wyatt et al., 2014).
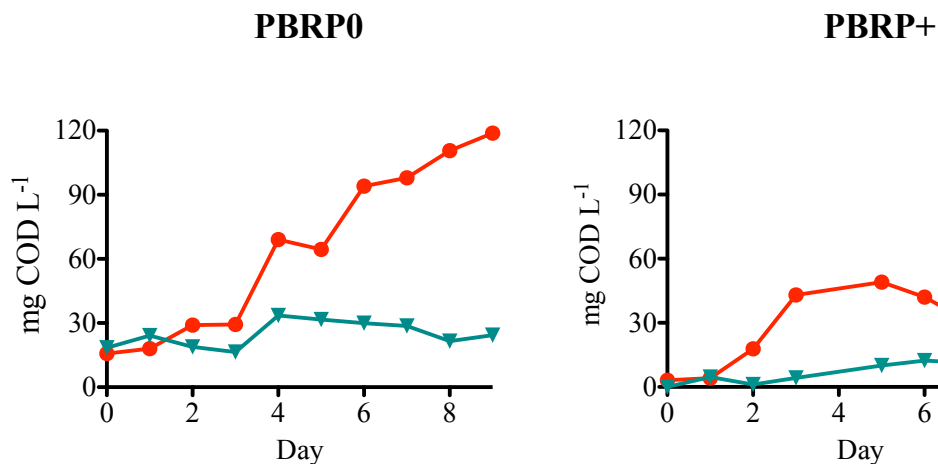
PBRP0

PBRP+

Figure 6.5 Total carbohydrates (red) and protein (teal) from the two PBR experiments.
In PBRP0, carbohydrates account for around 70% of the SCOD by the end of the experiment. In PBRP+, however, carbohydrates account for a much smaller fraction of the SCOD.

In PBRP+, carbohydrates accounted for only 39% of the SCOD, and the protein fraction contained 15% of the SCOD. Since the sum of these two fractions represented only about half of the SCOD in PBRP+, the main source of SMP in PBRP+ probably was not carbohydrates from EPS, but from other sources, such as the direct release of

utilization-associated products or biomass lysis/decay (Laspidou and Rittmann, 2002).

This difference in the composition of SMP further supports the notion that the increase in

SMP carbohydrates in PBRP0 was triggered by phosphate limitation, which did not occur

in PBRP+. Both PBRs showed much lower proportions of soluble protein than soluble

carbohydrates, even though EPS produced by *Synechocystis* is known to be 40% (w/w)

protein (Panoff et al., 1988), indicating that the carbohydrate fraction of *Synechocystis* EPS

is more resistant to microbial degradation than the protein fraction. This helps to explain

the rise in soluble carbohydrates in PBRP0 with no concurrent increase in the soluble

proteins.

I used specific UV absorbance at a wavelength of 254 nm ($SUVA_{254}$) to estimate

the aromatic content of the PBR SMP. **Table 6.2** shows the A_{254} and $SUVA_{254}$ values from

the final day of operation of both PBRs. PBRP0 had a higher A_{254} than PBRP+, probably a

result of PBR having more total SMP.

Table 6.2 A_{254} and $SUVA_{254}$ on the final day of PBR operation. Both PBRs had similar $SUVA_{254}$ values		
	A_{254} **(cm^{-1})**	$SUVA_{254}$ **(L m^{-2} mg^{-1})**
PBRP0	0.27	0.40
PBRP+	0.17	0.41

However, both PBRs had similar $SUVA_{254}$ values. Therefore, the relative aromatic

content of SMP in *Synechocystis*-based PBRs was not affected by phosphate limitation. I

also measured fluorescence of chlorophyll in the SMP **(Figure 6.6)**. In PBRP0, the

fluorescence of the SMP decreased over time, while it increased in PBRP+. Thus,

chlorophyll (and possibly other pigment molecules) was more dominant in the SMP of

PBRP+ than in PBRP0. These pigments probably were released upon cell lysis, supporting

that a significant portion of the SMP in PBRP+ was derived from biomass lysis/decay, not

from EPS.
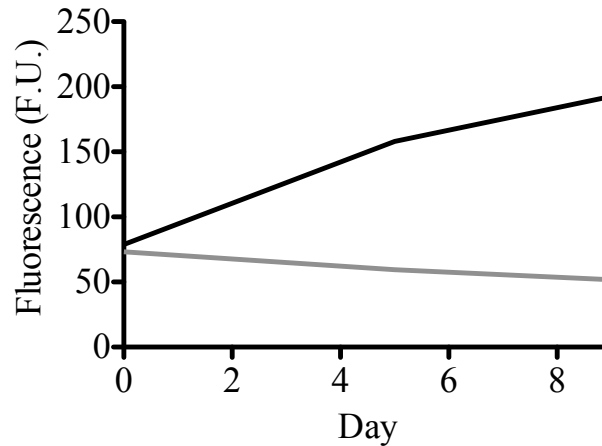
**Figure 6.6 Fluorescence from the SMP in the
two PBRs.** PBRP0 (grey line) showed a slight
decrease in fluorescence while PBRP+ (black line)
showed a great increase in fluorescence.

Microbial community analysis

I analyzed the microbial communities in both PBRs using high-throughput

sequencing of 16S rRNA gene libraries. **Figure 6.7** shows the bacteria present in both

PBRs over the course of each experiment at order-level definition. As expected, bacteria

from the order *Chroococcales*, to which *Synechocystis* belongs, dominated both PBRs. In

PBRP0, the most abundant heterotrophic bacteria were from the orders *Xanthomonadales*,

Bacillales, Rhizobiales, *Actinomycetales,* and *Caulobacteriales*. Upon inoculation (Day 0)

of PBRP0, *Xanthomonadales* were the most dominant heterotrophs. However, by Day 2

bacteria from the order *Bacillales* became the most dominant heterotrophs and remained as such until the end of the experiment (Day 9), while the *Xanthomonadales* diminished rapidly.
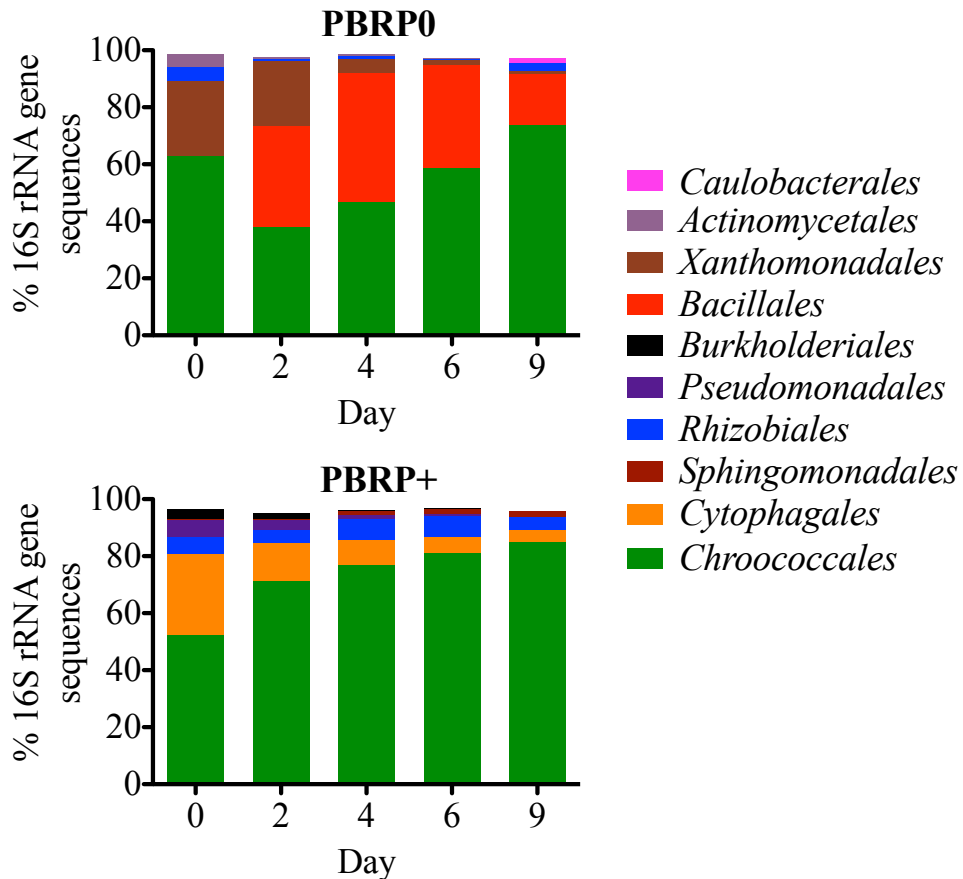
Figure 6.7 16S rRNA gene sequencing analysis of the two PBR experiments. In both PBRs, heterotrophic bacteria were detected, but each PBR had different types of heterotrophic bacteria present. In both PBRs, *Synechocystis* was the dominant microbe. However, PBRP0 had a substantially higher proportion of heterotrophic bacteria.

In PBRP+, the heterotrophic bacteria detected were from the orders *Cytophagales*, *Rhizobiales*, *Pseudomonadales*, *Sphingomonadales*, and *Burkholderiales*. *Cytophagales* were the dominant heterotrophic bacteria at the beginning of PBRP+ operation, but, decreased with time and, by the end of the experiment, were present in relatively the same

proportion as the *Rhizobiales*, representing about 4% of the 16S rRNA gene sequences. In PBRP0, the relative proportion of *Chroococcales* dropped between Day 0 and Day 2 and then increased. In contrast, the proportion of *Chroococcales* in PBRP$_+$ rose steadily over the duration of the experiment. Therefore, the microbial communities in both PBRs had heterotrophic bacteria present, but the ratios of *Chroococcales* to total heterotrophic bacteria and compositions of the heterotrophic communities were unique from one another.

To specifically track the growth of *Synechocystis*, I used qPCR to target only *Cyanobacteria*. **Figure 6.8** shows the number of 16S rRNA gene copies per liter from *Cyanobacteria* from both PBRs. In PBRP0, the 16S rRNA copies from *Cyanobacteria* increased slowly over the first few days and then remained relatively stable for the rest of the experiment. This indicates that the heterotrophic bacteria were likely being washed out of PBRP0, as the relative proportion of *Cyanobacteria* increased with no corresponding increase in the 16S rRNA gene copies from *Cyanobacteria*.

In contrast, the 16S rRNA gene copies from *Cyanobacteria* in PBRP+ rose rapidly at the beginning of the experiment and became stable after that. The qPCR data from both PBRs agree well with the OD_{730} and PCOD data that *Synechocystis* was the dominant microbe in both systems and that the bulk of the COD in the system was derived from *Synechocystis*. The qPCR, 16S rRNA gene sequencing, OD_{730}, and PCOD data also agree that PBRP+ had higher total amounts of *Synechocystis* and also higher relative proportion of *Synechocystis* than PBRP0. This supports that avoiding phosphate depletion improved production of *Synechocystis* biomass and enriched the community for *Synechocystis* in the PBR setting.
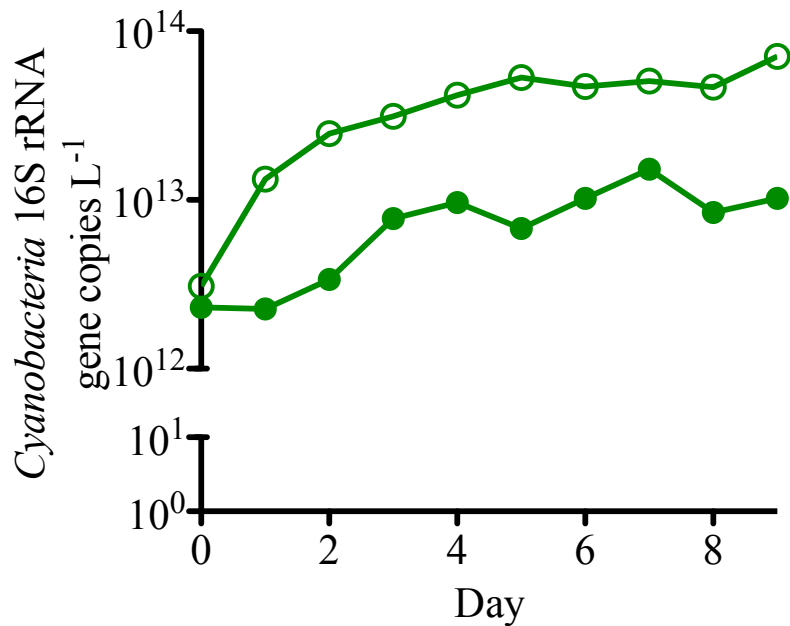
Figure 6.8 Measurement of 16S rRNA gene copies from
Cyanobacteria **in PBRP0 (closed circles) and PBRP+ (open
circles).** PBRP+ had more 16S rRNA gene copies per liter
than PBRP0, indicating a higher density of *Synechocystis* cells
in PBRP+.

Figure 6.9 shows high-throughput 16S rRNA gene sequence analysis of only the

heterotrophic bacteria from the two PBRs at genus-level definition on the final day of

operation. The most dominant heterotrophic bacterium in PBRP0 was a single species

belonging to the genus *Bacillus*. *Bacillus* spp. have been shown to produce extracellular

polysaccharases that can hydrolyze complex polysaccharides, such as glucan and xanthan

gum (Sutherland, 1999). Furthermore, some *Bacilliales* spp. are known to have the ability

to solubilize phosphate from organic and inorganic compounds (Rodríguez and Fraga,

1999).
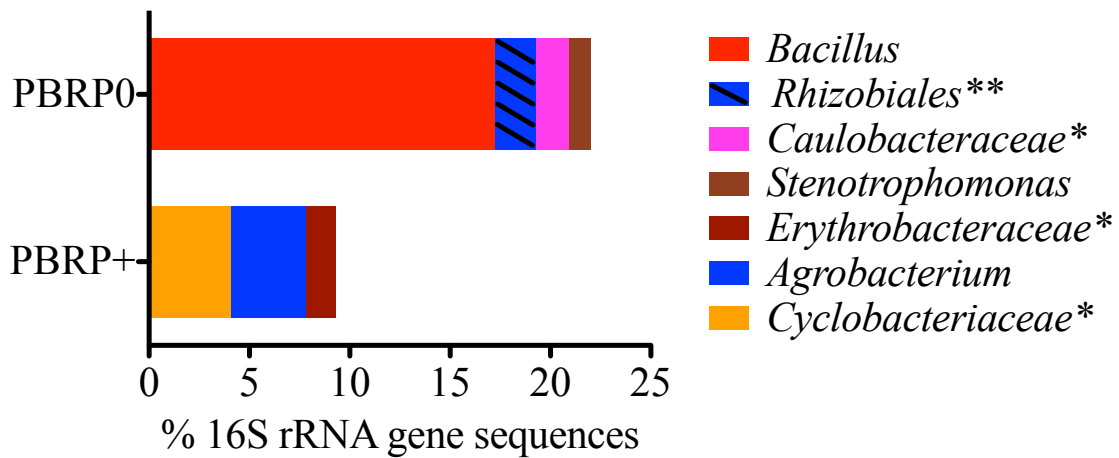
Figure 6.9 Identification of heterotrophic bacteria at the genus-level on the final day of PBR operation. The most abundant heterotrophic bacterium in PBRP0 was a single species belonging to the genus *Bacillus*, which represented the vast majority of the bacteria from the order *Bacillales*. In PBRP+, a single species belonging to the family *Cycolobacteriaceae* and a single species belonging to the genus *Agrobacterium* were the most dominant heterotrophic bacteria.

* A single operational taxonomic unit that was not defined below the family-level
** A single operational taxonomic unit that was not defined below the order-level

Thus, this bacterium may have also been involved in phosphate cycling in PBRP0 due to its ability to recycle phosphate from diverse sources. Other heterotrophic bacteria detected in PBRP0 included a single *Rhizobiales* sp., a single *Caulobacteraceae* sp., and a *Stenotrophomonas* sp.

In PBRP+, the most dominant heterotrophic bacteria belonged to a single species in the family *Cyclobacteriaceae* and a single species in the genus *Agrobacterium*. Members of the family *Cyclobacteriaceae* have previously been found in association with cultures of

the microalga *Dunaliella* sp. SAG 19.3 (Le Chevanton et al., 2013), as well as in association with macroalgae and have been isolated from numerous environments and have diverse metabolic capabilities (Anil Kumar et al., 2012). *Agrobacterium* spp. are common soil bacteria most studied for being the causative agent of crown gall tumors and other diseases in many plants (Matthysse, 2006). Thus, these bacteria are probably well suited to grow on different types of biomass. A single *Erythrobacteraceae* sp. was also detected in PBRP+.

I analyzed the SMP and microbial communities in two xenic PBR cultures of the model cyanobacterium *Synechocystis* sp. PCC6803. One PBR was limited by phosphate availability (PBRP0), while the other was not (PBRP+). PBRP0 produced less total biomass, but more SMP than PBRP+. Carbohydrates, probably originating from hydrolysis of EPS, dominated the SMP in PBRP0, while the SMP in PBRP+ appeared to be dominated by compounds released as a result of cell lysis or decay. Both PBRs showed relatively low concentrations of soluble protein. I detected heterotrophic bacteria in both PBRs. PBRP0 had a higher proportion of heterotrophic bacteria and less total *Synechocystis* than PBRP+. The greater proportion of heterotrophic bacteria in $PBRP_0$ surely was the result of the higher SMP release in this PBR. Because the purpose of the PBR is to generate lipid-rich *Synechocystis* biomass (Sheng et al., 2011b), it is most desirable to minimize SMP production, which represents a loss of energy and organic carbon. Thus, it is important to avoid nutrient limitations so that *Synechocystis* can use the available energy to produce biomass, rather than SMP.

Chapter 7

Conclusions and Recommendations for future work

7.1 Summary of Work

Cyanobacteria and eukaryotic microalgae are photoautotrophic microorganisms that have gained much attention as a useful source of biomass that can be used to produce transportation fuels and help to displace fossil fuel resources (Chisti, 2008; Rittmann, 2008). However, a number of technical barriers must be overcome to ensure the viability of these technologies on industrial scales. For example, it is generally accepted that large-scale cultures of photoautotrophic microorganisms must be viewed as biologically diverse microbial communities (Smith et al., 2009), yet few studies have assessed the implications of microbial ecology in photobioreactor (PBR) operations (Lakaniemi et al., 2012a; Lakaniemi et al., 2012b). As in natural systems, the growth of *Cyanobacteria* in PBRs is usually going to be associated with the growth of heterotrophic microorganisms, particularly bacteria (Li et al., 2011).

Interactions between microorganisms play important roles in many biotechnological processes including wastewater treatment and microbial fuel cell technologies. Often, the performance of these systems can be improved by optimizing the conditions such that the microbial communities carry out the desired processes (Rittmann et al., 2006). This same logic holds true for PBRs, as heterotrophic bacteria can positively or negatively affect the growth of cyanobacteria. Examples of positive effects would be providing carbon dioxide, reducing oxygen saturation, increasing the solubility of micronutrients, and recycling nutrients from decying biomass (Giroldo et al., 2003; Keshtacher-Liebson et al., 1995; Mouget et al., 1995). However, some heterotrophic bacteria may prey upon *Cyanobacteria*

and cause a termination of the culture (Radhidan and Bird, 2001). Thus, it is critical to

mitigate the negative effects of heterotrophic bacteria while promoting the positive effects.

This work focused on understanding the microbial ecology in (PBR) cultures of

Synechocystis sp. PCC6803 (*Synechocystis*).

In *Synechocystis*-based PBRs, soluble microbial products (SMP) derived from

extracellular polymeric substances (EPS) and decaying biomass probably are the major

electron donors and carbon sources available for heterotrophic bacteria to use for growth

(Laspidou and Rittmann, 2002; Merkey et al., 2009). Thus, understanding the origin,

composition, and fate of SMP is critical to understanding the linkage between

Synechocystis and heterotrophic bacteria in these systems.

7.2 Conclusions and Synthesis

Chapter 2 focused on understanding the phylogenetic distribution of heterotrophic

bacteria that associate with *Synechocystis*-based PBRs through culturing methods,

including isolation and enrichment of bacteria, and through culture-independent high-

throughput 16S rRNA gene sequencing. The work demonstrated that a wide variety of

bacterial taxa could be found in association with *Synechocystis*-based PBRs, including

bacteria from the phyla *Proteobacteria, Bacilli*, *Bacteroidetes*, *Actinobacteria*, and

Firmicutes. These results were further confirmed through high-throughput 16S rRNA gene

sequencing in Chapters 4, 5, and 6.

I expected that a high diversity of heterotrophic bacteria would be found in

association with *Synechocystis*-based PBRs, as this has been documented for other

microalgal systems (Berg et al., 2009; Carney et al., 2014; Eiler and Bertilsson, 2004;

Krohn-Molt et al., 2013; Li et al., 2011). Furthermore, I expected that the microbial communities in *Synechocystis*-based PBRs would be similar to those in natural settings in terms of the types of heterotrophic bacteria present. This was confirmed, as the heterotrophic bacteria found in association with *Synechocystis*-based PBRs were common soil and freshwater bacteria, some of which had previously been found in association with *Cyanobacteria* in natural systems (Berg et al., 2009; Livermore et al., 2013; Newton et al., 2011). Taken together, these data indicate that these diverse taxa of heterotrophic bacteria all possess the functional genes necessary to succeed in *Synechocystis*-based PBRs.

In Chapter 3, I expanded upon this by investigating the growth kinetics of heterotrophic bacteria that were isolated or enriched as a part of the work in Chapter 2. Here, I measured the growth of these heterotrophic bacteria on several different labile carbon substrates and on recalcitrant carbon substrates. I found that the growth rates of the heterotrophic bacteria from the PBRs were similar to those of heterotrophic bacteria from oligotrophic environments (Cho and Giovannoni, 2004; Eiler et al., 2003). To predict the growth of heterotrophic bacteria in PBR settings, I used a mathematical modeling approach using the empirically derived kinetic constants to represent the PBR as a chemostat bioreactor. The model results showed that concentrations of labile substrates above 1 mg COD/L could support the growth of heterotrophic bacteria at hydraulic retention times well below the typical operating range of *Synechocystis*-based PBRs. Thus, the work in this chapter set forth the important notion that heterotrophic bacteria will almost certainly be present in mass cultivations of *Synechocystis* and will likely be an intrinsic part of PBR operations.

The work in Chapter 4 was conducted under the major hypothesis that, in 16S rRNA gene based assays, *Synechocystis* would be overwhelmingly dominant due to being present in higher cell numbers and due to the high degree of polyploidy (carrying multiple genome copies in each cell) found in *Synechocystis* (Chisholm and Binder, 1995; Griese et al., 2011). The goal of Chapter 4 was to develop a molecular subtraction method to specifically remove *Synechocystis* 16S rRNA genes from pools of DNA extracted from *Synechocystis*-based PBRs. The purpose of this was to improve the resolution of heterotrophic bacteria in 16S rRNA gene based assays. However, the technique did not significantly improve the resolution of non-*Synechocystis* bacteria in high-throughput 16S rRNA gene sequencing analyses of PBR microbial communities. This was due mostly to the sensitivity of the high-throughput sequencing technology. From this, I rejected the hypothesis that *Synechocystis* was overwhelmingly dominant in 16S rRNA gene-based assays and concluded that high-throughput sequencing was sufficient to capture the true bacterial diversity in PBR cultures. This work also demonstrated that, in some *Synechocystis*-based PBRs, 16S rRNA gene sequences from heterotrophic bacteria greatly outnumber those from *Synechocystis*.

In Chapter 5, I investigated the effect of the inoculum on the structure of PBR microbial communities. First, I showed that four PBRs that were operated under identical conditions produced different biomass concentrations but that two of the PBR experiments, which were started using the same inoculum culture, produced the most similar biomass concentrations while the other two, each started with unique inocula, produced different biomass concentrations. I then showed that the microbial communities in the two PBRs

that were started using the same inoculum culture were very similar in terms of the types

and relative abundances of heterotrophic bacteria present in the PBR. However, the PBRs

that were started using different inoculum cultures each had unique microbial communities

in terms of the heterotrophic bacteria detected and their relative abundances. I then

expanded upon this work by conducting a series of batch experiments in which I compared

the microbial communities in flask cultures to the microbial communities in the inoculum

cultures used to start the different flasks. I found that the flask microbial communities

were most similar to the microbial communities in the inoculum culture that as used to start

the flask in terms of both the types of heterotrophic bacteria detected and the relative

abundance of the heterotrophic bacteria. From this, I concluded that the microbial

community in the inoculum used to start a PBR culture has a very strong impact on the

structure of the microbial community that develops in that PBR.

The work in Chapter 6 focused on understanding the relationship between

phosphorus availability, SMP production, and microbial community structure in PBRs. I

found that a phosphate-limited PBR had higher concentration of SMP that was correlated

with lower biomass density and higher relative proportion of heterotrophic bacteria than

did a PBR that had ample available phosphate. Furthermore, the phosphate-limited PBR

had a higher ratio of SMP to biomass than did the PBR with ample phosphate. The SMP in

the phosphate limited PBR was dominated by carbohydrates that were probably derived

from *Synechocystis* EPS, while the SMP in the PBR with ample phosphate had a lower

proportion of carbohydrates and appeared to be mostly derived from biomass decay, due to

a higher relative proportion of proteins and aromatic compounds. These data led me to

conclude that, under phosphate-limited conditions, *Synechocystis* shunts excess electrons and photoassimilated carbon to the production of EPS. Conversely, in conditions with ample phosphate, *Synechocystis* can use the electrons and photoassimilated carbon to produce cell mass. Thus, maintaining phosphate availability in *Synechocystis*-based PBRs is critical for managing SMP production. In turn, this manages the heterotrophic population by removing the most readily available substrates. These data strongly agree with previous studies in natural systems showing that phytoplankton produce more dissolved organic matter in low-nutrient conditions than they do in nutrient replete conditions (Unnithan et al., 2013).

Initially, I had hypothesized that the polyploidy of *Synechocystis* (Griese et al., 2011) would cause it to be greatly overestimated in 16S rRNA gene-based molecular analyses of PBR microbial communities. However, the high-throughput sequencing data presented in Chapters 4-6 indicated that this was not the case. Indeed, in some cases, the relative abundance of 16S rRNA gene sequences assigned to *Synechocystis* was lower than that of the 16S rRNA gene sequences assigned to taxa of heterotrophic bacteria. This indicates that, in some PBRs, heterotrophic bacteria can exist in vastly greater cell numbers than does *Synechocystis*. In terms of the microbial community structure, Chapters 2, 4, 5, and 6 showed that some PBR microbial communities are dominated by a single heterotrophic bacterium while others have a more even distribution of several types of heterotrophic bacteria. Furthermore, these chapters showed that once heterotrophic bacteria had colonized a PBR, the community did not change greatly over time so long as there were no changes to the operational parameters of the PBR.

132

7.3 Recommendations for future work

Effects of heterotrophic bacteria on growth of *Synechocystis*

A critical continuation of the work in Chapter 2 is to determine the effects the different heterotrophic bacteria isolated from PBR cultures have on the growth of *Synechocystis*. The first goal of this study would be to determine which bacteria, if any, promote the growth of *Synechocystis* in controlled co-cultures. One study showed that, in general, the addition of heterotrophic bacteria decreased the maximum growth rate of a microalgal species, although no mechanism for this was proposed (Le Chevanton et al., 2013), while another showed that the addition of heterotrophic bacteria increased the growth of microalgae by recycling organic carbon as carbon dioxide (Bai et al., 2014). If a suitable co-culture partner were to be identified, it could be used as a "probiotic" to control the microbial community in *Synechocystis*-based PBRs (Verschuere et al., 2000).

Metagenomics and metatranscriptomics to discover genes important for heterotrophic growth in PBRs

Comprehensive understanding of heterotrophic bacteria in PBRs requires knowledge of the genes most important for colonization and sustained growth in PBRs. As demonstrated throughout this work, diverse phylotypes of heterotrophic bacteria are associated with PBR cultures, meaning that the genes that confer success in the PBR are equally widespread. Metagenomic studies would help to uncover the most abundant genes, which would inform about the most important substrates in the PBR. Furthermore, metagenomic studies would help determine which heterotrophic bacteria are most

responsible for hydrolysis of large polymers such as EPS and which heterotrophic bacteria consume the lower molecular weight compounds. Metatranscriptomic studies can uncover temporal shifts in gene expression (Gilbert et al., 2008). PBR metagenomes will certainly be dominated by sequences from *Synechocystis*. However, as demonstrated in Chapters 4, 5, and 6, deep sequencing techniques are sensitive enough to detect gene sequences from heterotrophic bacteria even in a high background of *Synechocystis* genes.

Analysis of extracellular enzyme activity in PBRs

Another method to uncover the function of heterotrophic bacteria in PBRs is through direct measurement of extracellular enzyme activity. Extracellular enzymes such as ß-glucosidases are critical for the biodegradation of EPS (Sutherland, 1999), while peptidases, and alkaline phosphatases are important for biodegradation of polypeptides and for remineralization of phosphate from biomass, respectively (Morrissey et al., 2013). Bacterial extracellular enzymes have been shown to be important for the cycling of carbon and other nutrients in marine and soil habitats (Cañizares et al., 2011; Dang et al., 2008; Piontek et al., 2011). Thus, these enzymes probably play an equally important role in sustaining heterotrophic growth in *Synechocystis*-based PBRs. An exploration of extracellular enzyme activity in PBRs would be a strong addition to the metagenomic work described above.

Couple PBRs with water treatment

Another application of PBR technologies is coupling production of microalgal biomass with treatment of wastewater streams (Carney et al., 2014; Su et al., 2011;

Unnithan et al., 2013). Interactions between photosynthetic and heterotrophic microorganisms will be especially important in these systems as most wastewater streams have heterotrophic bacteria present (Carney et al., 2014; Su et al., 2011). Already, several groups have shown promising results for using microalgae or cyanobacteria to remove nitrogen and phosphorous from municipal or industrial wastewater streams (Mata et al., 2010).

References

Abed RMM, Dobretsov S, Sudesh K. 2009. Applications of *Cyanobacteria* in biotechnology. *J. Appl. Microbiol.* **106**:1–12.

Abed RMM, Zein B, Al-Thukair A, de Beer D. 2007. Phylogenetic diversity and activity of aerobic heterotrophic bacteria from a hypersaline oil-polluted microbial mat. *Syst. Appl. Microbiol.* **30**:319–30.

Abed RMM. 2010. Interaction between *Cyanobacteria* and aerobic heterotrophic bacteria in the degradation of hydrocarbons. *Int. Biodeterior. Biodegradation* **64**:58–64.

American Public Health Association, American Water Works Association WEF. 1998. Standard Methods for the Examination of Water and Wastewater. Ed. Lenore Clesceri, Arnold Greenberg, Andrew Eaton 20th ed.

Anil Kumar P, Srinivas TNR, Madhu S, Sravan R, Singh S, Naqvi SWA, Mayilraj S, Shivaji S. 2012. *Cecembia lonarensis* gen. nov., sp. nov., a haloalkalitolerant bacterium of the family *Cyclobacteriaceae*, isolated from a haloalkaline lake and emended descriptions of the genera *Indibacter*, *Nitritalea* and *Belliella*. *Int. J. Syst. Evol. Microbiol.* **62**:2252–8.

Bai X, Lant P, Pratt S. 2014. The contribution of bacteria to algal growth by carbon cycling. *Biotechnol. Bioeng.* **112**:688-95.

Barreiro DL, Prins W, Ronsse F, Brilman W. 2013. Hydrothermal liquefaction (HTL) of microalgae for biofuel production: State of the art review and future prospects. *Biomass and bioenergy* **53**:113–27.

Berg KA, Lyra C, Sivonen K, Paulin L, Suomalainen S, Tuomi P, Rapala J. 2009. High diversity of cultivable heterotrophic bacteria in association with cyanobacterial water blooms. *ISME J.* **3**:314–25.

Biddanda B, Ogdahl M, Cotner J. 2001. Dominance of bacterial metabolism in oligotrophic relative to eutrophic waters. *Limnol. Oceanogr.* **46**:730–39.

Böni J, Shah C, Flepp M, Lüthy R, Schüpbach J. 2004. Detection of low copy numbers of HIV-1 proviral DNA in patient PBMCs by a high-input, sequence-capture PCR (Mega-PCR). *J. Med. Virol.* **72**:1–9.

Bratbak G, Thingstad TF. 1985. Phytoplankton-bacteria interactions: an apparent paradox? Analysis of a model system with both competition and commensalism. *Mar. Ecol. - Prog. Ser.* **25**:23–30.

Brennan L, Owende P. 2010. Biofuels from microalgae—A review of technologies for production, processing, and extractions of biofuels and co-products. *Renew. Sustain. Energy Rev.* **14**:557–77.

Buchan A, LeCleir GR, Gulvik CA, González JM. 2014. Master recyclers: features and functions of bacteria associated with phytoplankton blooms. *Nat. Rev. Microbiol.* **12**:686–98.

Button DK. 1985. Kinetics of nutrient-limited transport and microbial growth. *Microbiol. Rev.* **49**:270–97.

Cañizares R, Benitez E, Ogunseitan OA. 2011. Molecular analyses of β-glucosidase diversity and function in soil. *Eur. J. Soil Biol.* **47**:1–8.

Caporaso JG, Lauber CL, Walters WA, Berg-Lyons D, Lozupone CA, Turnbaugh PJ, Fierer N, Knight R. 2010a. Global patterns of 16S rRNA diversity at a depth of millions of sequences per sample. *PNAS.* **108**:4516-22.

Caporaso JG, Kuczynski FD, Stombaugh J, Bittinger K, Bushman FD, Costello EK, Fierer N, Pena AG, Goodrich JK, Gordon JI, Huttley GA, Kelley ST, Knights D, Koenig JE, Ley RE, Lozupone CA, McDonald D, Muegge BD, Pirrung M, Reeder J, Sevinsky JR, Turnbaugh PJ, Walters WA, Widmann J, Yatsunenko T, Zaneveld J, Knight R. 2010b. QIIME allows analysis of high-throughput community sequencing data. *Nat. Methods* **7**:335–36.

Caporaso JG, Lauber CL, Walters WA, Berg-Lyons D, Huntley J, Fierer N, Owens SM, Betley J, Fraser L, Bauer M, Gormley N, Gilbert JA, Smith G, Knight R. 2012. Ultra-high-throughput microbial community analysis on the Illumina HiSeq and MiSeq platforms. *ISME J.* **6**:1621-24.

Carney LT, Reinsch SS, Lane PD, Solberg OD, Jansen LS, Williams KP, Trent JD, Lane TW. 2014. Microbiome analysis of a microalgal mass culture growing in municipal wastewater in a prototype OMEGA photobioreactor. *Algal Res.* **4**:52-61.

Le Chevanton M, Garnier M, Bougaran G, Schreiber N, Lukomska E, Bérard JB, Fouilland E, Bernard O, Cadoret J-P. 2013. Screening and selection of growth-promoting bacteria for *Dunaliella* cultures. *Algal Res.* **2**:212–22.

Chisholm SW, Binder BJ. 1995. Cell cycle regulation in marine *Synechococcus* sp. strains. *Appl. Environ. Microbiol.* **61**:707–17.

Chisti Y. 2007. Biodiesel from microalgae. *Biotechnol. Adv.* **25**:294–306.

Chisti Y. 2008. Biodiesel from microalgae beats bioethanol. *Trends Biotechnol.* **26**:126–31.

Chisti Y. 2013. Constraints to commercialization of algal fuels. *J. Biotechnol.* **167**:201–14.

Cho J, Giovannoni SJ. 2004. Cultivation and growth characteristics of a diverse group of oligotrophic marine gammaproteobacteria. *Appl. Environ. Microbiol.* **70**:432–440.

Dang H, Zhu H, Wang J, Li T. 2008. Extracellular hydrolytic enzyme screening of culturable heterotrophic bacteria from deep-sea sediments of the Southern Okinawa Trough. *World J. Microbiol. Biotechnol.* **25**:71–9.

Dionisi HM, Harms G, Layton AC, Gregory IR, Parker J, Hawkins SA, Robinson KG, Sayler GS. 2003. Power analysis for real-time PCR quantification of genes in activated sludge and analysis of the variability introduced by DNA extraction. *Appl. Environ. Microbiol.* **69**:6597–604.

Dubois M, Gilles KA, Hamilton JK, Rebers PA, Smith F. 1956. Colorimetric method for determination of sugars and related substances. *Agriculture* **28**:350–56.

Ducat DC, Way JC, Silver PA. 2011. Engineering *Cyanobacteria* to generate high-value products. *Trends Biotechnol.* **29**:95–103.

Eiler A, Bertilsson S. 2004. Composition of freshwater bacterial communities associated with cyanobacterial blooms in four Swedish lakes. *Environ. Microbiol.* **6**:1228–43.

Eiler A, Langenheder S, Bertilsson S, Tranvik LJ. 2003. Heterotrophic bacterial growth efficiency and community structure at different natural organic carbon concentrations. *Appl. Environ. Microbiol.* **69**:3701–09.

Fenu A, Wambecq T, Thoeye C, De Gueldre G, Van de Steene B. 2011. Modelling soluble microbial products (SMPs) in a dynamic environment. *Desalin. Water Treat.* **29**:210–7.

Fisher ML, Allen R, Luo Y, Curtiss R. 2013. Export of extracellular polysaccharides modulates adherence of the cyanobacterium *Synechocystis*. *PLoS One* **8**:e74514.

Fortuna AM, Marsh TL, Honeycutt CW, Halteman WA. 2011. Use of primer selection and restriction enzymes to assess bacterial community diversity in an agricultural soil used for potato production via terminal restriction fragment length polymorphism. *Appl. Microbiol. Biotechnol.* **91**:1193–202.

Gilbert JA, Field D, Huang Y, Edwards R, Li W, Gilna P, Joint I. 2008. Detection of large numbers of novel sequences in the metatranscriptomes of complex marine microbial communities. *PLoS One* **3**:e3042.

Giroldo D, Augusto A, Vieira H. 2003. Relative increase of deoxy sugars during microbial degradation of an extracellular polysaccharide released by a tropical freshwater *Thalassiosira* sp. (*Bacillariophyceae*). *J. Phycol.* **39**:1109–15.

Griese M, Lange C, Soppa J. 2011. Ploidy in *Cyanobacteria. FEMS Microbiol. Lett.* **323**:124–31.

Gross R, Leach M, Bauen A. 2003. Progress in renewable energy. *Environ. Int.* **29**:105–22.

Gur-Reznik S, Katz I, Dosoretz CG. 2008. Removal of dissolved organic matter by granular-activated carbon adsorption as a pretreatment to reverse osmosis of membrane bioreactor effluents. *Water Res.* **42**:1595–605.

Holmberg A, Blomstergren A, Nord O, Lukacs M, Lundeberg J, Uhlén M. 2005. The biotin-streptavidin interaction can be reversibly broken using water at elevated temperatures. *Electrophoresis* **26**:501–10.

Huang WJ, Lai CH, Cheng YL. 2007. Evaluation of extracellular products and mutagenicity in *Cyanobacteria* cultures separated from a eutrophic reservoir. *Sci. Total Environ.* **377**:214–23.

Huang XP, Huang LM, Yue WZ. 2003. The characteristics of nutrients and eutrophication in the Pearl River estuary, South China. *Mar. Pollut. Bull.* **47**:30–6.

Hube AE, Heyduck-Söller B, Fischer U. 2009. Phylogenetic classification of heterotrophic bacteria associated with filamentous marine *Cyanobacteria* in culture. *Syst. Appl. Microbiol.* **32**:256–65.

Hulatt CJ, Thomas DN. 2010. Dissolved organic matter (DOM) in microalgal photobioreactors: a potential loss in solar energy conversion? *Bioresour. Technol.* **101**:8690–7.

Ikeuchi M, Tabata S. 2001. *Synechocystis* sp. PCC 6803 - a useful tool in the study of the genetics of *Cyanobacteria. Photosynth. Res.* **70**:73–83.

Imai A, Fukushima T, Matsushige K, Hwan Kim Y. 2001. Fractionation and characterization of dissolved organic matter in a shallow eutrophic lake, its inflowing rivers, and other organic matter sources. *Water Res.* **35**:4019–28.

Jarusutthirak C, Amy G. 2006. Role of soluble microbial products (SMP) in membrane fouling and flux decline. *Environ. Sci. Technol.* **40**:969–74.

Jiang T, Kennedy MD, De Schepper V, Nam SN, Nopens I, Vanrolleghem PA, Amy G. 2010. Characterization of soluble microbial products and their fouling impacts in membrane bioreactors. *Environ. Sci. Technol.* **44**:6642–8.

139

Kaltschmitt M, Thran D, Smith KR. 2003. Renewable energy from biomass. *Encycl. Phys. Sci. Technol.* **14**:203–28.

Kelly EN, Schindler DW, Hodson P V, Short JW, Radmanovich R, Nielsen CC. 2010. Oil sands development contributes elements toxic at low concentrations to the Athabasca River and its tributaries. *PNAS.* **107**:16178-83.

Keshtacher-Liebson E, Hadar Y, Chen Y. 1995. Oligotrophic bacteria enhance algal growth under iron-deficient conditions. *Appl. Environ. Microbiol.* **61**:6–9.

Kim HW, Vannela R, Zhou C, Harto C, Rittmann BE. 2010a. Photoautotrophic nutrient utilization and limitation during semi-continuous growth of *Synechocystis* sp. PCC6803. *Biotechnol. Bioeng.* **106**:553–63.

Kim HW, Vannela R, Zhou C, Rittmann BE. 2010b. Nutrient acquisition and limitation for the photoautotrophic growth of *Synechocystis* sp. PCC6803 as a renewable biomass source. *Biotechnol. Bioeng.* **108**:277–85.

Knoop H, Zilliges Y, Lockau W, Steuer R. 2010. The metabolic network of *Synechocystis* sp. PCC 6803: systemic properties of autotrophic growth. *Plant Physiol.* **154**:410–22.

Koeck DE, Pechtl A, Zverlov VV, Schwarz WH. 2014. Genomics of cellulolytic bacteria. *Curr. Opin. Biotechnol.* **29**:171–83.

Kovárová-Kovar K, Egli T. 1998. Growth kinetics of suspended microbial cells: from single-substrate-controlled growth to mixed-substrate kinetics. *Microbiol. Mol. Biol. Rev.* **62**:646–66.

Krohn-Molt I, Wemheuer B, Alawi M, Güllert S, Schmeisser C, Grundhoff A, Daniel R, Streit WR. 2013. Metagenome survey of a multispecies and alga-associated biofilm revealed key elements of bacterial-algal interactions in photobioreactors. *Appl. Environ. Microbiol.* **79**:6196–206.

Labarre J, Chauvat F, Thuriaux P. 1989. Insertional mutagenesis by random cloning of antibiotic resistance genes into the genome of the cyanobacterium *Synechocystis* strain PCC 6803. *J. Bacteriol.* **171**:3449–57.

Lai YS, Parameswaran P, Li A, Baez M, Rittmann BE. 2014. Effects of pulsed electric field treatment on enhancing lipid recovery from the microalga, *Scenedesmus*. *Bioresour. Technol.* **173**:457–61.

Lakaniemi AM, Intihar VM, Tuovinen OH, Puhakka JA. 2012a. Growth of *Chlorella vulgaris* and associated bacteria in photobioreactors. *Microb. Biotechnol.* **5**:69–78.

Lakaniemi AM, Intihar VM, Tuovinen OH, Puhakka JA. 2012b. Growth of *Dunaliella tertiolecta* and associated bacteria in photobioreactors. *J. Ind. Microbiol. Biotechnol.* **39**:1357–65.

Laspidou CS, Rittmann BE. 2002. A unified theory for extracellular polymeric substances, soluble microbial products, and active and inert biomass. *Water Res.* **36**:2711–20.

Li N, Zhang L, Li F, Wang Y, Zhu Y, Kang H, Wang S, Qin S. 2011. Metagenome of microorganisms associated with the toxic cyanobacteria *Microcystis aeruginosa* analyzed using the 454 sequencing platform. *Chinese J. Oceanol. Limnol.* **29**:505–13.

Li P, Cai Y, Shi L, Geng L, Xing P, Yu Y, Kong F, Wang Y. 2009. Microbial degradation and preliminary chemical characterization of *Microcystis* exopolysaccharides from a cyanobacterial water bloom of Lake Taihu. *Int. Rev. Hydrobiol.* **94**:645–55.

Liu L, Li Y, Li S, Hu N, He Y, Pong R, Lin D, Lu L, Law M. 2012. Comparison of next-generation sequencing systems. *J. Biomed. Biotechnol.* **2012**:251364.

Liu WT, Marsh TL, Cheng H, Forney LJ. 1997. Characterization of microbial diversity by determining terminal restriction fragment length polymorphisms of genes encoding 16S rRNA. *Appl. Environ. Microbiol.* **63**:4516–22.

Liu X, Fallon S, Sheng J, Curtiss R. 2011a. CO2-limitation-inducible green recovery of fatty acids from cyanobacterial biomass. *PNAS.* **108**:6905–8.

Liu X, Sheng J, Curtiss R. 2011b. Fatty acid production in genetically modified *Cyanobacteria*. *PNAS.* **108**:6899–904.

Livermore JA, Emrich SJ, Tan J, Jones SE. 2013. Freshwater bacterial lifestyles inferred from comparative genomics. *Environ. Microbiol.* **16**:746-58.

Löffler FE, Sun Q, Li J, Tiedje JM. 2000. 16S rRNA gene-based detection of tetrachloroethene-dechlorinating *Desulfuromonas* and *Dehalococcoides* species. *Appl. Environ. Microbiol.* **66**:1369–74.

Mata TM, Martins AA, Caetano NS. 2010. Microalgae for biodiesel production and other applications: A review. *Renew. Sustain. Energy Rev.* **14**:217–32.

Matthysse AG. 2006. The genus *Agrobacterium*. In: Dworkin, M, Falkow, S, Rosenberg, E, Schleifer, KH, Stackebrandt, E, editors. *The Prokaryotes*. Springer New York, pp. 91–114.

Merkey B V, Rittmann BE, Chopp DL. 2009. Modeling how soluble microbial products (SMP) support heterotrophic bacteria in autotroph-based biofilms. *J. Theor. Biol.* **259**:670–83.

Miller PD, Robert W. 2011. Should fracking stop? *Nature.* **477**:271–75.

Morrissey EM, Berrier DJ, Neubauer SC, Franklin RB. 2013. Using microbial communities and extracellular enzymes to link soil organic matter characteristics to greenhouse gas production in a tidal freshwater wetland. *Biogeochemistry*. **117**:473-90.

Morton O. 2006. A new day dawning? Silicon Valley sunrise. *Nature.* **443**:19–22.

Mouget JL, Dakhama A, Lavoie MC, de la Noue J. 1995. Algal growth enhancement by bacteria: Is consumption of photosynthetic oxygen involved? *FEMS Microbiol. Ecol.* **18**:35–44.

Newton RJ, Jones SE, Eiler A, McMahon KD, Bertilsson S. 2011. A guide to the natural history of freshwater lake bacteria. *Microbiol. Mol. Biol. Rev.* **75**:14–49.

Ni BJ, Rittmann BE, Yu HQ. 2011a. Soluble microbial products and their implications in mixed culture biotechnology. *Trends Biotechnol.* **29**:454–63.

Ni BJ, Xie WM, Chen YP, Fang F, Liu SY, Ren TT, Sheng GP, Yu HQ, Liu G, Tian YC. 2011b. Heterotrophs grown on the soluble microbial products (SMP) released by autotrophs are responsible for the nitrogen loss in nitrifying granular sludge. *Biotechnol. Bioeng.* **108**:2844–52.

Ontiveros-Valencia A, Ilhan ZE, Kang D-W, Rittmann B, Krajmalnik-Brown R. 2013. Phylogenetic analysis of nitrate- and sulfate-reducing bacteria in a hydrogen-fed biofilm. *FEMS Microbiol. Ecol.* **85**:158–67.

Ortiz-Marquez JCF, Nascimento MD, Zehr JP, Curatti L. 2013. Genetic engineering of multispecies microbial cell factories as an alternative for bioenergy production. *Trends Biotechnol.* **31**:521–9.

Panoff JM, Priem B, Morvan H, Joset F. 1988. Sulphated exopolysaccharides produced by two unicellular strains of *Cyanobacteria*, *Synechocystis* PCC 6803 and 6714. *Arch. Microbiol.* **150**:558–63.

Parham NJ, Picard FJ, Peytavi R, Gagnon M, Seyrig G, Gagné P-A, Boissinot M, Bergeron MG. 2007. Specific magnetic bead based capture of genomic DNA from clinical samples: application to the detection of group B streptococci in vaginal/anal swabs. *Clin. Chem.* **53**:1570–6.

Pérez-Pantoja D, Donoso R, Agulló L, Córdova M, Seeger M, Pieper DH, González B. 2012. Genomic analysis of the potential for aromatic compounds biodegradation in *Burkholderiales*. *Environ. Microbiol.* **14**:1091–117.

Peterson CH, Anderson SS, Cherr GN, Ambrose RF, Anghera S, Bay S, Blum M, Condon R, Dean TA, Graham M, Guzy M, Hampton S, Joye S, Lambrinos J, Mate B, Meffert D, Sean P. 2012. A tale of two spills: novel science and policy implications of an emerging new oil spill model. *Bioscience* **62**:461–9.

Piontek J, Handel N, De Bodt C, Harlay J, Chou L, Engel A. 2011. The utilization of polysaccharides by heterotrophic bacterioplankton in the Bay of Biscay (North Atlantic Ocean). *J. Plankton Res.* **33**:1719–35.

Prasad S, Pratibha MS, Manasa P, Buddhi S, Begum Z, Shivaji S. 2013. Diversity of chemotactic heterotrophic bacteria associated with arctic *Cyanobacteria. Curr. Microbiol.* **66**:64–71.

Pulz O. 2001. Photobioreactors: production systems for phototrophic microorganisms. *Appl. Microbiol. Biotechnol.* **57**:287–93.

Purvina S, Bechemin C, Balode M, Verite C, Arnaud C, Maestrini SY. 2010. Release of available nitrogen from river-discharged dissolved organic matter by heterotrophic bacteria associated with the cyanobacterium *Microcystis aeruginosa. Est. J. Ecol.* **59**:184–96.

Radhidan KK, Bird DF. 2001. Role of predatory bacteria in the termination of a cyanobacterial bloom. *Microb. Ecol.* **41**:97–105.

Rees GN, Baldwin DS, Watson GO, Perryman S, Nielsen DL. 2004. Ordination and significance testing of microbial community composition derived from terminal restriction fragment length polymorphisms: application of multivariate statistics. *Antonie Van Leeuwenhoek* **86**:339–47.

Rinta-Kanto JM, Ouellette AJA, Boyer GL, Twiss MR, Bridgeman TB, Wilhelm SW. 2005. Quantification of toxic *Microcystis* spp. during the 2003 and 2004 blooms in western Lake Erie using quantitative real-time PCR. *Environ. Sci. Technol.* **39**:4198–205.

Rippka R, Deruelles J, Waterbury JB, Herdman M, Stainer RY. 1979. Generic assignments, strain histories and properties of pure cultures of *Cyanobacteria. J. Gen. Microbiol.* **111**:1–61.

Ritalahti KM, Amos BK, Sung Y, Wu Q, Koenigsberg SS, Loffler FE. 2006. Quantitative PCR targeting 16S rRNA and reductive dehalogenase genes simultaneously monitors multiple *Dehalococcoides* strains. *Appl. Environ. Microbiol.* **72**:2765–74.

Rittmann BE, McCarty PL. 2001. Environmental Biotechnology: Principles and Applications. New York: McGraw Hill Companies Inc.

Rittmann BE. 2008. Opportunities for renewable bioenergy using microorganisms. *Biotechnol. Bioeng.* **100**:203–12.

Rittmann BE, Hausner M, Löffler F, Love NG, Muyzer G, Okabe S, Oerther DB, Peccia J, Raskin L, Wagner M. 2006. A vista for microbial ecology and environmental biotechnology. *Environ. Sci. Technol.* **40**:1096–103.

Rittmann BE, Krajmalnik-Brown R, Halden RU. 2008. Pre-genomic, genomic and post-genomic study of microbial communities involved in bioenergy. *Nat. Rev. Microbiol.* **6**:604–12.

Rodriguez D, Longo A V, Zamudio KR. 2012. Magnetic capture hybridization of *Batrachochytrium dendrobatidis* genomic DNA. *J. Microbiol. Methods* **90**:156–9.

Rodríguez H, Fraga R. 1999. Phosphate solubilizing bacteria and their role in plant growth promotion. *Biotechnol. Adv.* **17**:319–39.

Ruiz V, Ilhan ZE, Kang DW, Krajmalnik-Brown R, Buitrón G. 2014. The source of inoculum plays a defining role in the development of MEC microbial consortia fed with acetic and propionic acid mixtures. *J. Biotechnol.* **182-183**:11–18.

Ryan RP, Monchy S, Cardinale M, Taghavi S, Crossman L, Avison MB, Berg G, van der Lelie D, Dow JM. 2009. The versatility and adaptation of bacteria from the genus *Stenotrophomonas*. *Nat. Rev. Microbiol.* **7**:514–25.

Sakai T, Ishizuka K, Kato I. 2003. Isolation and characterization of a fucoidan-degrading marine bacterium. *Mar. Biotechnol.* **5**:409–16.

Saxena RC, Adhikari DK, Goyal HB. 2009. Biomass-based energy fuel through biochemical routes: A review. *Renew. Sustain. Energy Rev.* **13**:167–178.

Schirmer A, Rude MA, Li X, Popova E, del Cardayre SB. 2010. Microbial biosynthesis of alkanes. *Science.* **329**:559–562.

Schmidt W, Drews G, Weckesser J, Mayer H. 1980. Lipopolysaccharides in four strains of the unicellular cyanobacterium *Synechocystis*. *Arch. Microbiol.* **127**:217–22.

Schütte UME, Abdo Z, Bent SJ, Shyu C, Williams CJ, Pierson JD, Forney LJ. 2008. Advances in the use of terminal restriction fragment length polymorphism (T-RFLP) analysis of 16S rRNA genes to characterize microbial communities. *Appl. Microbiol. Biotechnol.* **80**:365–80.

Sheng J, Kim HW, Badalamenti JP, Zhou C, Sridharakrishnan S, Krajmalnik-Brown R, Rittmann BE, Vannela R. 2011a. Effects of temperature shifts on growth rate and lipid

characteristics of *Synechocystis* sp. PCC6803 in a bench-top photobioreactor. *Bioresour. Technol.* **102**:11218–25.

Sheng J, Vannela R, Rittmann BE. 2011b. Evaluation of methods to extract and quantify lipids from *Synechocystis* PCC 6803. *Bioresour. Technol.* **102**:1697–703.

Sheng J, Vannela R, Rittmann BE. 2011c. Evaluation of cell-disruption effects of pulsed-electric-field treatment of *Synechocystis* PCC 6803. *Environ. Sci. Technol.* **45**:3795–802.

Smith CJ, Danilowicz BS, Clear AK, Costello FJ, Wilson B, Meijer WG. 2005. T-Align, a web-based tool for comparison of multiple terminal restriction fragment length polymorphism profiles. *FEMS Microbiol. Ecol.* **54**:375–80.

Smith VH, Sturm BSM, Denoyelles FJ, Billings SA. 2009. The ecology of algal biodiesel production. *Trends Ecol. Evol.* **25**:301–9.

Solomon S, Plattner GK, Knutti R, Friedlingstein P. 2009. Irreversible climate change due to carbon dioxide emissions. *PNAS.* **106**:1704–9.

Su Y, Mennerich A, Urban B. 2011. Municipal wastewater treatment and biomass accumulation with a wastewater-born and settleable algal-bacterial culture. *Water Res.* **45**:3351–8.

Sutherland IW. 1999. Polysaccharases for microbial exopolysaccharides. *Carbohydr. Polym.* **38**:319–28.

Tamura K, Peterson D, Peterson N, Stecher G, Nei M, Kumar S. 2011. MEGA5: molecular evolutionary genetics analysis using maximum likelihood, evolutionary distance, and maximum parsimony methods. *Mol. Biol. Evol.* **28**:2731–9.

Thompson DE, Rajal VB, De Batz S, Wuertz S. 2006. Detection of *Salmonella* spp . in water using magnetic capture hybridization combined with PCR or real-time PCR. *J. Water Health* **4**:67–75.

Torres CI, Krajmalnik-Brown R, Parameswaran P, Marcus AK, Wanger G, Gorby YA, Rittmann BE. 2009. Selecting anode-respiring bacteria based on anode potential: phylogenetic, electrochemical, and microscopic characterization. *Environ. Sci. Technol.* **43**:9519–24.

Uduman N, Qi Y, Danquah MK, Forde GM, Hoadley A. 2010. Dewatering of microalgal cultures: A major bottleneck to algae-based fuels. *J. Renew. Sustain. Energy* **2**:012701.

Unnithan VV, Unc A, Smith GB. 2013. Mini-review: A priori considerations for bacteria–algae interactions in algal biofuel systems receiving municipal wastewaters. *Algal Res.* **4**:35-40.

Vermaas WFJ. 1998. Gene modifications and mutation mapping to study the function of photosystem II. *Methods Enzymol.* **297**:293–310.

Verschuere L, Rombaut G, Sorgeloos P, Verstraete W. 2000. Probiotic bacteria as biological control agents in aquaculture. *Microbiol. Mol. Biol. Rev.* **64**:655–71.

Vogel F, Harf J, Hug A, Von Rohr PR. 2000. The mean oxidation number of carbon (MOC)-a useful concept for describing oxidation processes. *Water Res.* **34**:2689–702.

Weisburg WG, Barns SM, Pelletier DA, Lane DJ. 1991. 16S ribosomal DNA amplification for phylogenetic study. *J. Bacteriol.* **173**:697–703.

Weishaar JL, Aiken GR, Bergamaschi BA, Fram MS, Fujii R, Mopper K. 2003. Evaluation of specific ultraviolet absorbance as an indicator of the chemical composition and reactivity of dissolved organic carbon. *Environ. Sci. Technol.* **37**:4702–8.

Wyatt KH, Tellez E, Woodke RL, Bidner RJ, Davison IR. 2014. Effects of nutrient limitation on the release and use of dissolved organic carbon from benthic algae in Lake Michigan. *Freshw. Sci.* **33**:557-67.

Zavřel T, Sinetova MA, Búzová D, Literáková P, Červený J. 2015. Characterization of a model cyanobacterium *Synechocystis* sp. PCC 6803 autotrophic growth in a flat-panel photobioreactor. *Eng. Life Sci.* **15**:122–32.

Zhang H, Parameswaran P, Badalamenti J, Rittmann BE, Krajmalnik-Brown R. 2011. Integrating high-throughput pyrosequencing and quantitative real-time PCR to analyze complex microbial communities. *Methods Mol. Biol.* **733**:107–28.

Zhou C, Ontiveros-Valencia A, Cornette de Saint Cyr L, Zevin AS, Carey SE, Krajmalnik-Brown R, Rittmann BE. 2014. Uranium removal and microbial community in a H2-based membrane biofilm reactor. *Water Res.* **64**:255–64.

Ziv-El M, Popat SC, Parameswaran P, Kang DW, Polasko A, Halden RU, Rittmann BE, Krajmalnik-Brown R. 2012. Using electron balances and molecular techniques to assess trichoroethene-induced shifts to a dechlorinating microbial community. *Biotechnol. Bioeng.* **109**:2230–9.
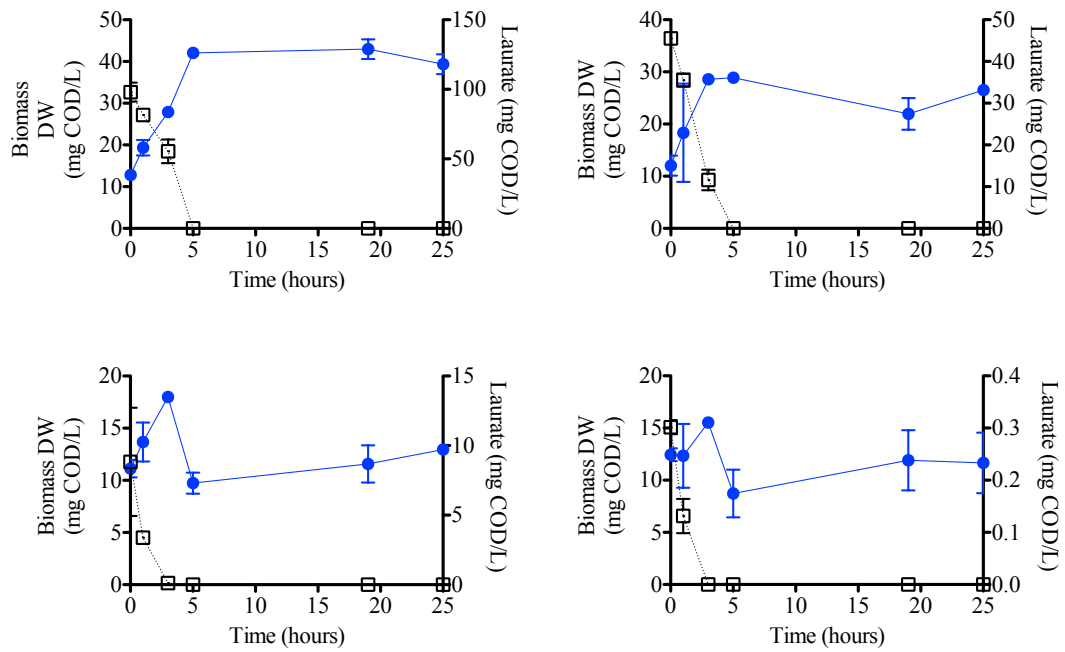
APPENDIX A

BACTERIAL GROWTH CURVES AND MONOD FITS
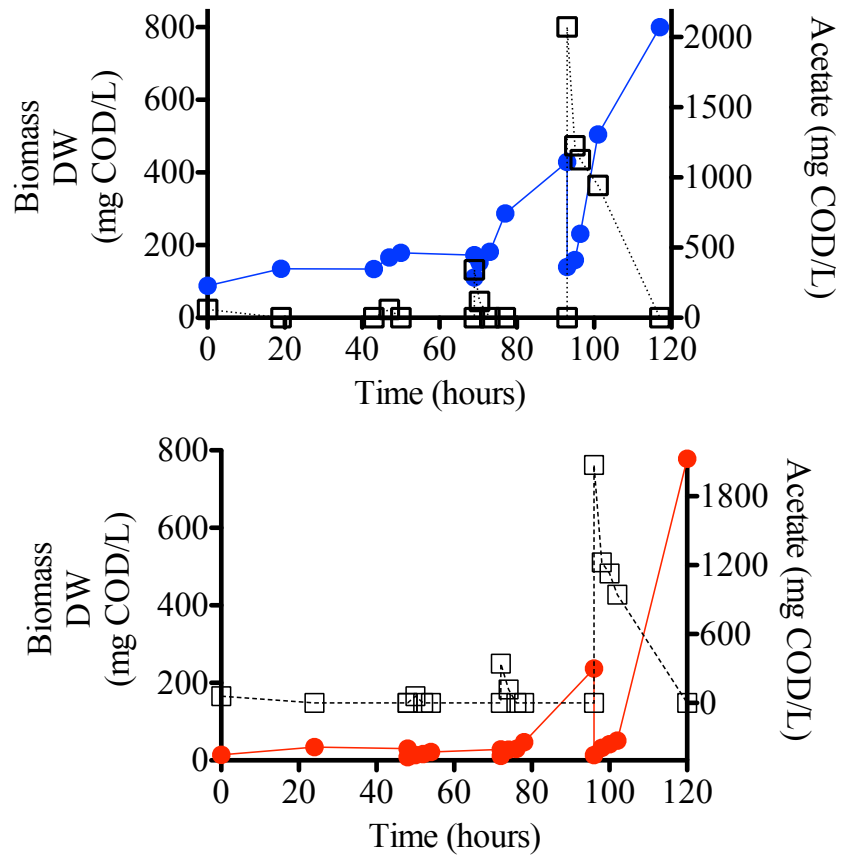
Figure A.1 Representative growth curves for *B2* (above blue) and *ENR1* (below red) on acetate (black) as a sole carbon source.
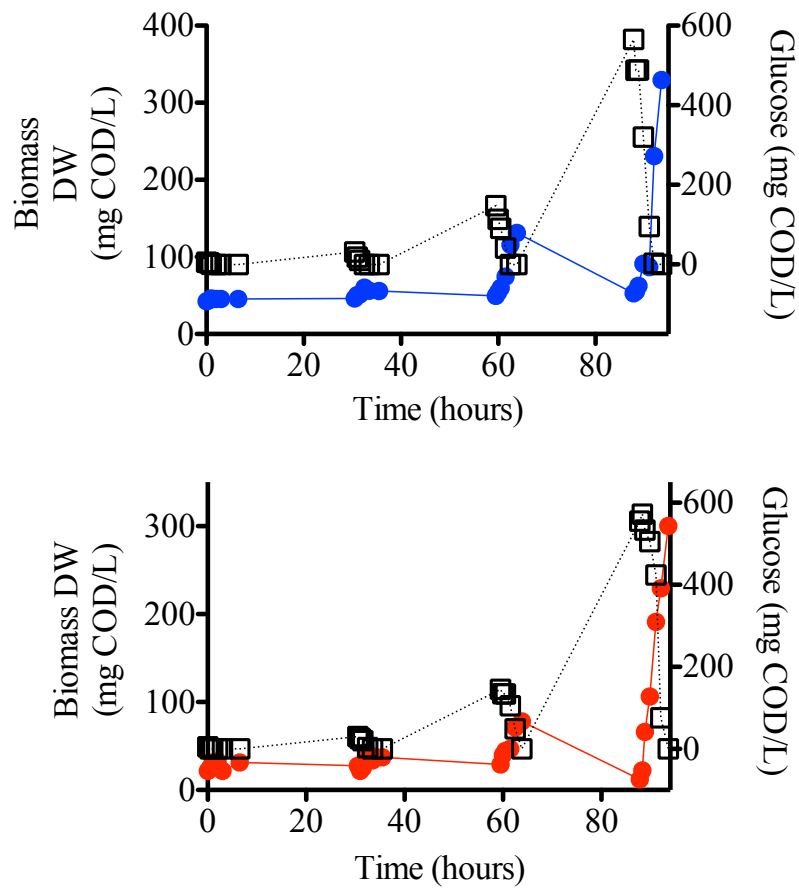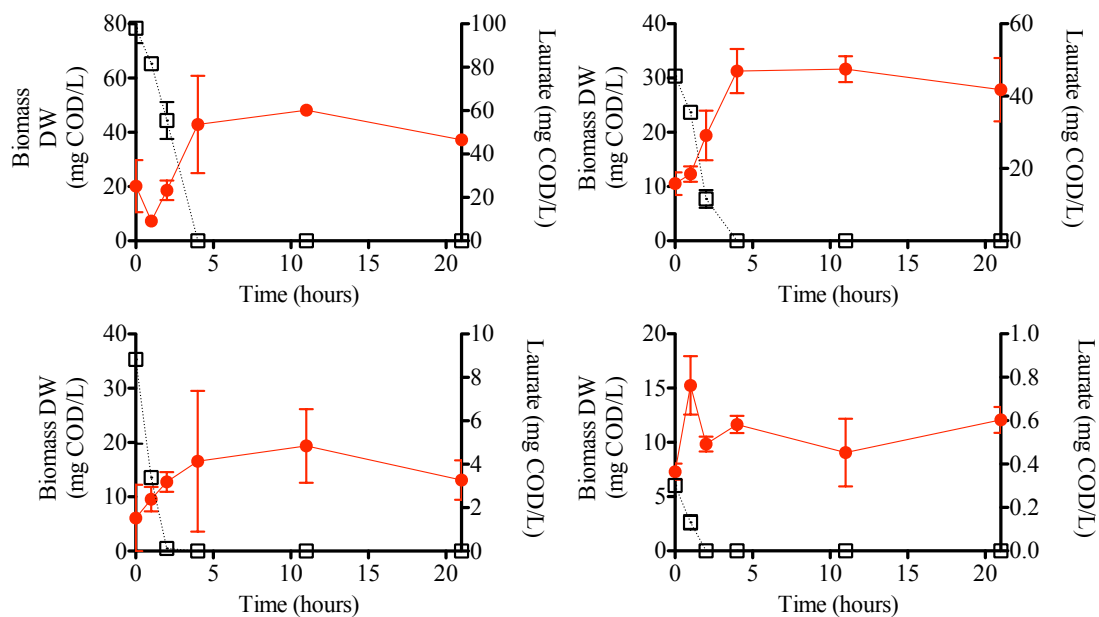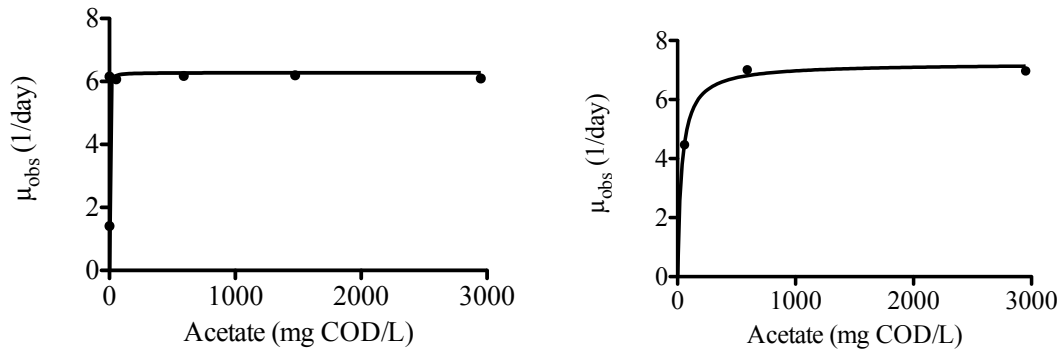
Figure A.2 Representative growth curves for *B2* (above blue) and *ENR1* (below red) on glucose (black) as a sole carbon source.
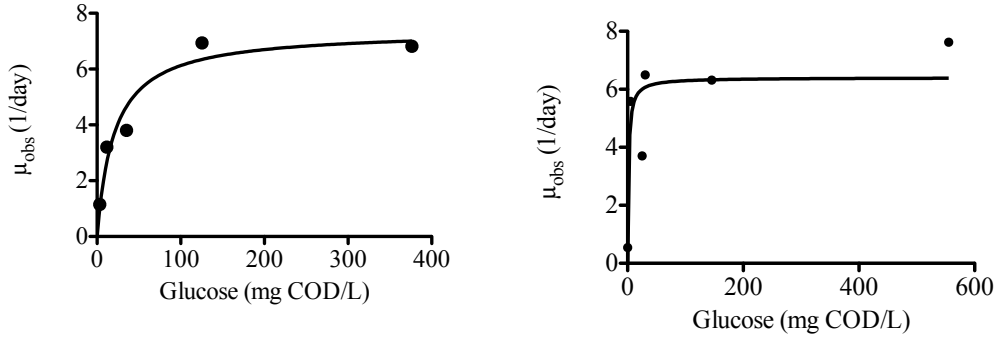
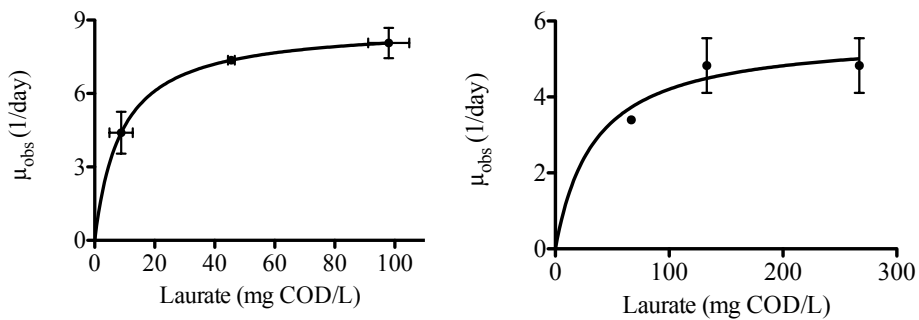**Figure A.3 Representative growth curves for *B2* (blue) on laurate (black) as a sole carbon source.**

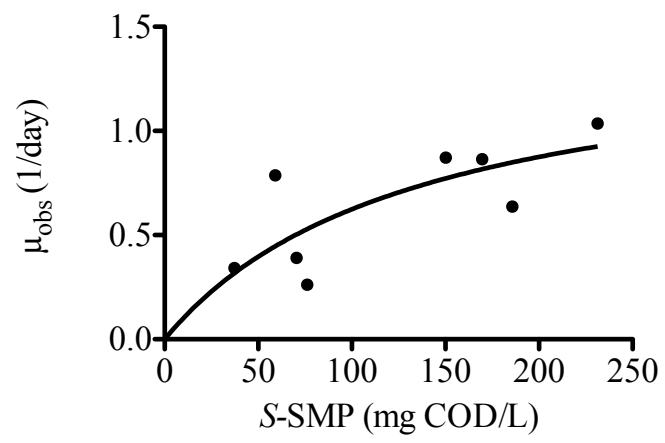**Figure A.4 Representative growth curves for *ENR1* (red) on laurate (black) as a sole carbon source.**

Figure A.5 Monod fits for growth of *B2* (left) and *ENR1* (right) on acetate as a sole carbon source.

A.6 Monod fits for growth of *B2* (left) and *ENR1* (right) on glucose as a sole carbon source.

A.7 Monod fits for growth of *B2* (left) and *ENR1* (right) on laurate as a sole carbon source.

Figure A.8 Monod fit for growth *ENR1* on *S*-SMP